SAND-79-0056
UNLIMITED RELEASE

ENHANCED GAS RECOVERY PROGRAM
THIRD ANNUAL REPORT
OCTOBER 1977 THROUGH SEPTEMBER 1978

D. A. NORTHROP AND C. L. SCHUSTER, EDITORS

Prepared by Sandia Laboratories, Albuquerque, New Mexico 87115
and Livermore, California 94550 for the United States Department of
Energy under Contract AT(29-1) 789

MARCH 1979

Sandia Laboratories
energy report

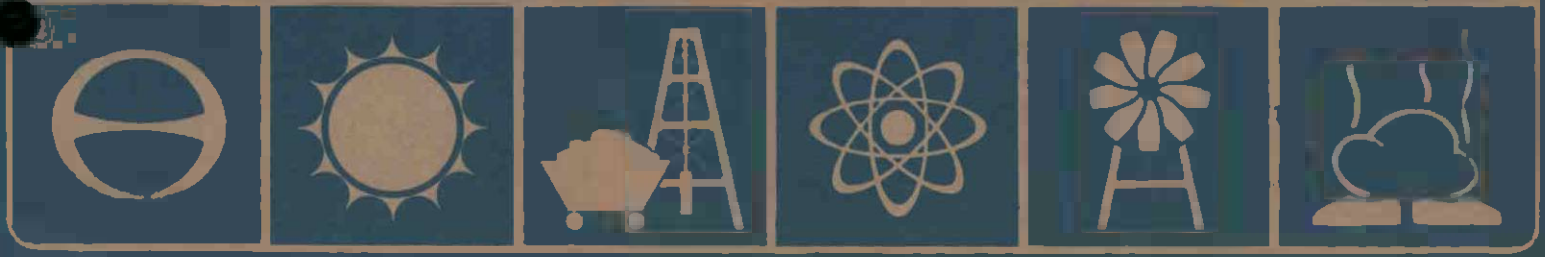

SF 2900-QQB(3-74)

Issued by Sandia Laboratories, operated for the United States Department of Energy by Sandia Corporation.

SF 1004-DF(11-77)

Printed in the United States of America

Available from National Technical Information Service
U.S. Dept. of Commerce
5285 Port Royal Road
Springfield, VA 22161

Price: Printed Copy: $5.50
Microfiche: $3.00

SAND79-0056
Unlimited Release

ENHANCED GAS RECOVERY PROGRAM

THIRD ANNUAL REPORT

October 1977 through September 1978

ABSTRACT

Massive hydraulic fracture mapping field experiments continued in FY 78 with the major activity being an improvement program for the surface electrical system. The potential measurement boxes were modified to accept two different radial inputs and to be continuously calibrated. These, coupled with an improved software capability, should provide higher signal to noise ratios and allow smaller, deeper and more symmetrical fractures to be detected.

Seismic signal analysis continued on the Nevada Test Site data and pointed the direction for the mineback activity. Although there was considerable scatter in the seismic locations, knowledge was gained into the source mechanism and planning for the geophone locations in future experiments. The borehole seismic system was successfully fielded on two experiments and fracture orientation was determined using the received seismic signals.

Sandia's continuing investigation of advanced borehole logging techniques has led to expanded involvement in the areas of nuclear magnetism logging, complex electromagnetic logging, and related interpretive problems.

Hydraulic and explosive fracturing experiments have been conducted adjacent to an existing tunnel complex at DOE's Nevada Test Site and

have been directly observed by subsequent mineback activities. Evaluation of a proppant distribution experiment has revealed a complex fracture system created in a complex geologic region with numerous faults and sharp variations in in situ stress. Evaluation of an experiment to examine hydraulic fracture behavior at a geologic formation interface is underway. Initial mineback has revealed that a fracture initiated in an ashfall tuff formation broke upwards into an overlying welded tuff formation with significantly different properties, most notably an order of magnitude higher modulus; coring is underway to further delineate the fracture systems. The question of fracture propagation at an interface is being addressed by analytical, numerical and experimental techniques. Small volume hydraulic fracturing is being developed as a diagnostic tool to measure in situ stresses and to evaluate expected fracture behavior. In conjunction with a nuclear containment program, it has been confirmed that confined explosive detonations produce containment cages of high residual stress around the cavity which severely inhibits the formation of radial fractures in communication with the cavity. In conjunction with a development program, it was shown that a tailored impulse from a propellant can create multiple fractures from a wellbore; twelve fractures (0.6 to 8 ft) were produced from a 20 lb propellant charge which gave pressure loading rates of 20 psi/sec and a peak pressure of 13,800 psi and no evidence of wellbore enlargement or crushing.

TABLE OF CONTENTS

		PAGE
I.	Introduction and Summary	4
II.	Massive Hydraulic Fracture Mapping and Characterization	11
	A. Surface Electrical Potential System	11
	1. Introduction	11
	2. Athabasca Tar Sands Fracturing Experiment	14
	3. GPE, Utah MHF Experiment	20
	4. Amoco Wattenberg Experiments	20
	B. Borehole Seismic System	30
	C. NTS Seismic Signal Analysis	38
	D. Downhole Stacked Hydrophone System	46
III.	Advanced Logging and Formation Evaluation	50
	A. Electric Logging	50
	B. Electromagnetic Logging	69
	C. Nuclear Magnetism Log	69
	D. Borehole Seismic System	71
	E. Acoustic Logging	71
IV.	Stimulation and Mineback Experiment Project	73
	A. Hole 5	74
	B. Hole 6	77
	C. Interface Studies	93
	D. Small Volume Hydraulic Fracturing	99
	E. Complementary Studies	106
	1. High Energy Gas Frac	106
	2. Nuclear Containment	109
V.	Publications, Presentations, and Communications	116

I. INTRODUCTION AND SUMMARY

Introduction

Sandia Laboratories conducts several projects which are part of the United States Department of Energy's (DOE) Enhanced Gas Recovery Program. One is the Massive Hydraulic Fracture Characterization Project whose objective is to develop instrumentation systems for characterizing fracture systems, formations, and other parameters contributing to enhanced gas recovery. Another is the Stimulation and Mineback Experiment Project whose objective is to understand, and thus improve, fracturing processes for stimulation of natural gas production from low permeability formations which contain a high potential resource. Another is the advanced logging for formation evaluation program being conducted for the Bartlesville Energy Technology Center in support of the Western Gas Sands Program. This report summarizes activities conducted under these projects during Fiscal Year 1978; October 1, 1977, through September 30, 1978.

The Massive Hydraulic Fracture Characterization Project began in 1974 with the initial application of Sandia's instrumentation capability in a joint experiment with El Paso Natural Gas in the Pinedale Field, Green River Basin, Wyoming. The initial effort was an attempt to measure the orientation and growth of a massive hydraulic fracture using both surface seismic recording and electrical potential mapping techniques. In the ensuing years, the surface seismic program has been discontinued because of its inability to map fractures from the surface. The electrical potential technique has grown and has been fielded on several experiments over the past four years. This instrumentation system has been deployed on both joint DOE-industry funded and private industry experiments on a non-transfer of funds basis. These experiments have covered a range of stimulation techniques in natural gas, petroleum, and tar sands recovery. This instrumentation system has

demonstrated the capability to determine fracture orientation induced by massive hydraulic fracturing; provide a measure of the asymmetry of fracture wings created; and provide some insight into the stimulation processes occurring within the reservoir.

The electrical potential technique is based upon the surface measurement of potential changes caused by a changing current electrode geometry. The current electrode is the fracture well and the conductive frac fluid, which, introduced into the subsurface formation, causes the geometry to change during the fracture operation. These potential changes are small and require extensive data collection and analysis to ascertain fracture orientation. Model calculations aid in the interpretation of fracture orientation and symmetry.

Recent program activities have focused upon the continued development of the surface electrical potential techniques (e.g., enhanced signal to noise ratios) and its application to a variety of reservoirs. In addition, there has been a broadening of project scope to develop other instrumentation systems and techniques for characterizing geological features such as sand lenses and natural fracture systems, effects due to different stimulation processes, and other factors affecting enhanced gas recovery. The original surface seismic program has been redirected and now emphasizes a borehole recording system that can be utilized in the fracture well. A continuing close relationship with industry is anticipated in these activities.

Current progress on Sandia's overall program of advanced borehole logging and formation evaluation lies primarily in the areas of nuclear magnetism and complex electromagnetic logging. A working relationship between Sandia and Chevron Oil Field Research Company is being developed to investigate the nuclear magnetic response of typical tight Western gas sands and the applicability of NMR measurements to the exploitation of such reservoirs. Work is continuing on the development of a computer

code to model the complex electromagnetic response of a borehole induction probe within a layered and invaded sequence of formations.

The Mineback Stimulation Test Project was initiated in FY 77. However, the program has built upon fracturing and mineback activities which have been conducted since 1974 in G-tunnel, at the Nevada Test Site, as part of a nuclear containment program sponsored by the Division of Military Applications under DOE. The commonality of objectives between the nuclear containment program and enhanced gas recovery activities is striking, and the continued close relationship between the two programs will be mutually beneficial.

Various stimulation techniques have been applied to the so-called unconventional natural gas resources, such as the western tight sands basins and the eastern Devonian shale formations, with varying, but generally non-economic, results. Massive hydraulic fracturing (MHF), as being practiced, is based upon extensive "conventional" fracturing experience, laboratory testing, and empirical design models; the extrapolation to the massive scale has not been generally successful. Dendritic, foam, gas, and chemical explosive fracturing techniques have been applied, and successes or failures are not well understood. Industry has often stated the need to perform experiments in an environment which allows for direct examination and evaluation.

Mineback evaluation provides this opportunity. A detailed physical description can be obtained directly and can be correlated with measured geologic material properties, in situ stress distributions, fluid behavior, and the operational parameters of the test. Supportive rock and fluid mechanics laboratory and modeling work will be performed to aid in this interpretation. The mineback also provides the opportunity for the calibration of instrumentation techniques under known conditions. Thus, mineback testing provides significantly more information than the evaluation of a commercial stimulation job which is based primarily upon gas production. Industry and service company participation in the

program will ensure that the results will impact the experience and knowledge base used in production; such industry interest has been high. The program will provide a unique opportunity to quantify and understand fracture behavior.

Sandia's projects derive their support from both the Eastern Gas Shales Project, Western Gas Sands Project, and Bartlesville Energy Technology Center, which are major parts of DOE's Enhanced Gas Recovery Program. Sandia's projects provide a broad supporting research and development capability. Activities are planned, conducted, and reported with the aim of contributing to the objectives of both the Eastern and Western Projects and to the overall development of Enhanced Gas Recovery technology.

Summary

The surface electrical potential experiments continued with three rather diverse fracturing sites. The first of these was a shallow horizontal fracture in a tar sand formation in Canada. This was the northernmost experiment we have conducted. The telluric current levels were much higher than had ever been encountered. The resulting telluric potential essentially masked the data obtained from the fracture, and the shape and orientation could not be determined.

The second surface electrical potential experiment was in the Unita Basin with Gas Producing Enterprises. A deep multizone fracture was planned using the limited entry technique to cause simultaneous stimulation of several pay zones. Although the total volume was high, the length of each fracture was not sufficient to cause a significant potential change.

The third set of experiments was conducted by Amoco in the Wattenburg field at an intermediate depth in the Sussex formation. Amoco desired to bring together on these experiments all the fracture mapping techniques that are available. The USGS and Texas A & M University also participated in these experiments. The wells were cored in the

fracture interval and completed open hole to facilitate both borehole televiewer and borehole television monitoring of the fractures. Core analysis will be done by both Amoco and Texas A & M. The tiltmeter was installed and data collected by M. D. Wood of the USGS. Sandia fielded the surface electrical potential system on all three experiments and collected data with the borehole seismic system on a portion of the two experiments. Sandia also had their Hewlett-Packard pressure gauge on site and recorded wellhead pressures on two experiments and downhole pressure on the third experiment. Analysis of the data collected on all three experiments was presented by all parties at a data exchange meeting held at Amoco.

Two seismic recording experiments were conducted during this fiscal year. During the Hole 6 fracturing experiments at the Nevada Test Site, seismic recordings were made, and the data are quite encouraging, as close-in seismic events were recorded. As an aid to determining the amount of chemical explosive detonated during a fracturing test, surface seismic recordings were also made at a Petroleum Technology Corporation (P.T.C.) experiment. This West Virginia test indicated that probably most of the explosive slurry did detonate as planned.

A second wireline tool utilizing a string of hydrophones is under development. This type of tool will allow fracture heights to be determined from the wellbore but not fracture orientations. The tool has some inherent advantages over the borehole seismic system. One of these is the fact that it will only be 1 ½" in diameter and can therefore be installed through tubing and be implaced during the actual fracturing experiment. As the hydrophones are pressure sensitive, the tool will not require clamping of the sidewall for obtaining data.

A logging task force was formed in February 1978, and was chartered to investigate the state-of-the-art in commercial geophysical logs as

well as logging research to determine which areas of concentration might be most beneficial to natural gas reservoir applications. Over numerous months of literature search, theory development, and interviews with production and research personnel from the petroleum industry, academic community, and logging service organizations, this task force has concluded that the areas of NMR and electromagnetics would provide the most benefit. In addition, continuing research and development of existing Sandia borehole neutronics programs is encouraged with petroleum applications in mind.

The Stimulation and Mineback experiment project has focused on the evaluation of two experiments conducted at the Nevada Test Site: one investigates the distribution of proppant produced by a hydraulic fracture (Hole 5), and the other examines fracture behavior at a geologic formation interface (Hole 6). The complex fracture system observed in the Hole 5 test has been substantiated by conducting small-volume fracturing tests in 16 intervals along two boreholes on either side of the Hole 5 region. Two hundred sixty feet of tunnel were subsequently driven along these boreholes, and complex geology with numerous faults and variable fracture behavior and in situ stress distributions were observed. The results indicate that complex hydraulic fracture can occur in regions of complex geology and in situ stresses. In the Hole 6 experiment, two hydraulic fractures were created above and below an ashfall tuff-welded tuff formation interface. These formations, respectively, have significantly different elastic moduli (0.5×10^6, 5.0×10^6 psi), Poisson's ratios (0.30, 0.21), and porosities (45, 13%). Fracture calculations were used to select volumes sufficient to create 50 ft high fractures of 600 ft total length; 256 and 117 bbls were injected at 6 bbls/min into the ash fall and welded tuff zones, respectively. Initial evaluation of this experiment has been made by mining along the interface. Preliminary observations include: (1) the first (lower) fracture easily penetrated the interface and broke

upwards into a formation of significantly higher modulus; (2) fracture length was 150 ft at the elevation of the interface; (3) the second (upper) fracture initiated in the same plane as the first fracture and propagated along it at several locations; (4) natural fractures in the welded tuff affected fracture behavior; (5) fracture widths were consistent with material properties, 5-10 mm and 2-5 mm in the ash-fall and welded tuffs, respectively, and (6) observed fracture orientation was the same as the azimuth determined by seismic instrumentation. Exploratory coring is being used to further delineate the fracture; initial results indicate penetration of the lower fracture at least 25 ft upwards into the welded tuff with significant branching and no additional lateral extension at the elevation of the interface.

In related studies not directly funded under this program, two areas have produced results of interest to enhanced gas recovery technology. Examination of several contained explosive experiments have confirmed the formation of a region of high residual stress and decreased permeability around the explosive cavity. The concept of a high energy gas fracture was tested which examined fracturing in the stress and strain-rate regions intermediate between the hydraulic and explosive fracturing extremes. At a particular selection which created peak pressures of 13,800 psi and pressure loading rate of $\sim$ 20 psi/μsec, mineback revealed that twelve fractures had been initiated from the wellbore, with seven of the twelve fractures having lengths from 2 to 8 ft in length. Thus, multiple fracture initiation is feasible and reasonable penetrations can be achieved.

II. MASSIVE HYDRAULIC FRACTURE MAPPING AND CHARACTERIZATION PROGRAM

A. Surface Electrical Potential System (SEPS)

1. Introduction

The measurement of induced surface potentials is being used in a research effort to map the orientation of fractures created by massive hydraulic fracturing (MHF). MHF is a natural gas production stimulation technique currently under development by many private companies for utilization in the tight gas sandstone reservoirs of the West and the Devonian shale formations of the East. Knowledge of the fracture system characteristics created by MHF is needed, during developmental testing, to assist in evaluating the effectiveness of the stimulation treatment and, during commercial utilization to optimize well placement.

Electrical prospecting is a well-known technique that is used in the investigation of geological structures beneath the surface of the earth. The approach taken is to determine the variation of the electrical constants of the earth's crust, and variation in resistivity is by far the greatest. The induced surface electrical potential method used in MHF characterization uses the variation in the resistivity contrast and is associated with the science (or art) of electrical prospecting. The casing of the well to be fractured is used as the probe for injecting current into the earth. A remote well casing serves as the return current probe. The induced potential distribution is measured at the surface of the earth on circumferences around the fracture well. Theoretically, before fracture, the equal potential lines form concentric circles with the fracture well as their center. During fracture, the well casing, along with the associated fracture, when filled with a conducting fluid, acts as a changing current injection electrode. As the fracture progresses, the change in electrode geometry causes a predictable distortion of the concentric circles formed by the vertical well casing alone.

The surface electrical potential data are taken by periodically recording the induced potential differences at the earth's surface between data probes (in concentric circles) placed every 15^{o} circumferentially around the fracture well, and a reference probe. The injected current is of a bipolar pulse form to minimize the effects of electrode polarization. Prior to fracture initiation, background data are taken to establish the induced potential levels around the fracture well at the data probes. This then becomes the reference data level for detecting the changes produced when the conductive fracture fluid alters the electrical geometry of the fracture well. This change in the fracture well current distribution, caused by fracture growth, alters the induced surface electrical potential around the fracture well. If the electrical potential measurements before, during and after the fracturing are compared, diagnostic information about the fracture is obtained.

Each potential measurement location consisted of a pair of potential probes driven into the earth and a potential measurement box (PMB). The probes are stainless steel stakes approximately two feet long. A wire from each probe was fed to a PMB located adjacent to the inner potential probe. The output from twelve PMB's were frequency multiplexed onto one coax cable. The coax cable fed power from the instrumentation van to each PMB and data via the frequency multiplex system from each PMB to the instrumentation van. Two coax cables thus fed the potential data between each probe pair from all 24 locations to the instrumentation van for processing and recording. Changes are being made to upgrade the system to include the addition of a reference circle. This reference circle is an electrical conductor having the same layout radius as the radius 1 data probes. The reference circle is connected to a reference probe located a distance 5 to 10 times the radius 1 data probe distance from the fracture well. This type of layout yields twice the data from the same number of data probes.

Each of the 48 data sources exist between a data probe and the reference probe. This additional data will possibly provide a data confidence factor if the data from each radius sets flags the same fracture direction. Changes in fracture direction may also be detectable. Further, the dual radii capability may provide a means of assessing fracture length and fracture growth rate. The data probe radii range from 1000 to 1800 feet and are determined from a mathematical model which considers such parameters as fracture depth and expected fracture length(s). The reference circle is connected to the reference probe via the instrumentation van. This enables the reference circle to be used as a common tie for both the fracture data acquisition and for calibration.

The PMB has been modified to include a radius 1-radius 2 select capability, a 1 HZ passive bandpass filter in front of the isolation amplifier, and a 4 pole active linear phase low pass filter. The active filter has a cut-off of 1.75 HZ which gives a data bandwidth from approximately .25 to 1.75 HZ. The 1 HZ bandpass filter helps eliminate probe to reference probe current flow via the isolation amplifier input impedance. The combined filter effects are to reduce that portion of the telluric spectrum outside the pulses fundamental frequency of $\frac{1}{2}$ HZ.

The reference circle is formed by a conductor within 24 - 500 ft, 6 conductor cables which are used to interconnect the 24 PMB's to the instrumentation van. These cables also supply power, control and calibrate inputs to the PMB's and carry the subcarrier VCO outputs back to the instrumentation van. The test control has been added, which interrelates all functional aspects of SEPS. The computer has been upgraded to a DEC PDP 11/34 and includes dual floppy and dual RK05 discs for better data handling. Digital outputs from the DR11-K control the Fluke 4216A programmable supply, the bipolar calibration source. The DR11-K, via the test control, controls the radius 1-radius 2

selection. The A and B sets of 12 subcarriers from the PMB's, containing either calibrate or radius-1 radius-2 data, is extracted from the 6 conductor cables in the TEST CONTROL and coupled to the A and B subcarrier discriminators. The outputs of these 24 data sources undergo analog to digital conversion in the ADK11-KT. When SEPS is a non-fielded configuration (stored in the instrumentation van), the TEST CONTROL extracts simulated radius 1-radius 2 levels from the calibrate source and makes them available as inputs to the PMB's. The SEPS has undergone hundreds of testing hours in this configuration.

The inability to pulse a downhole current probe to high current levels has limited the SEPS test capability. The pulser has been modified and now has an SCR for both pulse turn-on and turn-off. Turn-off failure had been the problem area.

In addition to changes in the SEPS hardware, improvements have been incorporated in the software which allows for more precise data acquisition, system testing, and performance monitoring.

The data acquisition program has been changed from BASIC to FORTRAN to allow for more efficient operation and possible foreground/background applications in the future.

2. Athabasca Tar Sands Fracturing Experiment

In July 1977, Sandia Laboratories, through a working relationship with AMOCO, was invited to participate in a massive hydraulic fracturing experiment to be conducted in the Athabasca tar sands of the Province of Alberta, Canada. The U. S. Geologic Survey, Office of Earthquake Studies, was also invited to participate. The purpose of the experiment was to determine whether it is possible to establish a reliable technique of creating horizontal fractures which will be in communication with wells drilled on commercial spacing. The Alberta Oil Sands Technology and Research Authority (AOSTRA) provided approximately 75% of the funding with the objective of developing oil sands and heavy

oil technology and Numac Oil and Gas Ltd., the project operator, provided the additional 25%. Sandia and USGS funding was provided by DOE.

The Athabasca Tar Sands deposit is located in the northeast quarter of the Province of Alberta, Canada, some 200 miles northeast of Edmonton (Fig. II-1). The test site was located on a lease held by Numac Oil & Gas Ltd. Access to the test site was by helicopter from Fort McMurray, forty miles to the northwest. All equipment required for the experiment arrived by rail from Edmonton. Six miles of roadway were built to move the equipment and supplies from the rail head to the test site.

The fracture well, F-1, was located in the central portion of the test site (Fig. II-2). An observation well, 0-1, was drilled approximately 25 feet from the fracture well using the information cored throughout the McMurray formation by picking the core point 10 feet above the Clearwater formation. In order to permit an open hole treatment, casing was set 10 feet above the bottom of the McMurray formation, and coring then continued 10 feet into the underlying Devonian formation. Two additional wells, 0-2 and 0-3, were drilled at distances of 200 feet from the F-1 well. These wells were used for observation throughout the experiment. The surface electrical potential array, Fig. II-3, was set up at a radius of 1000 feet around the F-1 well.

The fracture well (F-1) was drilled to a depth of 1170 ft, and casing was set to 1150 ft. Two fractures were performed. The first, in the open hole section, was in an attempt to create a horizontal fracture at the tar sands-Devonian shale interface at approximately 1160 feet. The second fracture was through the abrasajet cut in the casing at 1071 feet and into the tar sands formation.

The initial portion of the first fracture was performed on October 3, 1977, (open hole, tar sands-Devonian shale interface, 1160 feet). During this operation, 11,760 gallons of gelled water were pumped. Fracture pressure varied from 200 to 870 psi. Flow rates ranged

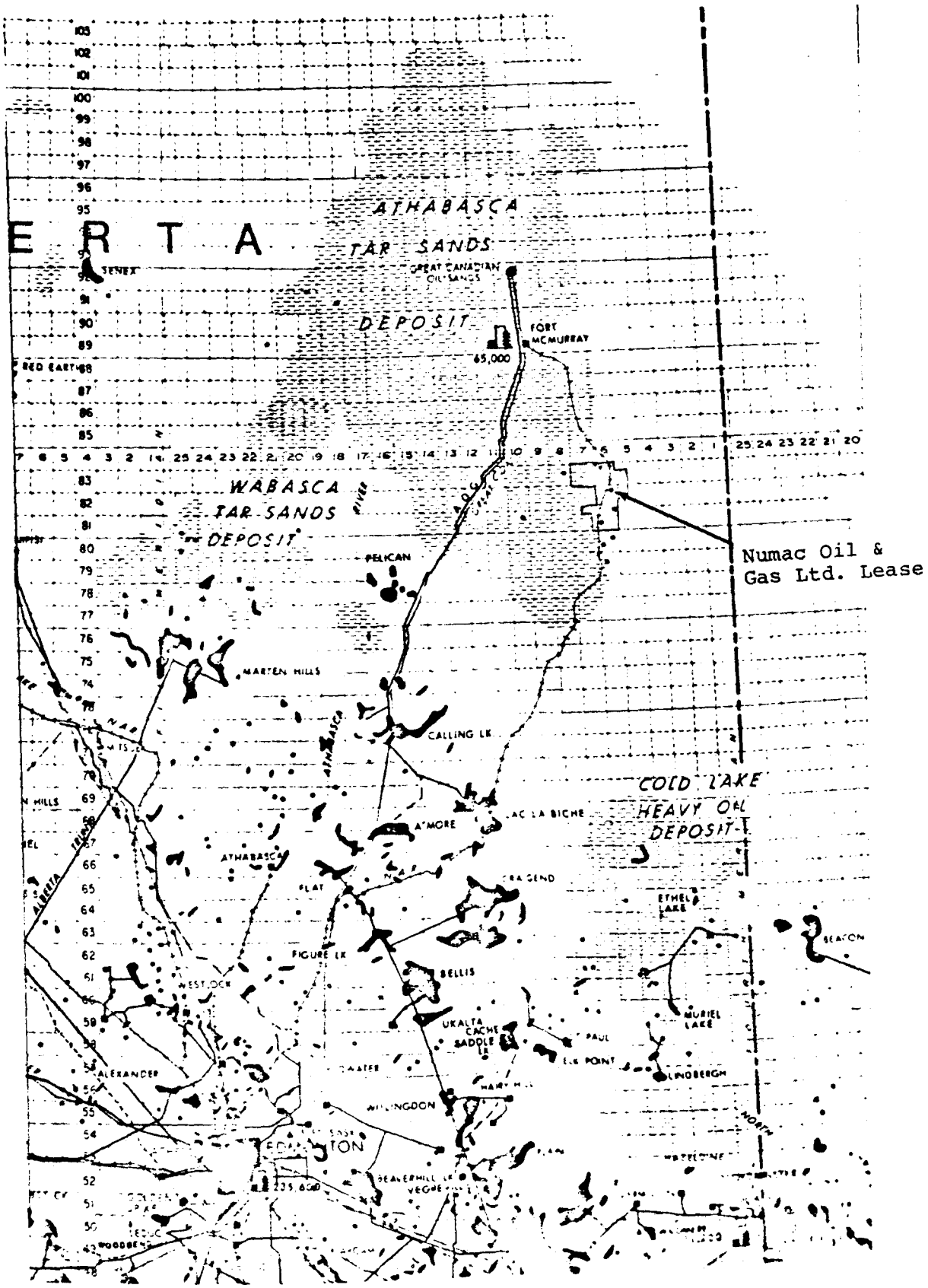

Fig. II-1 Athabasca Tar Sands Deposit

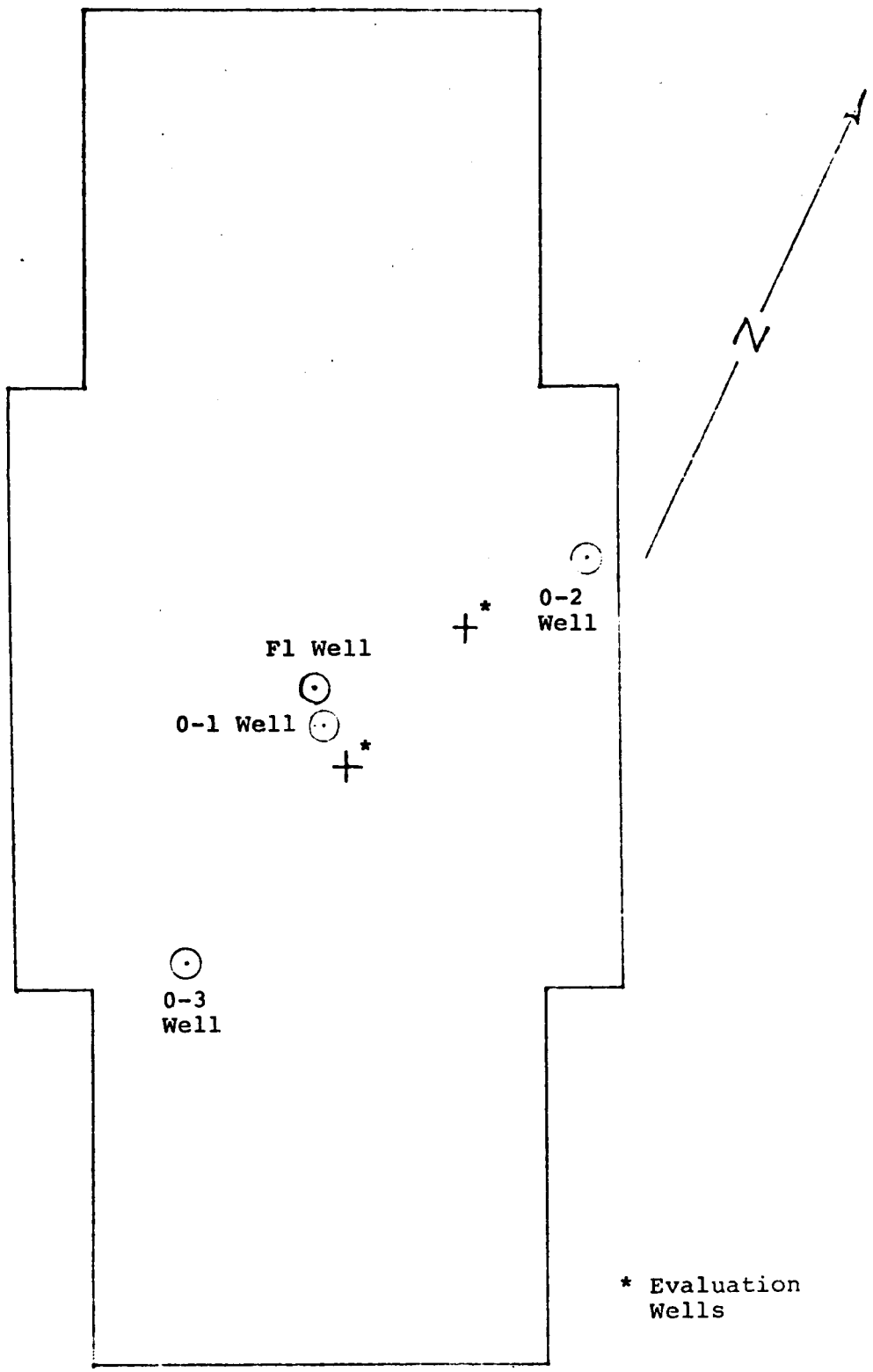

Fig. II-2 Test Site

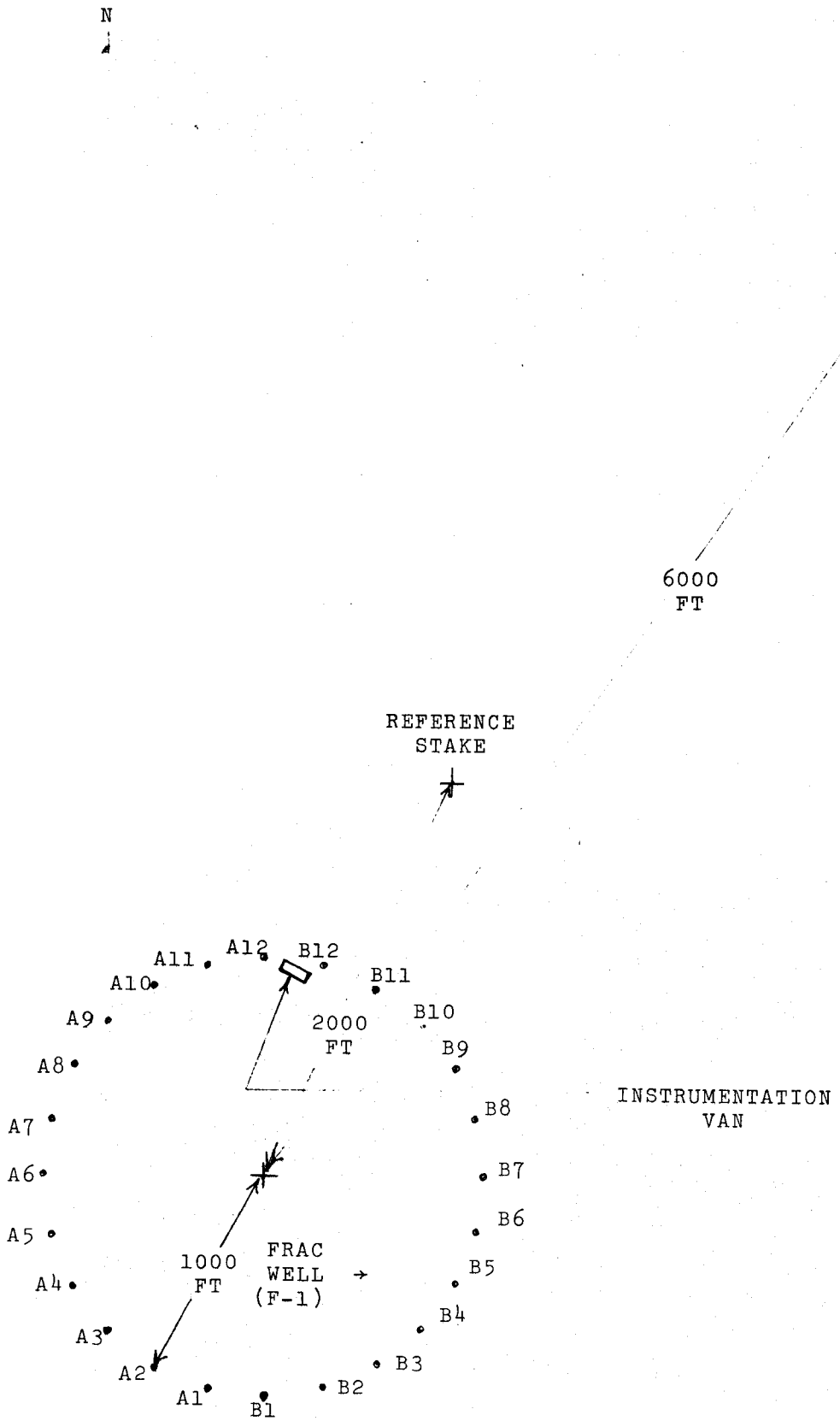

Fig. II-3 Surface Electrical Potential Layout

from 82 to 336 gallons per minute. The Amoco downhole TV camera was located in the open hole portion of the well, and surface potential and tilt measurements were made. This portion of the experiment lasted approximately six hours. Temperature logs were run on the well after this pump. Due to an unexpected temperature response in the well, the second portion of the fracture was delayed until October 4, while additional temperature logs were run. During the second portion of the first fracture, 67,284 gallons of colored (uranine) grout were pumped. Surface potentials and tilt measurements were performed. This second portion of the first fracture required approximately six hours.

The second fracture was performed on October 6, 1977. This fracture procedure was through the abrasajet cut in the casing at 1071 feet and into the tar sands formation. Red dye was added to the grout. 73,330 gallons were pumped; fracture pressures ranged from 100 to 400 psi, and flow rates were between 180 and 953 gallons per minute.

The surface electrical potential fracture mapping instrumentation system was designed to detect the direction of vertical fractures, the predominant form used in enhanced gas and oil recovery procedures. The Surmont Project hydrofracture experiment was designed to be a horizontal fracture, implicitly excluding direction. The response of the surface electrical potential instrumentation to this type of fracture would be non-conclusive. The presence of this instrumentation system, therefore, could only be to attempt to determine if the fracture propagated vertically.

Post-test analysis of the surface electrical data failed to reveal any specific fracture orientation.

Two evaluation wells have been drilled by Numac, one 100 feet to the northeast and one 50 feet to the southeast of the fracture well. Core samples from both wells failed to reveal any colored grout.

3. G.P.E. Utah MHF Experiment

On November 21, 1977, Sandia participated in G.P.E.'s MHF experiment in their Natural Buttes #22 well located approximately 32 miles south of Vernal, Utah; the fracture was performed by Dowell. The experiment was designed to create fractures through 35 perforations, at depths of 6838, 6844, 6847, 6898, 6924, 6981, 7007, 7022, 7105, 7122, 7148, 7358, 7495, 7499, 7570, 7750, 7875, 7954, 7956, 8016, 8018, 8022, 8029, 8037, 8049, 8051, 8220, 8237, 8454, 8470, 8474, 8492, 8500, 8531, and 8550 feet, in the Mesa Verde formation. Pumping started at 1305 hours and continued through 1756 hours. A total of 547-740 gallons were pumped at rates up to 2310 gallons per minute.

The surface electrical potential system was the only fracture mapping system deployed for the experiment. The test site layout is shown in Figure II-4. Extremely rugged terrain prevented the installation of potential measurement boxes in a 75° sector west of the well.

Surface potential measurements were taken at two-minute intervals during the experiment. During the early period of pumping, the surface potential had a wider dispersion than had been observed on previous hydrofracture experiments and no definite orientation was discernable.

4. Amoco Wattenberg Experiments

Sandia Laboratories participated with Amoco in a series of hydraulic fracture mapping experiments in their Wattenberg field near Ft. Lupton, Colorado. Three fracture experiments were conducted between January 31 and March 8, 1978. The Horst #1 well, located 5.1 miles west-northwest of Ft. Lupton (Fig. II-5), was fractured on January 31 and February 1. Jeffers #1, 4.7 miles west-northwest of Ft. Lupton, was completed on February 15, 1978. The final well, Carlson C-1, 1.7 miles west of Ft. Lupton, was fractured March 7 and 8, 1978. All these wells were an open hole completion into the Sussex formation. A fracture radius of approximately 1500 feet was anticipated on each well.

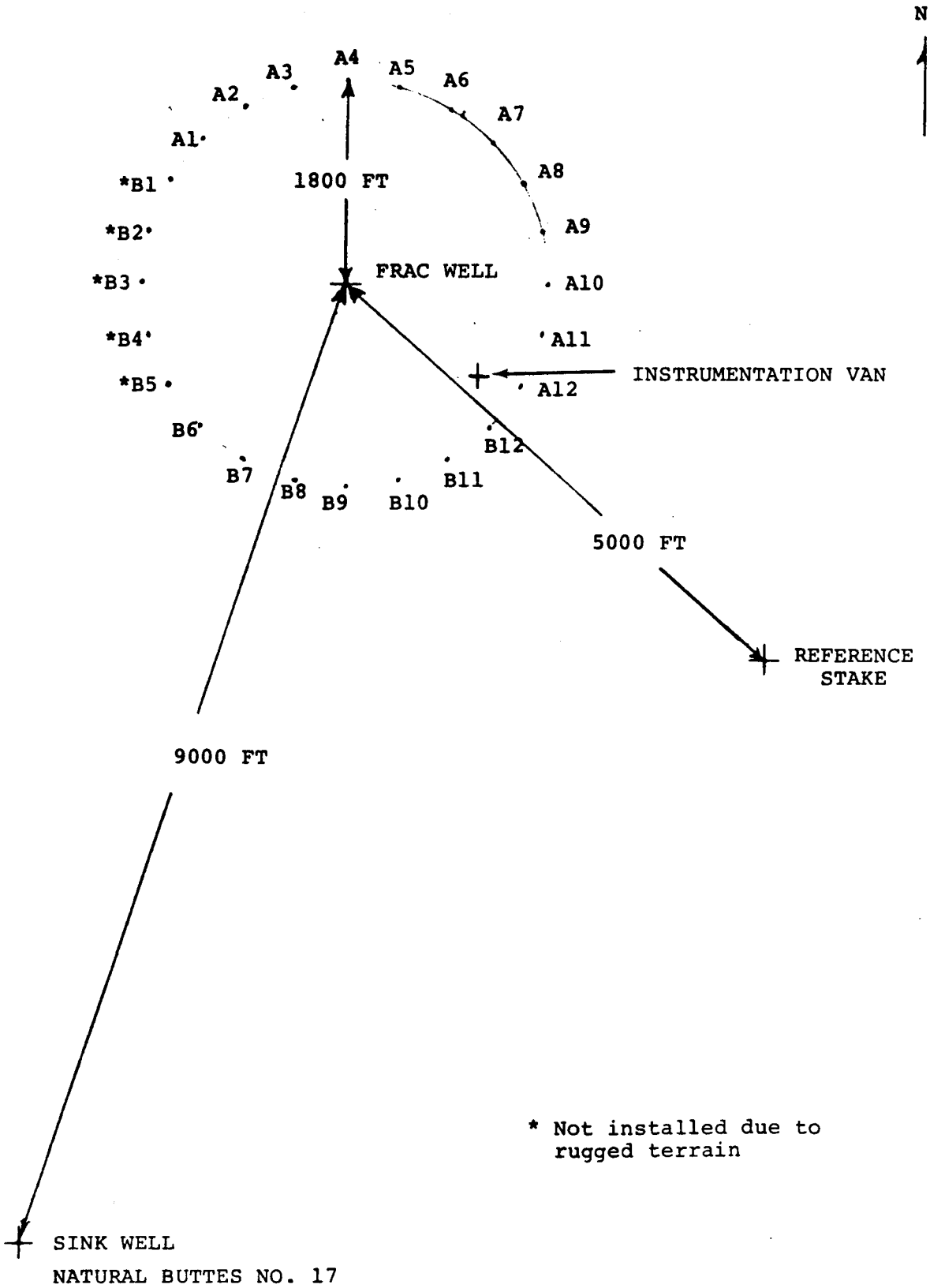

Fig. II-4 Test Site - Natural Buttes No. 22

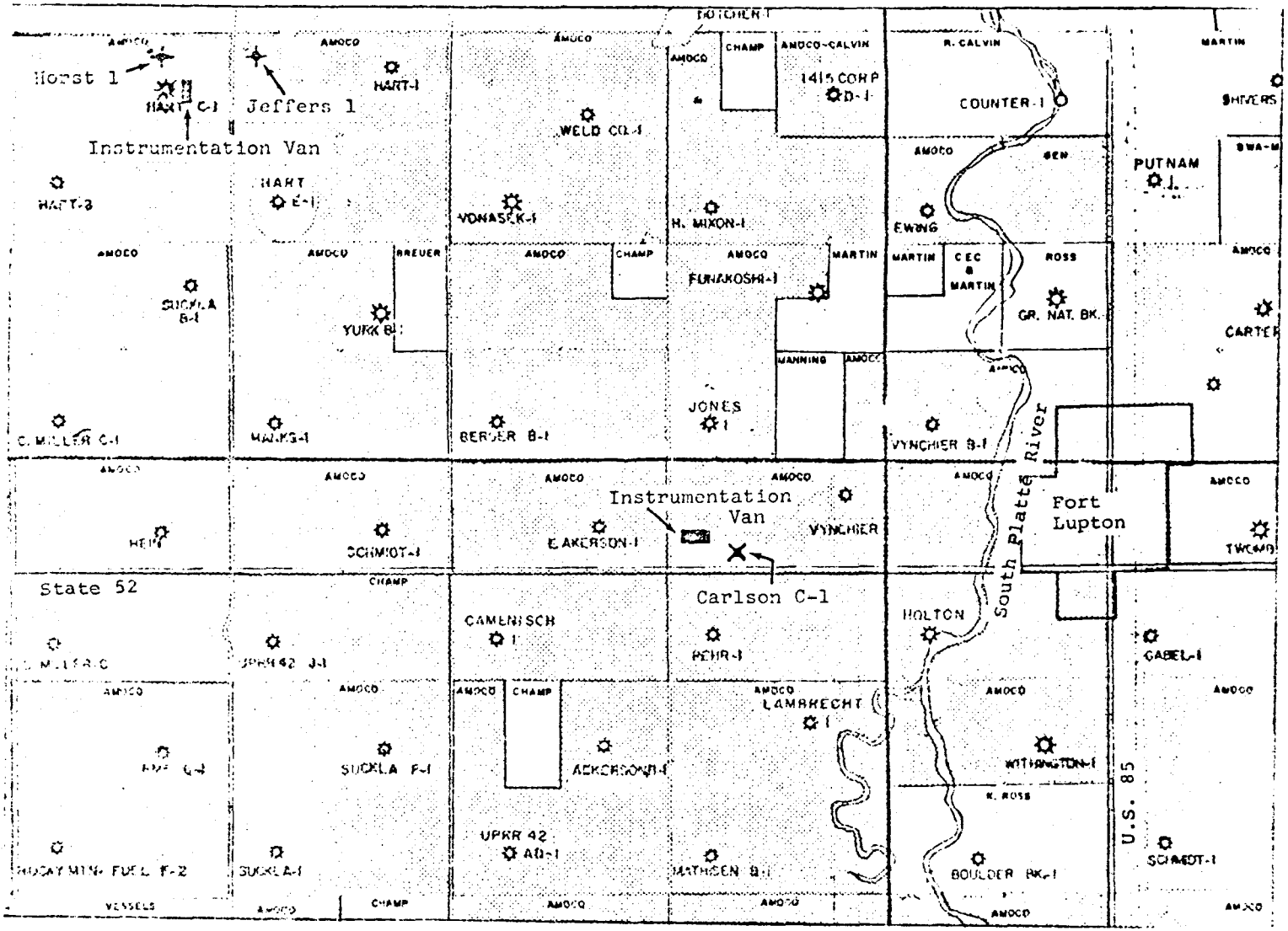

Fig. II-5 Wattenberg Field - Amoco

The Horst experiment was conducted in two steps. Step 1 consisted of a breakdown procedure using 15,800 gallons of gelled water containing 3% KCL. Step 2, performed a day later, was the main fracture of 122,400 gallons of fracture fluid with 228,000 pounds of proppant.

Instrumentation consisted of the Surface Electrical Potential System (SEPS), a three-axis wall-clamp geophone tool downhole near the fracture interface (at a depth of 4775 feet) and a special Hewlett-Packard quartz recording pressure system monitoring the surface pressure at the wellhead. During the breakdown (Step 1) the pressure was increased until the first indication of breakdown occurred. The well was then shut in for approximately 6 minutes. During this listening period, the geophone system recorded the seismic activity. The flow rate was then increased from zero to 5 BPM until 5000 additional gallons were pumped. This required approximately 23 minutes. The well was shut in for 8 minutes (approx.) listening time. Five-thousand additional gallons were pumped at 10 BPM, requiring 11.5 minutes (approx). After another 8 minutes of shut-in time, 5000 more gallons were pumped at 20 BPM. This required approximately 6 minutes. The well was shut-in for 10 minutes after which controlled flow-back was initiated.

During both the pumping and flow back intervals, the geophone outputs were completely masked by noise. The smallest amount of flow induced extreme seismic activity.

The SEPS was active throughout the entire procedure of Step 1, using the well casing as the current injection probe. Figure II-6 illustrates the SEPS layout around the Horst well for both steps of the experiment. Data acquisition for Step 1 (breakdown) began at 9:24 a.m. and concluded at 12:27 p.m.

The SEPS portion of Step 2 attempted to utilize the downhole current probe for current injection at the open-hole portion of the well. The current probe had to be abandoned because of a failure in the current switching system portion of SEPS. The SEPS portion of the experiment

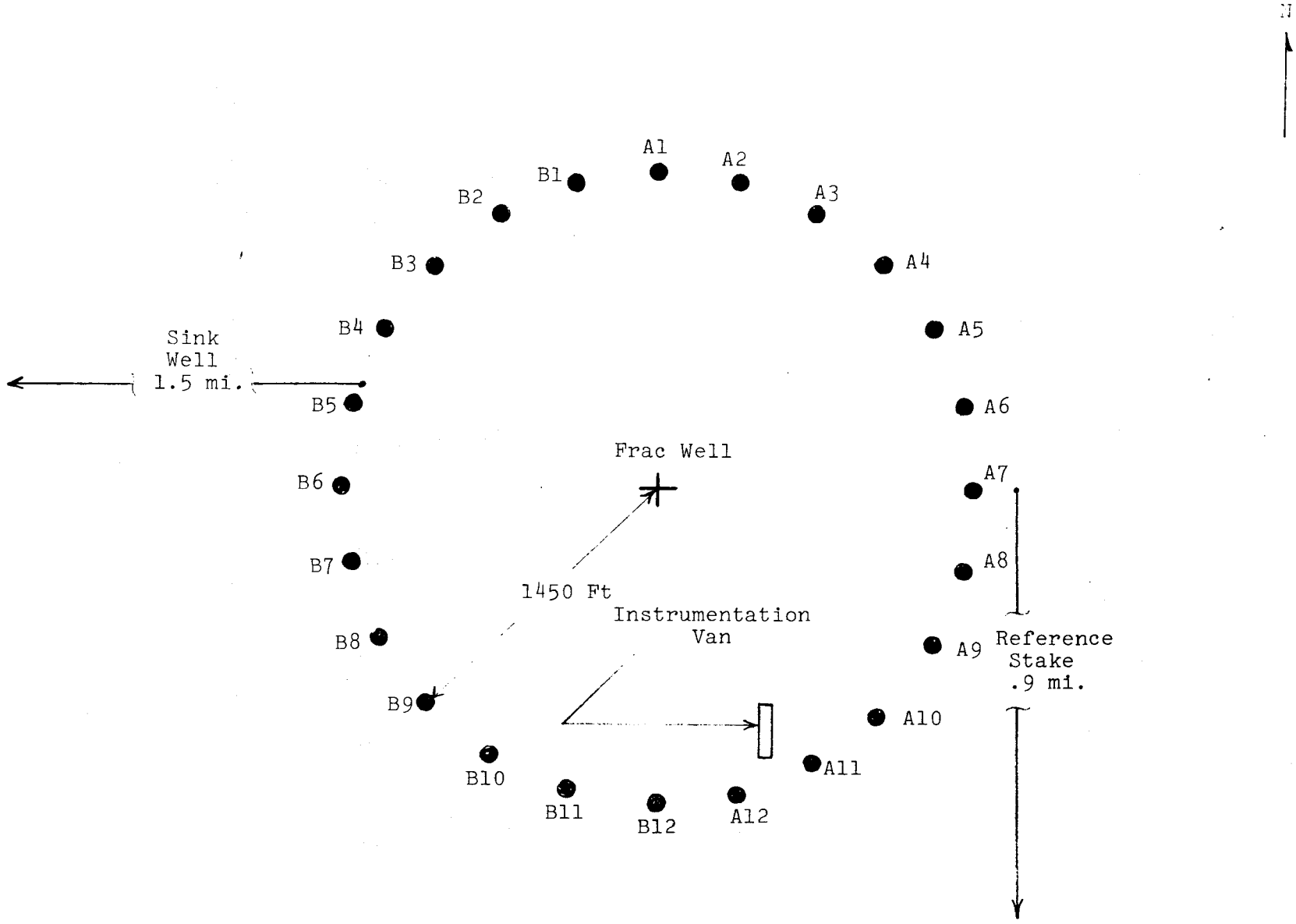

Fig. II-6 Horst 1 Well - SEPS Layout

was accomplished utilizing the well casing for the current injection probe.

Data acquisition on the SEPS began at 12:44 and continued until 16:03. The fracture fluid flow started at 13:05 and continued to 15:30. The flow rate was changed between 20 and 30 BPM several times during the fracture procedure. This had the purpose of assessing the response of the surface tilt meters.

Analysis of the SEPS data failed to indicate a definite fracture orientation; however, it did indicate a general trend of North-South with a symmetrical fracture growth.

The Hewlett-Packard recording pressure gauge monitored the casing pressure during breakdown. Tubing pressure was monitored during the main fracture. Several interesting pressure phenomena were observed.

The Jeffers experiment was conducted February 15, 1978. This well was located approximately 1/2 mile east of the Horst #1 well and the instrumentation van was not moved from the Horst site. The main fracture procedure used 121,620 gallons of gelled water and 228,000 pounds of proppant.

On this experiment, Amoco placed their TV camera downhole during the breakdown phase. Upon inserting the camera into the well and starting downhole, the camera developed a water leak, and this portion of the experiment was cancelled. Tubing was then hung in the well and Sandia attempted to use the downhole current probe for the SEPS measurements. Again, a failure in the current switching system portion of SEPS forced the current injection probe to be moved to the fracture well casing. Figure II-7 illustrates the SEPS layout around the Jeffers well for the main fracture procedure.

Two sink wells were used during this experiment in order to determine what possible effect they might have on fracture directional analysis. Data acquisition on the SEPS begin at 09:39 and continued through 13:06. Breakdown occurred at 10:01 (950 psi) and flow

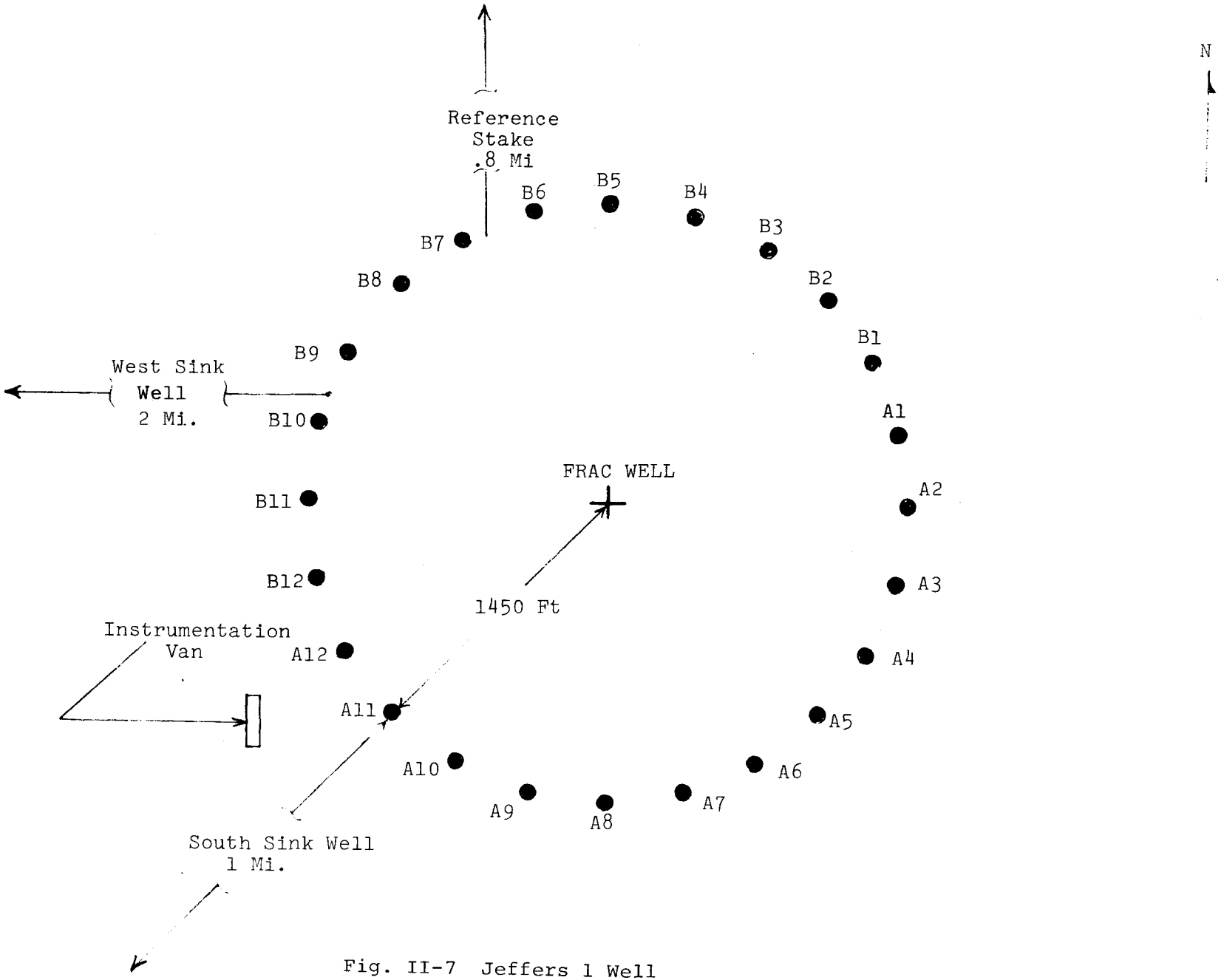

Fig. II-7 Jeffers 1 Well

terminated at 12:38. Flow rate varied between 11 and 27 BPM. Analysis of the SEPS data utilizing the two current returns independently and eliminating noise indicated a symmetric N30°W to S30° fracture orientation.

After the downhole current probe was removed, it was decided to utilize the tubing for the H-P pressure gauge. The pressure gauge was inserted in the tubing and lowered to approximately 50 feet above the fracture. Except for intermittent operation during very high flow rates, an excellent pressure record was obtained. Several flow rate changes were made in the pumping program and the resulting changes in bottom hole pressure can be seen on the pressure records (Fig. II-8).

The Carlson C-1 experiment was a 2-step procedure. The breakdown portion on March 7 used 18,700 gallons of 3% KCL gelled water from steam cleaned tanks to enhance the probability of being able to see with the Amoco camera. Instrumentation included the SEPS, the 3-axis geophone package and the Hewlett-Packard recording pressure gauge.

The SEPS utilized the well casing for the current injection probe for both steps of the procedure. Figure II-9 illustrates the SEPS layout at the Carlson well for both steps of the procedure. Data acquisition for Step 1 (break-down) on the SEPS began at 08:58 and continued at 11:50. Breakdown occurred at 09:12, and after a shutdown at 10:27, pumping continued until 12:05. Due to a failure in communications, the SEPS was not active after the shutdown period.

Data acquisition on the SEPS for the main fracture on March 8 (Step 2) began at 09:00 and continued until 11:35. Flow began at 09:13 and continued until 11:07. Flow rates ranged from 21 to 34 BPM. Analysis of the SEPS data failed to indicate a definite fracture orientation; however, again a general North-South symmetrical fracture could be interpreted from the data.

The 3-axis wall-clamp geophone package was located in the lubricator above the fluid insertion point before main fracture pumping started.

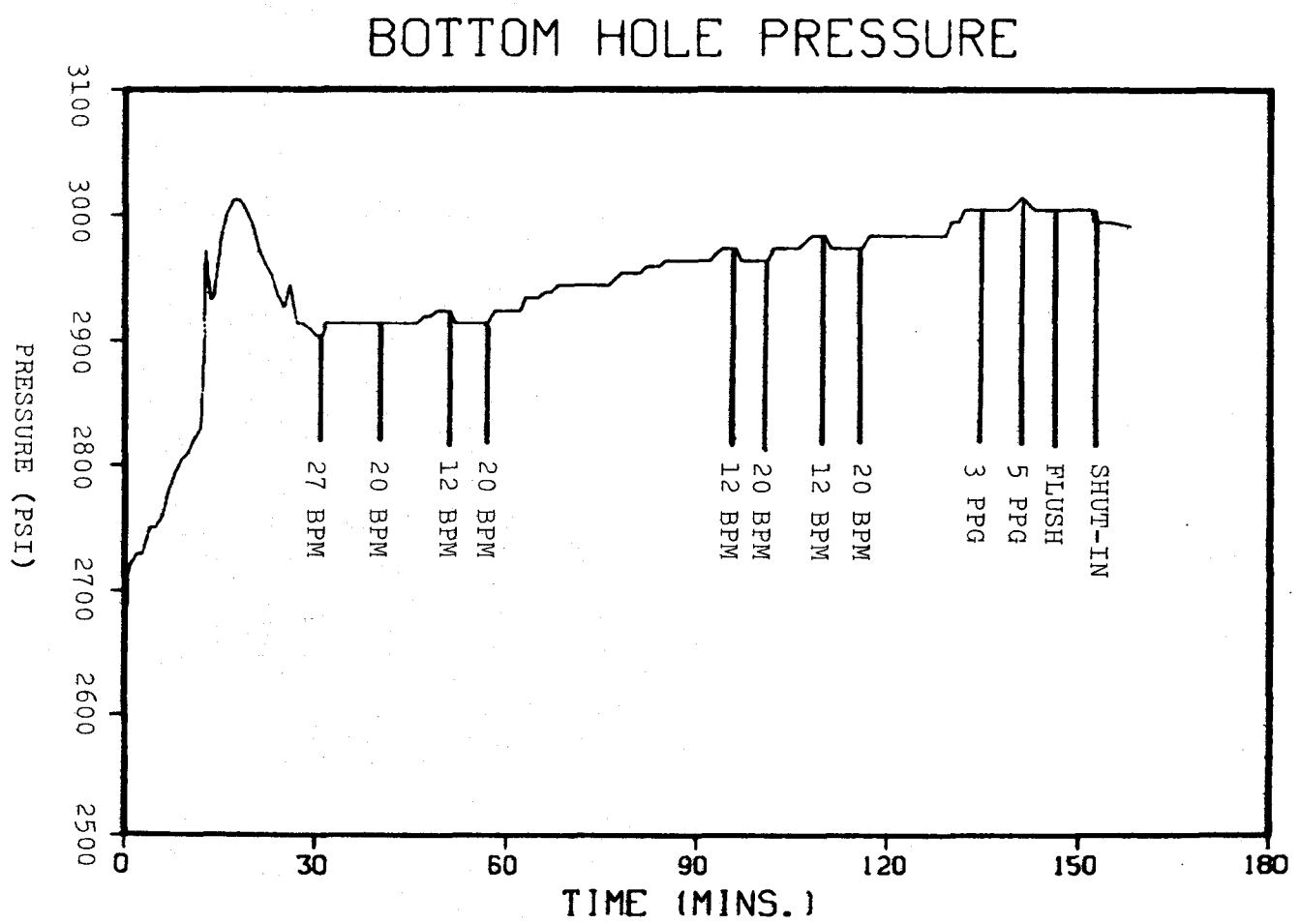

Fig. II-8 Downhole Pressure Jeffers Well No. 1

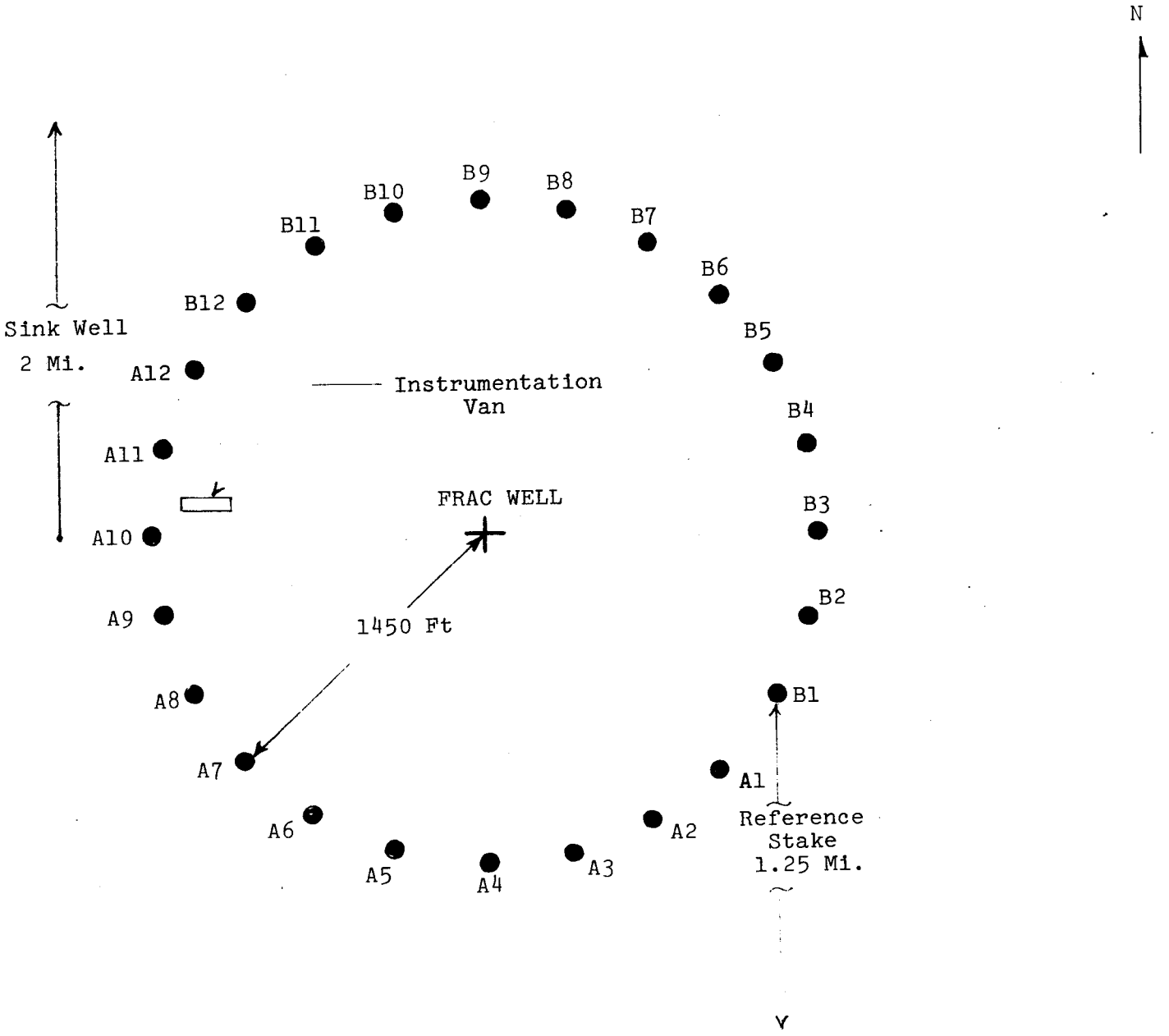

Fig. II-9. Carlson C-1 Well

Immediately following shut-in, the package was landed 50 feet above the cashing shoe and clamped in place. Data was acquired for approximately 6 hours.

B. Borehole Seismic System

The borehole seismic system was fabricated using commercially available components where possible. These components were integrated into an overall system that would allow operation of a single conductor wire line. The single conductor wire line provides power to the electronics, control to the clamping arm, monitoring circuitry for the clamping arm, and the return path for the multiplexed output from the geophones. The lower section of the system is the orientation package which contains its own power supply package, camera, and orientation unit. Either of two orientation units can be used: 1) a compass unit for operation in an open hole, and 2) a gyroscopic unit for operation in a cased hole. The configuration and dimensions of this system are shown in Fig. II-10. The system is 3-5/8" in diameter and up to 16 feet long and is capable of being clamped into boreholes from 4-1/2" up to 15" in diameter.

Two horizontal and one vertical geophone produced by Mark Products (Model L-25A) were selected for use in this system. The output of these geophones is amplified by a specially designed amplifier, each of which then feeds a voltage controlled oscillator (VCO). The three geophone VCO signals are multiplexed with a VCO signal that monitors the clamp arm operation and then transmitted to the surface. Figure II-11 is a block diagram of the downhole system. The geophone VCO's are standard IRIG frequencies and allow a 2 KHz bandwidth signal to be transmitted to the surface from each geophone. Magnetic tape recordings at the surface are made to allow for future data analysis. The entire system has been pressure tested and found to operate satisfactorily up to pressures of 12,000 psi.

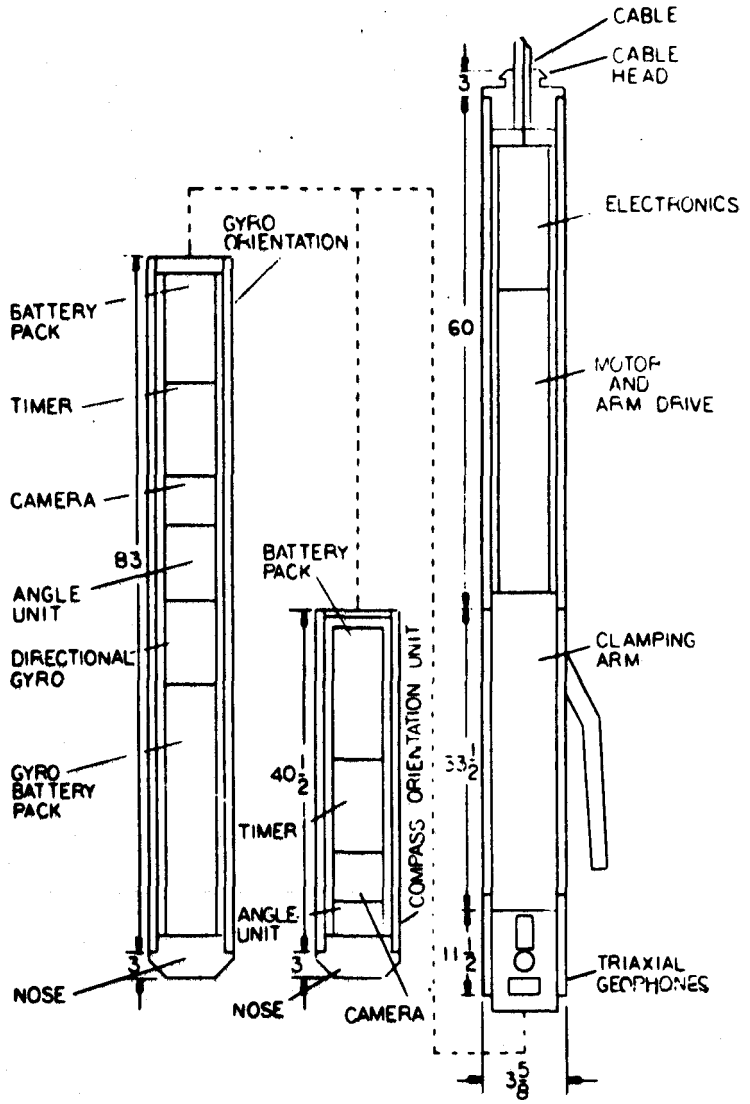

Fig. II-10 Borehole Seismic System Configuration and Dimensions (inches)

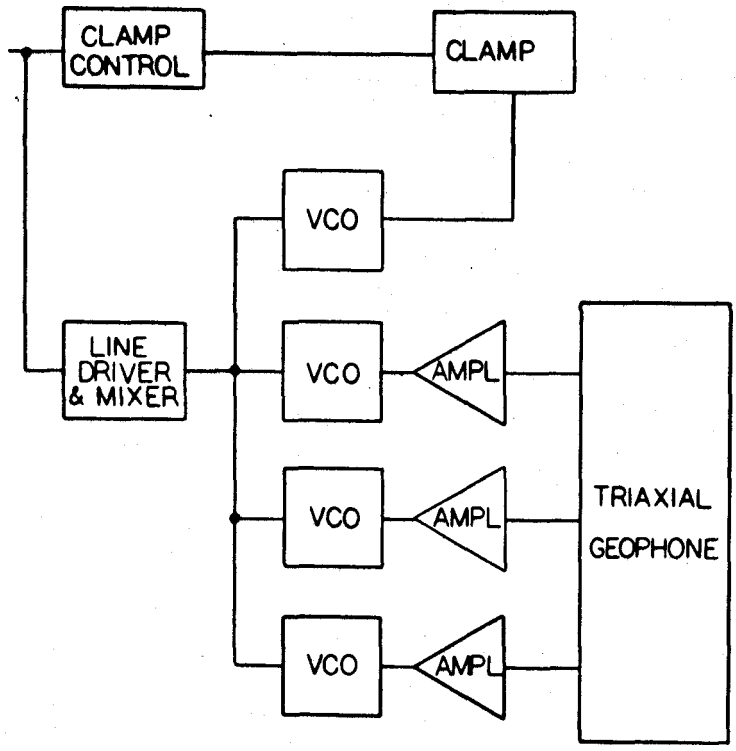

Fig. II-11 Block diagram of the borehole seismic system

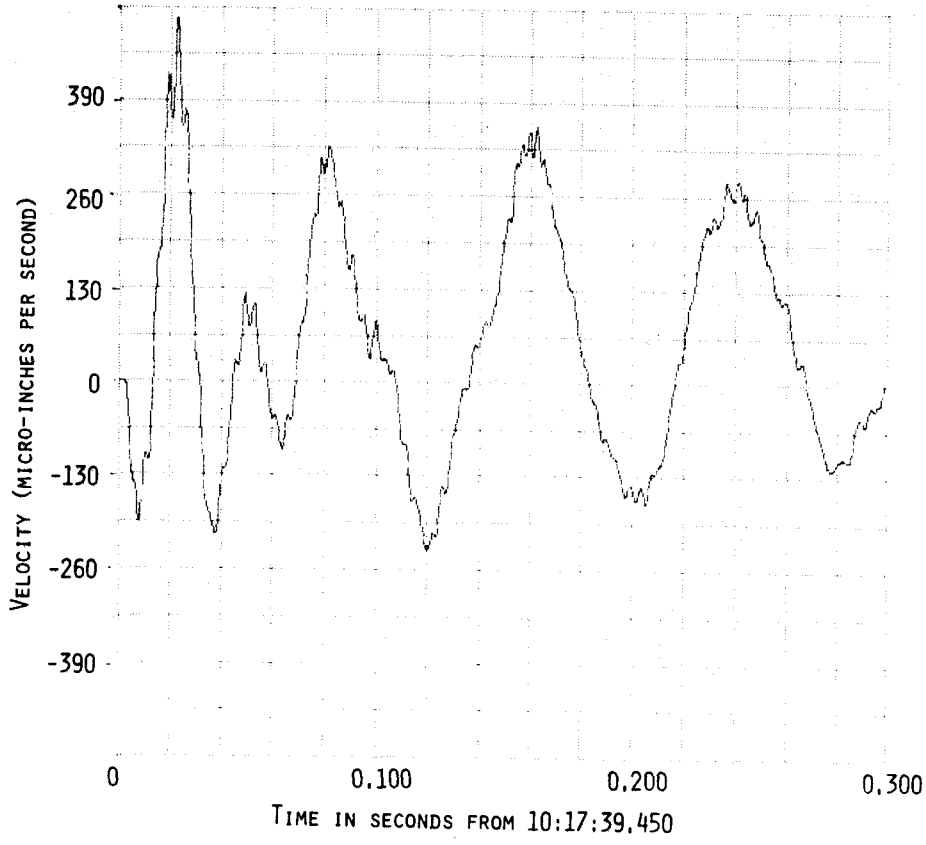

Fig. II-12 Test #1 example of low frequency oscillation

In January of 1978, Sandia Laboratoies participated in the first fracturing experiment utilizing the wire line seismic package with Amoco in the Wattenberg area. Amoco had drilled and completed a hole into the Sussex formation with an open hole completion. The borehole seismic package was lowered and clamped in position in the open hole section prior to the initiation of pumping from the surface. The package remained in the hole during the entire breakdown pump, which contained only fluid and no proppant. The breakdown pump was divided into three 5000 gallon phases after the initial breakdown was achieved with a quiet period inserted after each phase. A quiet period was also inserted immediately after the breakdown and also during flow-back. Any amount of fluid flow caused sufficient seismic disturbances that seismic signals in the presence of the noise would have been undetectable. During the shutdowns, several seismic signals were observed.

The seismic signals observed appeared to fall into three classes or categories of signals. The first category appears to be a high frequency impulsive type of signal which is arriving at the geophone package and causing either the geophone or their mounts to go into a resonance mode of oscillation. The origin of these impulsive signals is not understood but has been speculated to be caused by either thermal cracking, fault slippage along the fracture face, or closing motions of the fracture face. If the resonance problems in the geophones and mounts could be resolved, then the direction to these signal sources could be determined, and if a P-wave and S-wave is present, the distance to the origin could also be determined.

The second category of signals appears to be associated with these impulsive signals but has evidently had the higher frequencies attenuated to a low enough level as not to cause the packages to go into resonance. These signals appear to have created pressure waves

within the fracture edges and oscillating from one end to the other, or from the top to the bottom of the fracture. If this supposition is correct, the frequency of the oscillations can be directly related to the fracture height and fracture length. That is, a pressure wave would travel through the fracture as an increase in pressure until it reached a boundary. Here it would be refracted as a decrease in pressure. Thus, one cycle of pressure change would require two transverses of the fracture face. Figures II-12 and 13 are examples of this oscillatory type signal. The supposition is that the low frequency component (Figure II-12) is governed by the fracture length and the higher frequency (Figure II-13) by the fracture height. If one uses a velocity of propagation for fluids slightly reduced because of the containment, the approximate fracture size is 75 x 250 feet.

An interesting side note is that the size did not change dramatically between pumps. Apparently, the total size was essentially achieved during the initial 5000 gallon phase and the next two pumps only inflated the original fracture.

The third category of signals occurred only following the shut-in after breakdown occurred. These signals appear to be measuring the near field fracture displacements as the fracture is closing during shut-in. The fracture orientation obtained by wellbore televiewer agrees with the orientation obtained by these displacements. Figure II-14 is a representative example of this seismic motion. If one integrates the area under the curve of particle velocity, one obtains the displacement; this displacement is on the order of one microinch for each of these signals. With a total of approximately 100 signals during this shut-in period, total fracture face motion is probably in the neighborhood of 100 microinches. This appears to be a quite reasonable number and could be accounted for by fracture tip extension or leak-off from the fracture face.

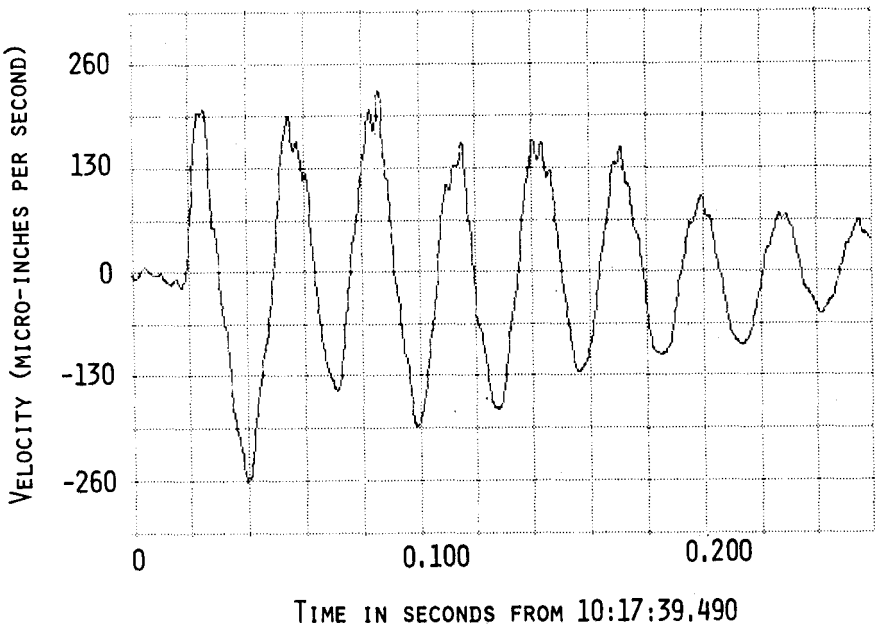

Fig. II-13 Test #1 example of high frequency oscillation

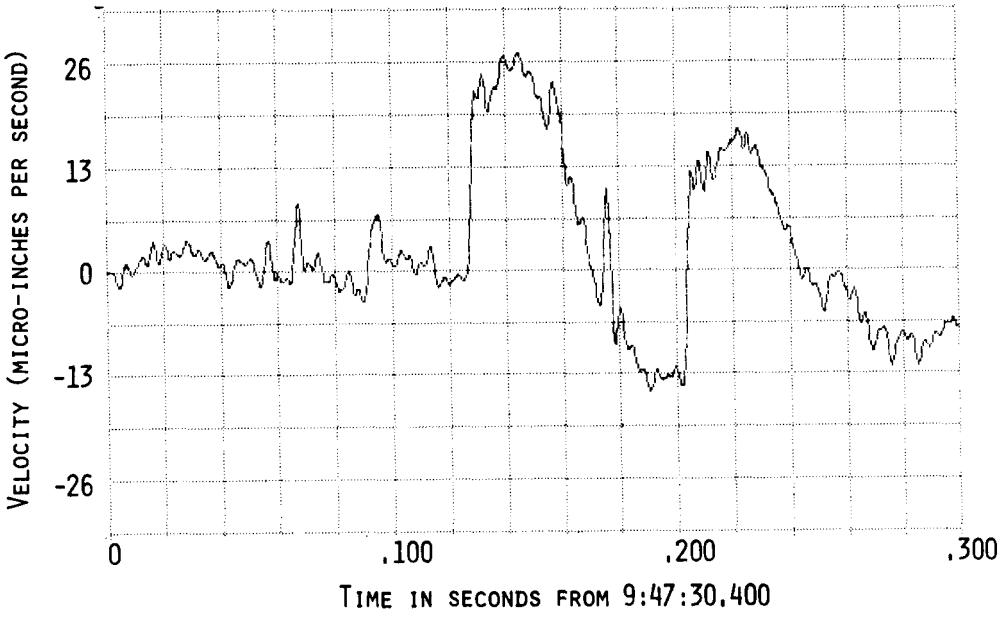

Fig. II-14 Test #1 example of near field displacement signal

The second experiment using the borehole seismic system was conducted in March of 1978. Amoco again provided a well for this fracturing experiment. The seismic system was located in a lubricator above the wellhead during the main fracture pump of approximately 124,000 gallons of fluid, and 228,000 pounds of sand. At the conclusion of the main pump, the borehole seismic package was lowered to a depth of 50 feet above the fracture interval in the cased portion of the hole. The system was then clamped into position and data recording initiated. During the data recording period, no flowback occurred as the well was shut-in. Data recording continued for six hours after the system was emplaced. During that time, numerous signals were recorded that appeared to be similar to the category 1 and 2 signals seen during the first experiment. It should be noted that the category 3 signals were only seen in the first experiment after a small volume of fluid had been pumped for the initial breakdown and were not seen after 5000 gallons had been pumped. On this experiment, none of these signals were found after the entire pumping operation was completed. The category 2 signals that occurred in this experiment arrived at the geophones with a different orientation relative to the geophone mount compared to Test No. 1. As the apparent orientation of these signals changed, it suggests that the signals are external to the seismic system and not related to the method of mounting. Figure II-15 is an example of one of the signals received during the second experiment. The frequency of this signal suggests that it was created by the fracture oscillating from the top to the bottom of the fracture with a fracture height of approximately 50 feet.

Apparently, several types of seismic activities are associated with massive hydraulic fracturing. The occurrence of these seismic activities should provide a useful means for evaluating fracture geometries. By using a wire line seismic system that is located near the fracture interval, these signals can more readily be recorded for

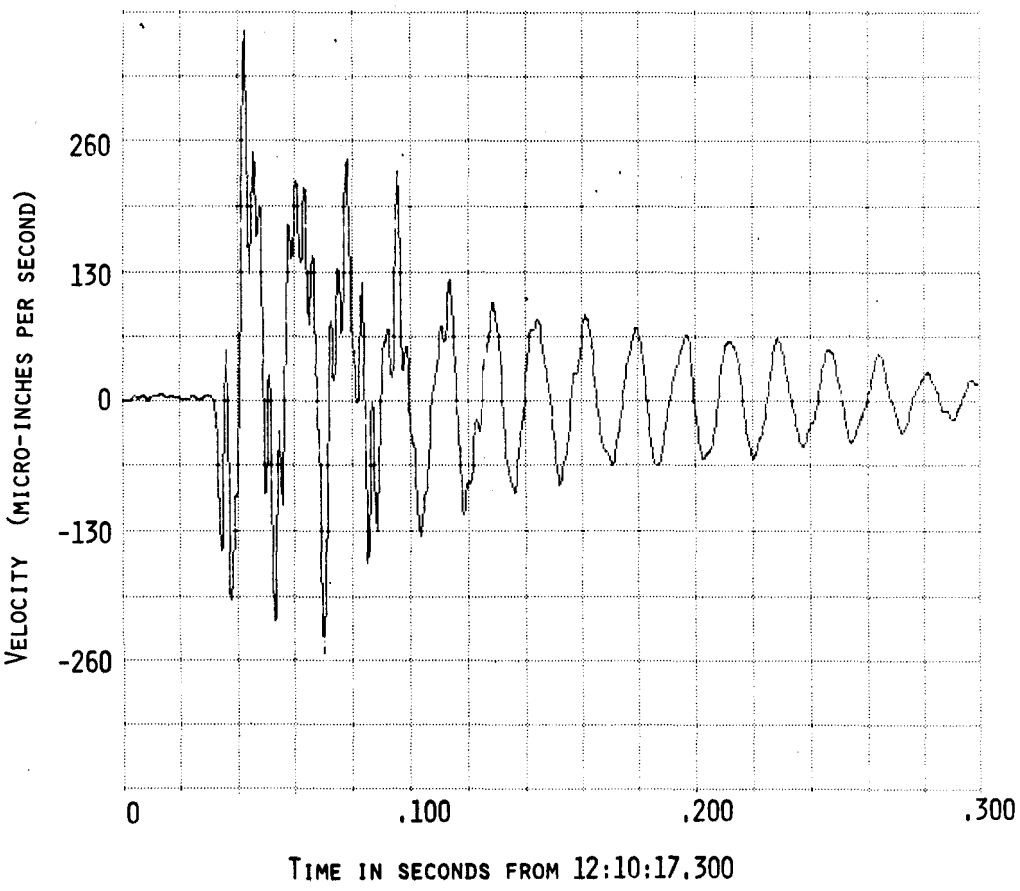

Fig. II-15 Test #2 example of high frequency oscillation

analysis. The preliminary conclusions based upon two experiments suggest that fracture orientation can be determined and that the fracture height and length may also be determined. These assumptions need to be verified continuing the test and evaluation program. The implications of determining fracture orientation using the wire line tool surely is an intriguing idea for the future planning of well locations in a field to be developed utilizing massive hydraulic fracturing.

C. N.T.S. Seismic Signal Analysis

During August 1977, a hydraulic fracture experiment was conducted at the Nevada Test Site.[1] The formation to be fractured was located adjacent to a tunnel complex that allowed for the installation of a seismic array. Four stations with three-axis geophones were located approximately 200 feet from the bottom of the wellbore that was fractured.

The design called for four seismic locations located on a 50-foot square with three orthogonally mounted geophones at each location. These holes were drilled from the tunnel complex, the geophones were located and oriented and then grouted into position with an impedance matching grout. Geophone signal leads were brought from the boreholes into amplifiers located in the tunnel and their outputs multiplexed to a recording system located at the tunnel face. Figure II-16 shows a plan view of the existing tunnel, the borehole, and the geophone location.

The hydraulic fracture was conducted from the surface of the mesa into an open-hole section of the wellbore. The bottom portion or rat hole had been filled with pea gravel and a packer set at a depth of 1352. This allowed for an open-hole section of 6 feet for the hydraulic fracture. Fracture design called for a pad of 1200 gallons

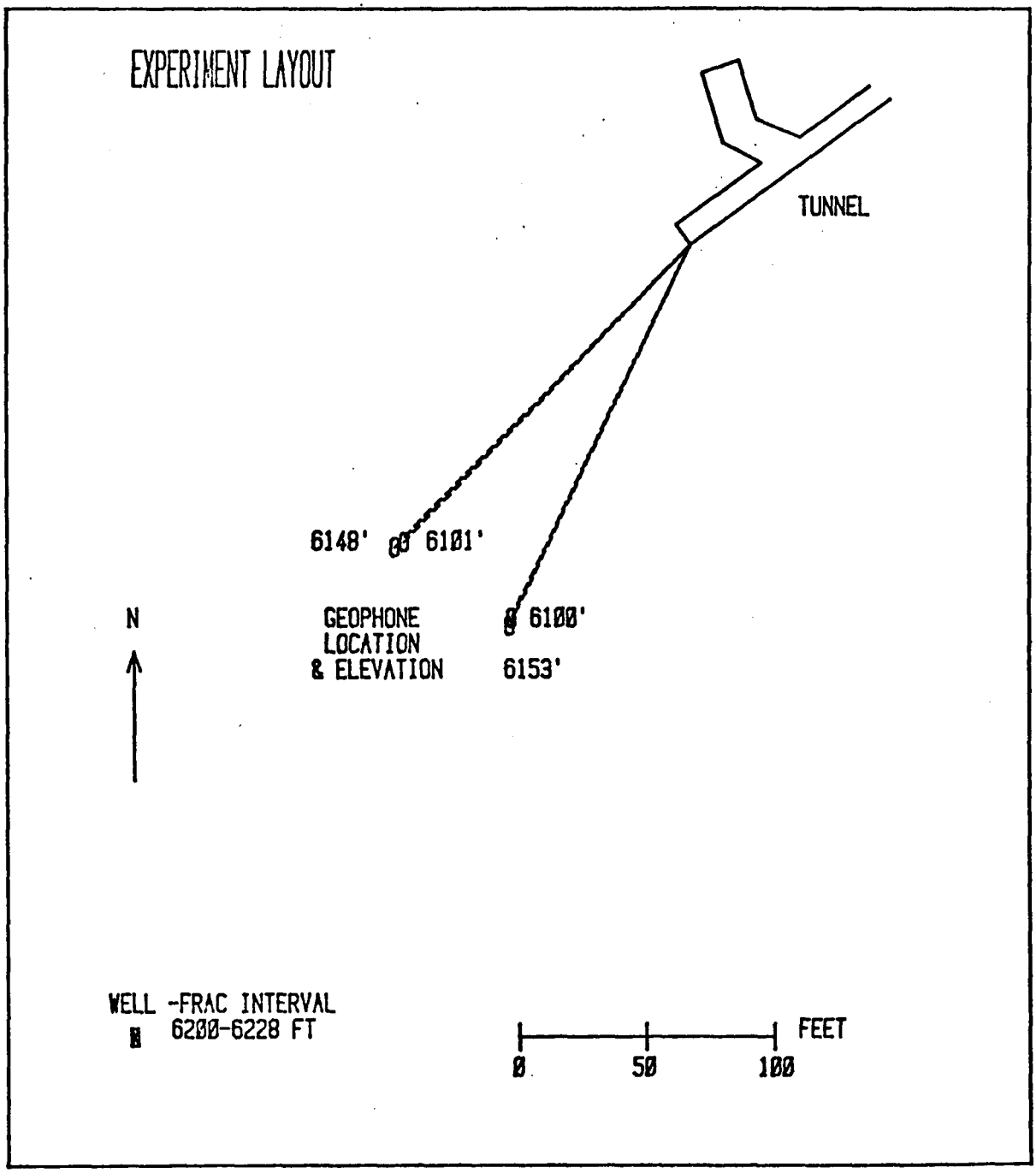
EXPERIMENT LAYOUT
TUNNEL
6148'
6101'
6100'
N
GEOPHONE
LOCATION
& ELEVATION
6153'
WELL -FRAC INTERVAL
6200-6228 FT
FEET
0
50
100

Figure II-16

followed by two pumps of 4000 gallons each with different colored grout. The design of the fracturing experiment was such that the mineback could locate the fracture and determine if it had remained within the ashfall tuff zone or had fractured out of zone into a welded tuff zone.

Seismic recordings were made prior to, during and after the hydrofrac pumping. The downhole pressure, flow rate, and seismic events during the pumping period are shown in Figure II-17. As can be seen from the flow rate, there were several shut-ins during the experiment due to equipment problems on the surface.

A very interesting and important result of the seismic signals detected was that they only occurred during pumping intervals. The seismic signals recorded in Fig. II-17 are only the signals that were readily detectable above the noise level on analog playback records. This level is estimated to be 10 microns per second of amplitude. An example of one of these signals received at a three-axis geophone location is shown in Figure II-18. The arrival of the P-wave and S-wave is pointed out in this figure. As can be easily seen, the S-wave energy is considerably higher than the P-wave energy. For analysis of these signals, it is necessary to determine both the P-wave and S-wave velocities in medium where the seismic signals are created. These velocities were determined prior to the hydrofrac experiment by using hammer blows in the tunnel and recording seismic propagation times. With three-axis geophones located at four locations, several techniques can be utilized for locating the seismic source. These techniques utilize the P-wave and S-wave velocities from single stations or in combinations of stations.

The arrival times of the P-waves and S-waves cannot be determined at present by a computerized method. The best method appears to be by trained individuals determining the first breaks in the seismic records. This results in a rather arbitrary selection of arrival times.

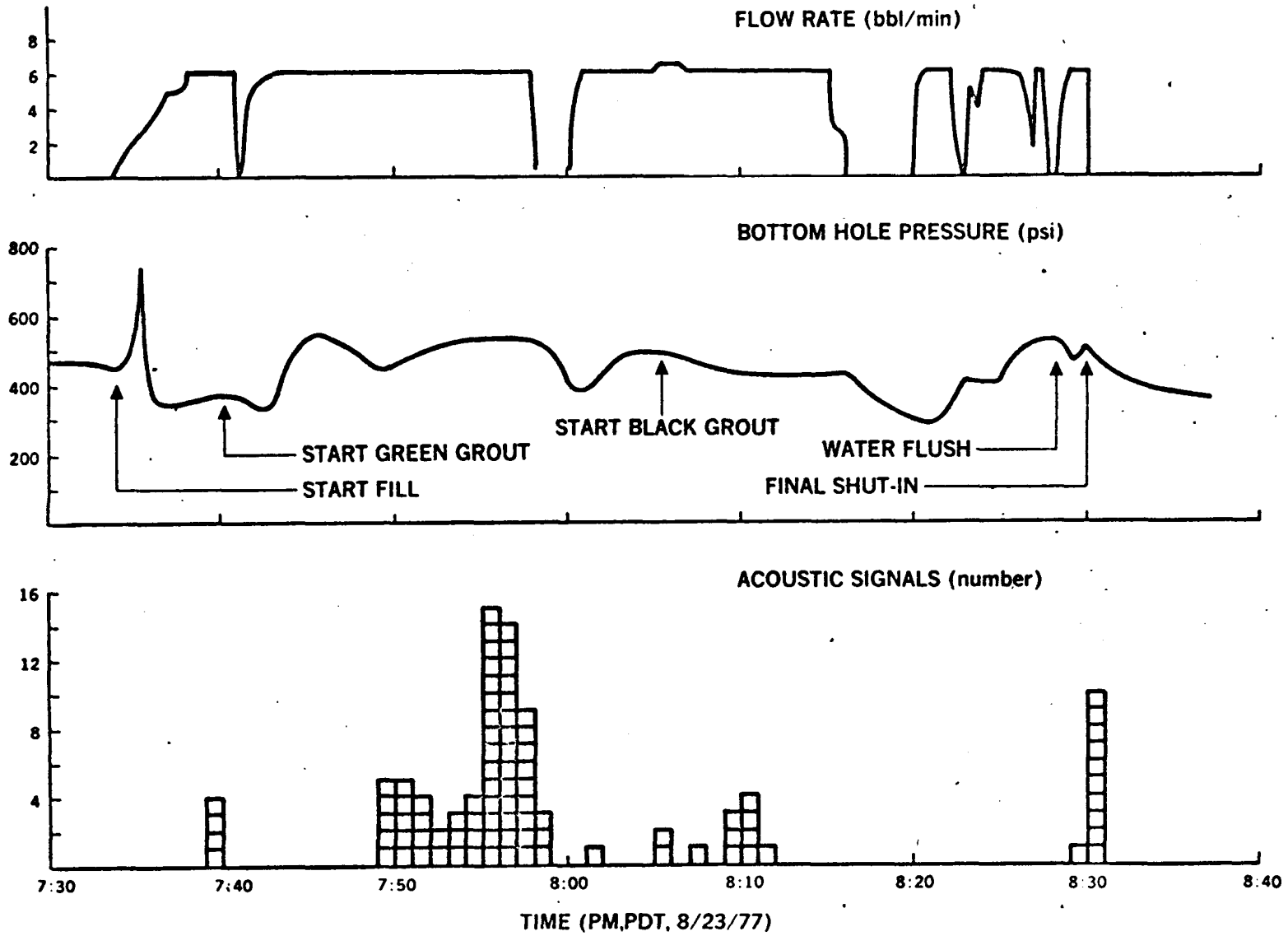

Figure II-17 Hole 6 - Formation Interface Test, Lower Frac

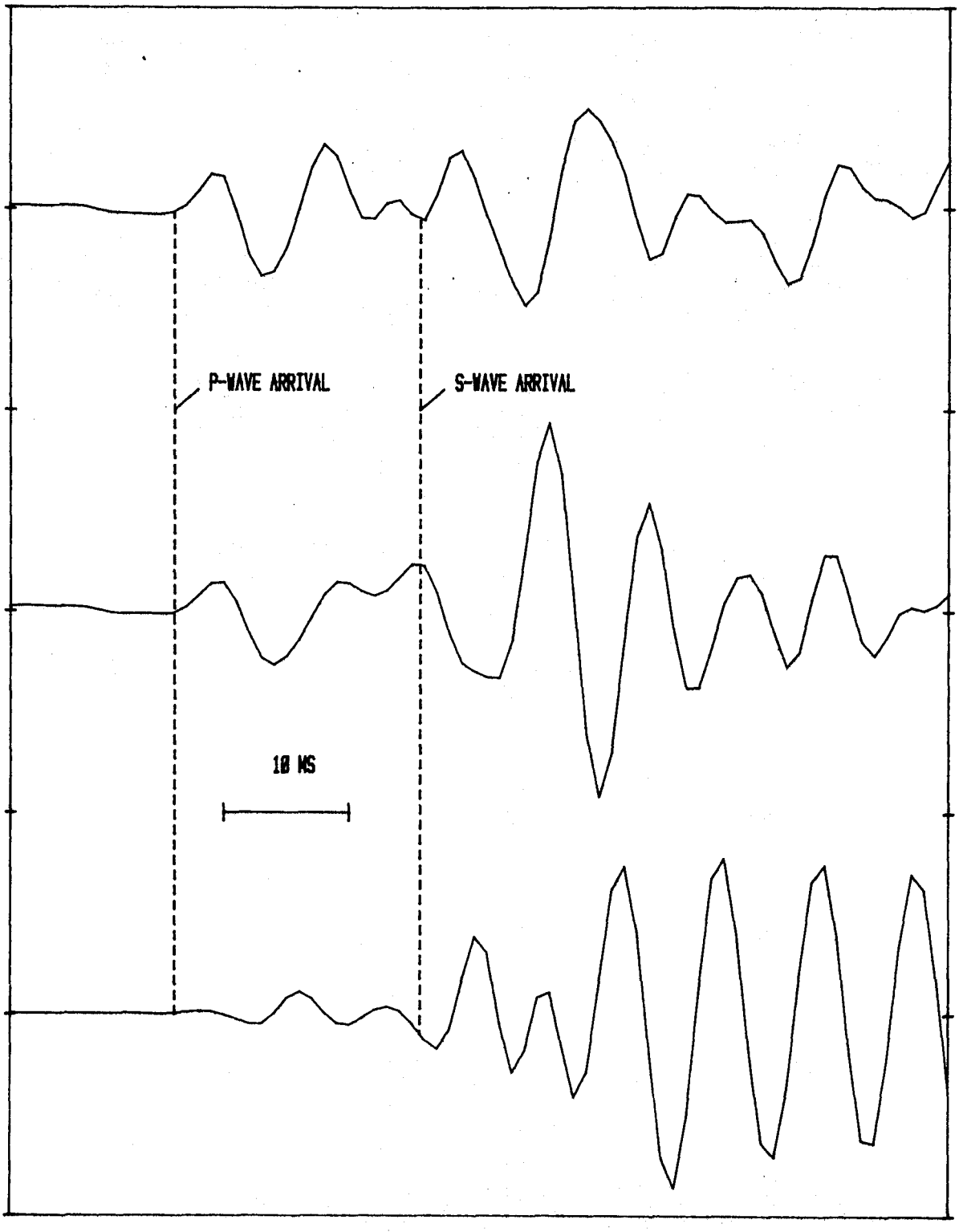

Figure II-18. Typical Seismic Signal Received During Hydraulic Fracturing on Hole #6 Experiment

The vector solution to the P-wave arrivals can be somewhat automated by computing the Lissajous pattern of the arriving P-wave. One difficulty that was encountered during the analysis for location of seismic sources was the small dimension of the geophone array relative to the distance to the seismic source and the large dimension of the hydraulic fracture. On future experiments, a seismic recording array will be sized to allow for larger baselines and be placed in better position relative to the fracture design.

The most successful method of data analysis turned out to be the P-S wave solutions from four stations when all four solutions were in good agreement. The measure of success was the lack of scatter in the data and a source location that agreed with the true location as determined by the mineback. Although it is believed that the source signals were not originating from the induced hydraulic fracture but to the side of it, this small discrepancy could not be seen in the dispersion of the data. The results of this analysis are shown in Figures II-19 and 20. Overlying the data plots are the actual locations that were observed in the mineback phase. As can be seen, these locations would be adequate to guide a mineback program or a coring program for locating hydraulic fractures.

During the mineback, several natural fractures were observed which were crossing, or at high angles to, the induced fracture. Some of these natural fractures contained fracture fluid and are believed to be the cause of the majority of the seismic signals observed. As the natural fracture became lubricated with the frac fluid and the in-situ stress field being oriented according to the induced fracture, the state of stress on the natural fracture would allow for fault slip type of motions along these natural fractures. These fractures were observed to be a few centimeters in length up to possibly 10 meters in length. This appears to agree quite well with the interpretation of the seismic data.

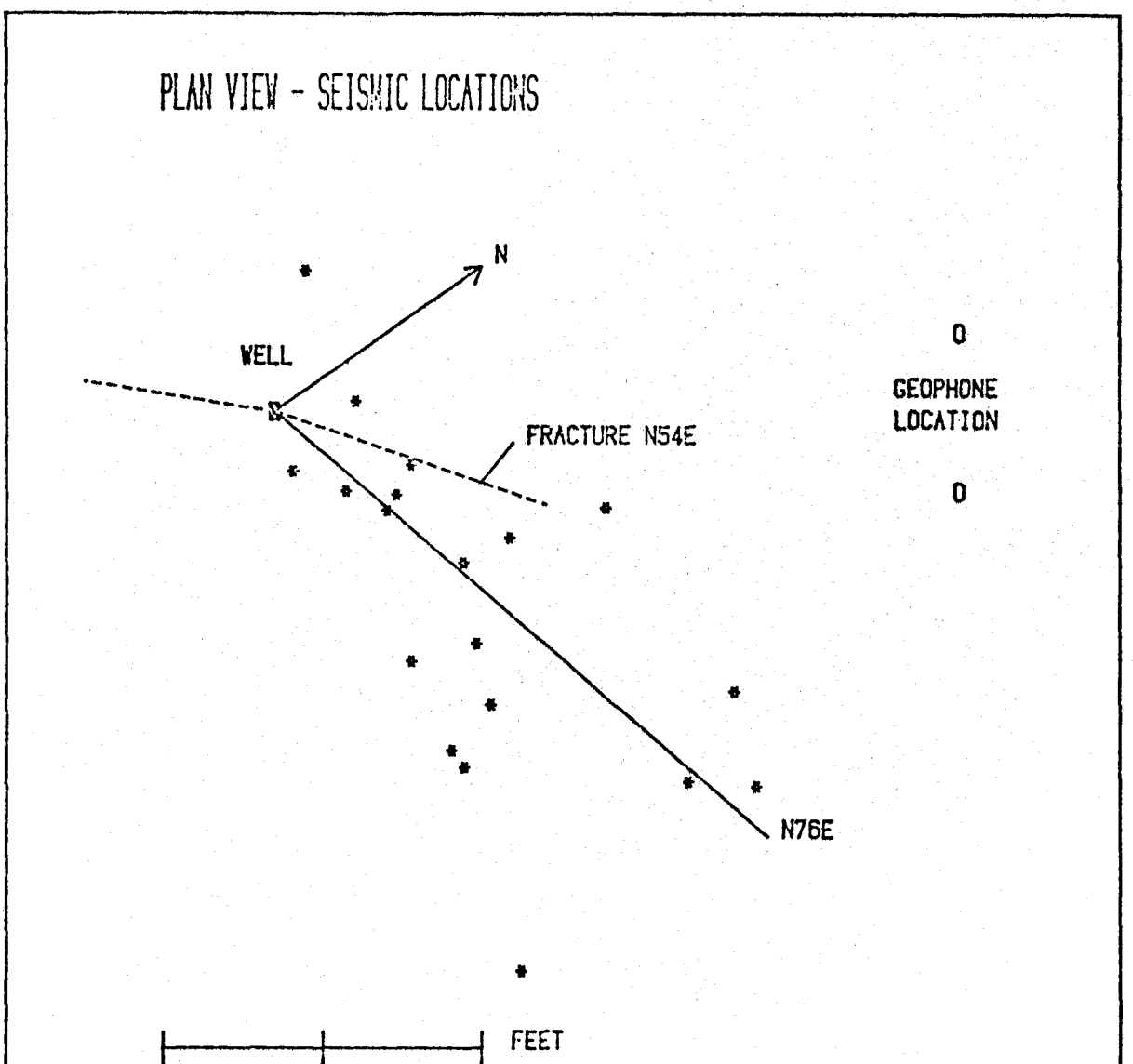
PLAN VIEW - SEISMIC LOCATIONS
N
WELL
FRACTURE N54E
GEOPHONE
LOCATION
N76E
FEET
0
50
100

Figure II-19

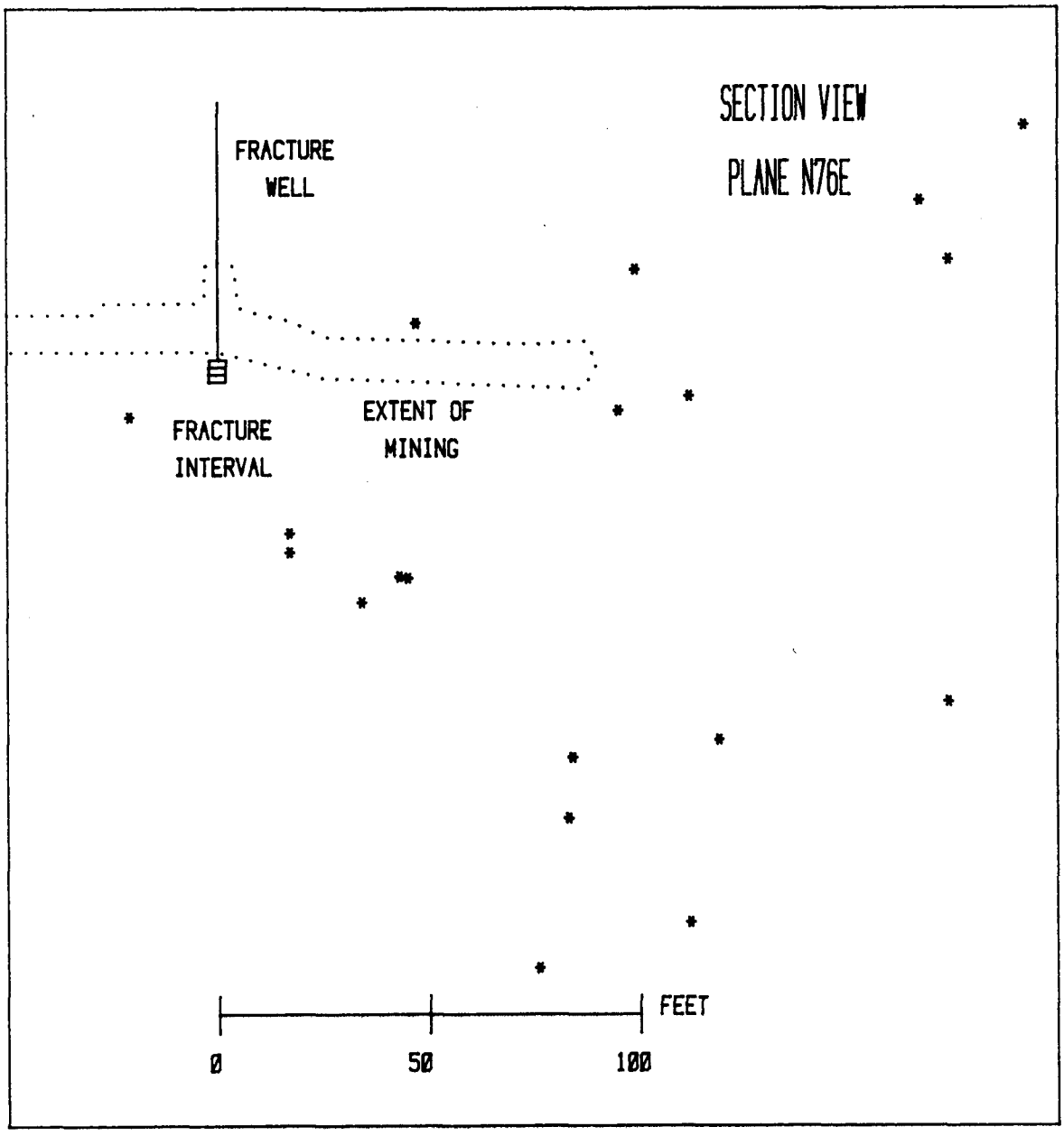
SECTION VIEW
PLANE N76E
FRACTURE
WELL
FRACTURE
INTERVAL
EXTENT OF
MINING
FEET
0
50
100

Fig. II-20

Future experiments will take advantage of the insight gained from this experiment where the base leg of the seismic locations was too short relative to the fracture dimensions. A much longer base leg with comparable dimensions to fracture lengths would have been more desirable from an accuracy of source location standpoint.

D. Downhole Stacked Hydrophone System

The idea of using compressional waves as an aid in the investigation of oil and gas formation is not new. It was established early that the compressional wave propagation velocity depends on the lithology and porosity of a formation.[2] One of the basic tools used as an aid in determining formation porosity and helpful in interpreting seismic records has been the acoustic velocity log. The log is a recording, as a function of depth, of the time required for a compressional acoustic wave to travel a unit distance of formation. There are various configurations of the velocity logging tool, however, the basic tool consists of a transmitter and two receivers, both incorporated in the logging tool. The prime measurement is the difference in time between the arrival of acoustic signal at the receivers. The acoustic wave radiates outward from the transmitter. In addition to traveling through the borehole with the propagation velocity dependent on the characteristic of the drilling mud, the wave is refracted at the formation interface and travels through the formation with a velocity which is dependent on the lithology and porosity of the formation. In general, acoustic wave velocity is higher in the formation than in the drilling mud, and in measuring from first arrival times the propagation velocity in the formation can be determined. The depth of penetration of the acoustic wave into the formation is a function of transmitter to receiver spacing. Deeper formation penetration is realized with an increased distance between transmitter and receiver. Measurements in the past have indicated that the acoustic velocity in the invaded zone

around the well can be substantially different from that in the deeper uncontaminated zone.[3] Therefore, it is desirable to extend the spacing to the maximum possible length. An acoustic velocity system making use of this principle is being constructed for evaluation and test.

The system includes a continuous acoustic single frequency transmitting source at the surface and a linear array of hydrophone transducers, used as receivers, downhole. The frequency source at the surface transmits a monofrequency signal through the formation which is received by the downhole hydrophone array. The phase and amplitude differences between the hydrophone receivers are measured. Propagation velocity through the formation is obtained from the phase difference measurements. Measurements of amplitude differences should provide information on attenuation through the formation. The control and recording system at the surface consists of a desk-top size computer capable of interfacing with and controlling the acoustic signal source, a gain-phase meter, and other peripheral devices including a printer and plotter.

In addition to formation diagnostics, the hydrophone system under development will be evaluated for downhole detection of passive acoustic signals for the purpose of hydraulic fracture diagnostics. Early experiments in techniques to detect and map hydraulic fractures have shown that acoustic signals in the 100 to 2,000 Hz frequency range have been detected by a downhole hydrophone immediately following a hydraulic fracturing operation.[4] At the conclusion of pumping, these signals continued at about a constant rate throughout a 30 minute period while the well was shut-in. Only one detector was employed therefore, it was not possible to obtain information on source locations. Because of fracture depth the seismic or acoustic signals produced by a fracture, when measured at the earth's surface, have such a low signal-to-noise ratio that their detection is highly improbable.[5] Signal detection from

fractures thus requires that the sensor receivers be deployed near the fracture source.

Most of the receiving and recording part of the system is on hand. The design specification for the downhole hydrophone package has been completed and development contracts let for the fabrication of six hydrophone transducers. The downhole hydrophone package consists of a stainless steel rod approximately 30 feet in length and 1.5 inches in diameter. The stainless steel rod contains four hydro-acoustic transducers spaced at 10 feet intervals. The electronics for the transducers includes an acoustic amplifier, a constant-bandwidth voltage controlled oscillator (VCO), and a mixer-line driving amplifier. This is contained in the section of rod between the top two transducers. The electrical power required for the downhole package is supplied from the surface through a single conductor armour shielded cable. The frequency multiplexed VCO signals from the downhole package are carried to the surface by the same cable. The signals are recorded at the surface on magnetic tape. Subcarrier discriminators separate each hydrophone signal and time differences of fracture related signals are determined. The time difference between the hydrophone receivers give two dimensional signal source locations (no azimuthal control).

The hydrocoustic transducer section of the downhole package is on order and delivery of 6 transducer units is expected in November of 1978. Assembly of the first downhole package is expected to begin in late Fall of 1978.

Although the design and fabrication of the acoustic transducer element in itself is well within the state of the art, the mechanical housing and its design is a task which has not been attempted in the past. Therefore, in order to establish a backup source, 6 transducers have been ordered from a second manufacturer. The approach that each supplier has to the housing of the transducer element and its over-all

strength in the mechanical support are completely different. Both systems will be evaluated. The second system is expected to be ready for assembly in late February, 1979.

References

1. Warpinski, N. R., Northrop, D. A., Schmidt, R. A., "Direct Observation of Hydraulic Fractures: Behavior at a Formation Interface," Sandia Laboratories Report SAND78-1935, October 1978.
2. Pirson, S. J., "Handbook of Well Log Analysis," Prentice-Hall, Inc., Englewood Cliffs, NJ, 1963.
3. Gretener, P. E. F., "An Analysis of the Observed Time Discrepancies Between Continuous and Conventional Well Velocity Surveys," Geophysics, Vol. 26, No. 1, February 1961.
4. Power, D. V., Schuster, C. L., Hay, R., and Twombly, J., "Detection of Hydraulic Fracture Orientation and Dimensions in Cased Wells," SPE 5626, presented at the SPE 50th Annual Fall Meeting, Dallas, TX September 25 - October 1, 1975.
5. McCann, R. P., Hay, R. G., and Bartel, L. C., "Massive Hydraulic Fracture Mapping and Characterization Program, First Annual Report: August 1975 - July 1976," Sandia Laboratories Report SAND77-0286, June 1977.

III. ADVANCED LOGGING AND FORMATION EVALUATION

(T. L. Dobecki, 4733; P. C. Lysne, 2355;
C. N. Vittitoe, 4231)

Currently available borehole logs and analysis techniques have been developed to accommodate the needs of the petroleum geophysicist for the "normal" petroleum reservoir. Physical characteristics of those reservoirs of prime interest to the Enhanced Gas Recovery Program are such that these "normal" reservoirs logs and analysis are not accurate, if at all applicable. Included in these physical characteristics are very low permeability (< 100 microdarcy) and significant shale or clay content. The net result is that permeability determinations from pumping tests are often weeks in duration and that S_w calculations are sorely in error. In response to these problems, Sandia has initiated a research and development program to assess those logs which are currently available, those which are still at a research level, and the basic physics of such logs to determine which, if any, offer promise toward solving the problems posed by such tight, claey formations. To date, our activities have concentrated upon a) basic electrical (non-inductive) logging, b) electromagnetic (induction) logging, c) nuclear magnetism (NML) logging, d) borehole neutronics, and e) acoustic logging. The progress and findings of each individual investigation are presented in the following sub-sections.

A. Electric Logging (Non-Inductive)

Mud filtrate invasion is dependent upon several parameters including, among others, pore size, mud type, and formation permeability. It is felt that an accurate measure of invasion depth as a function of time for a constant hydrostatic head would be a valuable contribution to a scheme for measuring permeability in situ. As the problem usually involves detection of a boundary between waters of different salinity, it is also felt that some variation on electrical resistivity logging tools would be the most attractive approach.

The basic premise is that if layering in the subsurface can be defined through the use of expanding electrode arrays (Wenner or Schlumberger Configuration) on Earth's surface, then this same principle may be applied to an expanding array of electrodes within a borehole in order to measure concentric layering (invaded zone) around the borehole. Inversion of electrical resistivity data taken on the Earth's surface is often accomplished through the use of master curves (e.g. Wetzel and Mooney; Orellana and Mooney; Compagnie Generale de Geophysique) depicting theoretical measured apparent resistivity versus electrode spacing for given thicknesses and resistivity ratios of two-, three-, and four-layered subsurfaces. Comparison of actual field data with the theoretical curves enables interpretation. If a similar set of theoretical curves could be developed for the case of an electrode array within a borehole, this would provide the means of determining the depth of invasion.

In actuality, the borehole plus invaded zone in a thick, homogeneous interval represents three concentric zones of differing electrical resistivity (Figure III-1). These are: Zone 1 (resistivity = ρ_1), the borehole and contained fluids; Zone 2 (resistivity = ρ_2), the invaded zone; and Zone 3 (resistivity = ρ_3), the natural, non-invaded formation. In most modeling calculations, Zone 1 (the "borehole effect") is sometimes neglected. It is felt that, for our purposes, Zone 1 should be included. Therefore, before developing the mathematics for the three-layered system, attention is first directed to the two-layered, or borehole with no invasion, case.

In order to solve for apparent resistivity for a given electrode spacing, it is necessary first to solve for the electrical potential. Referring to Figure III-2, the potential at a point P = P(0,0,Z) on the borehole axis due to axial, point coordinate system, P_o = (0,0,0) is given by

$$V_P = V_o + V_1 \qquad (1)$$

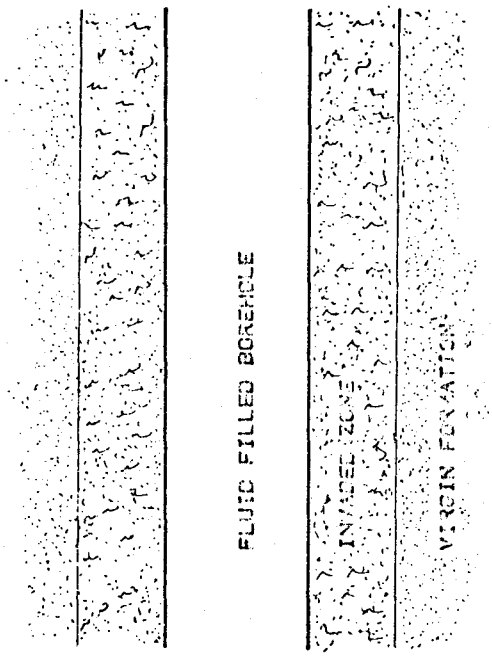

Fig. III-1. Illustration of the three zones of differing resistivity surrounding and including a fluid-filled borehole.

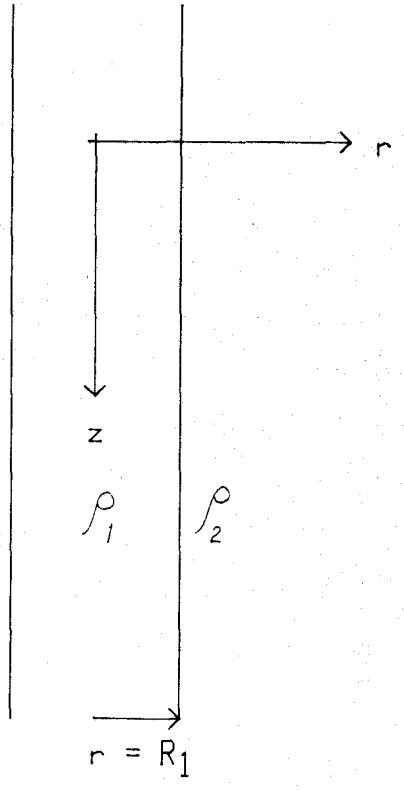

Fig. III-2. Model of two-layered (non-invaded) borehole system. The resistivities are: Zone 1 ($r < R_1$) = ρ_1; Zone 2 ($r \geq R_1$) = ρ_2.

where $V_o = \frac{I\rho_1}{4\pi z}$ is the "normal" potential, and V_I is the perturbing potential due to the boundary at $r = R_1$. The potential at a point in the formation (Zone 2) will be called simply V_2. V_P and V_2 must be solutions to LaPlace's Equation and satisfy certain boundary conditions. LaPlace's Equation in cylindrical coordinates, utilizing the azimuthal symmetry of this problem, is

$$\frac{\partial^2 V}{\partial r^2} + \frac{1}{r}\frac{\partial V}{\partial r} + \frac{\partial^2 V}{\partial z^2} = 0 \tag{2}$$

By separation of variables we seek a solution of the form:

$$V(r,z) = R(r) \times Z(z) \tag{3}$$

Substituting (3) in (2) and dividing by R x Z, we find:

$$\frac{1}{R}\frac{d^2R}{dr^2} + \frac{1}{Rr}\frac{dR}{dr} = -\frac{1}{z}\frac{d^2Z}{dz} \tag{4}$$

For (4) to be valid for all z and r values, each side of (4) must be equal to a constant which will be called, arbitrarily, m^2. Therefore,

$$\frac{d^2Z}{dz^2} = -m^2 z \tag{5}$$

$$\frac{r^2 d^2R}{dr^2} + \frac{r dR}{dr} - (m^2 r^2)R = 0 \tag{6}$$

The solution to (5) is simply:

$$Z = A \cos(mz) + B \sin(mz) \tag{7}$$

but, since the potential should be the same at $z = \pm z$, $B = 0$, or:

$$Z = A \cos(mz) \tag{8}$$

Equation (6) is a form of the modified Bessel's Equation whose solution is:

$$R = C\, I_o(mr) + D\, K_o(mr) \tag{9}$$

Therefore, the solution of the general potential at a point (r,z) is:

$$V = \int_0^\infty (E\ I_o(mr) + F\ K_o(mr))\ \cos(mz)dm\ . \tag{10}$$

Zone 1 contains the points r = 0, and since $K_o(0)\to\infty$, this implies F = 0 for Zone 1. Zone 2 contains the points r = ∞, and since $I_o(\infty)\to\infty$, E = 0 for Zone 2. Therefore:

$$V_p = V_o + \int_0^\infty E\ I_o(mr)\cos(mz)dm \tag{11}$$

$$V_2 = \int_0^\infty F\ K_o(mr)\cos(mz)dm\ . \tag{12}$$

All that remains is to utilize the boundary conditions and solve for E and F. This will not be presented in its entirety; only the boundary conditions and an expansion of 1/z (in "normal" potential term) in cylindrical coordinates will be given.

The boundary conditions are:

$$\text{B.C.(1)}\quad V_p = V_2 \text{ at } r = r_1 \tag{13}$$

$$\text{B.C.(2)}\quad \frac{1}{\rho_1}\frac{\partial Vp}{\partial r} = \frac{1}{\rho_2}\frac{\partial V_2}{\partial r} \text{ at } r = R_1 \tag{14}$$

The expansion of 1/z in cylindrical coordinates which is necessary to apply the boundary conditions is:

$$\frac{1}{z} = \frac{2}{\pi}\int_0^\infty \cos(mz)K_o(mr)dm \tag{15}$$

The resulting solution for E is:

$$E = \frac{I(\rho_2 - \rho_1)}{2(\pi)^2}\Bigg/\left(\frac{\rho_2}{\rho_1}\frac{I_1(mR_1)}{K_1(mR_1)} + \frac{I_o(mR_1)}{K_o(mR_1)}\right) \tag{16}$$

Substituting (16) into (11), we find the final expression for potential measured on the borehole axis for an axial current source.

$$V_p = \frac{I\rho_1}{4\pi z} + \frac{I(\rho_2 - \rho_1)}{2(\pi)^2} \int_o^\infty \frac{K_o(mR_1)K_1(mR_1)\cos(mz)\,dm}{\frac{\rho_2}{\rho_1} I_1(mR_1)K_o(mR_1) + I_o(mR_1)K_1(mR_1)} \qquad (17)$$

We have applied numerical integration for the solution of (17) to determine V_p for a suite of z values and resistivity ratios. From the values of potential measured, it is possible to calculate the apparent electrical resistivity. Figures III-3 and III-4 show derived normalized apparent resistivity ($\rho a/\rho_1$) versus normalized electrode spacing (spacing ÷ borehole radius) for various values of the ρ_1/ρ_2 ratio. The curves look very much like those curves developed for two-layer surface resistivity models except for the overshoot and undershoot of the curves with respect to the final value of the ratio. A similar overshoot has been observed in curves published by Seigel[1] after a Russian translation and by Kunz and Moran.[2] It is felt, then, that the overshoot is a real occurrence. With that, master curves for the two-layer, non-invasion situation have been compiled for both the "normal" (Figures III-3 and 4) and "modified Schlumberger" (III-5 and 6) arrays of borehole electrical probes. For the normal array, the spacing, A, is the distance between the current and potential probes. For the modified Schlumberger array, the spacing, A_o, is the distance from the current probe to the midpoint between the potential probes. Note that the overshoot for $\rho_2/\rho_1 > 1$ (Figure III-3) increases in magnitude as the ρ_2/ρ_1 ratio increases (63% overshoot for $\rho_2/\rho_1 = 100$ versus 107% overshoot for $\rho_2/\rho_1 = 1000$). Also, the peak position of the overshoot is found at greater electrode separations for increased ρ_2/ρ_1 values. This clearly means that for typical borehole fluid-formation resistivity contrasts, the measured value of apparent resistivity only indicates the true formation resistivity if the electrode spacing is large (10-1000X)

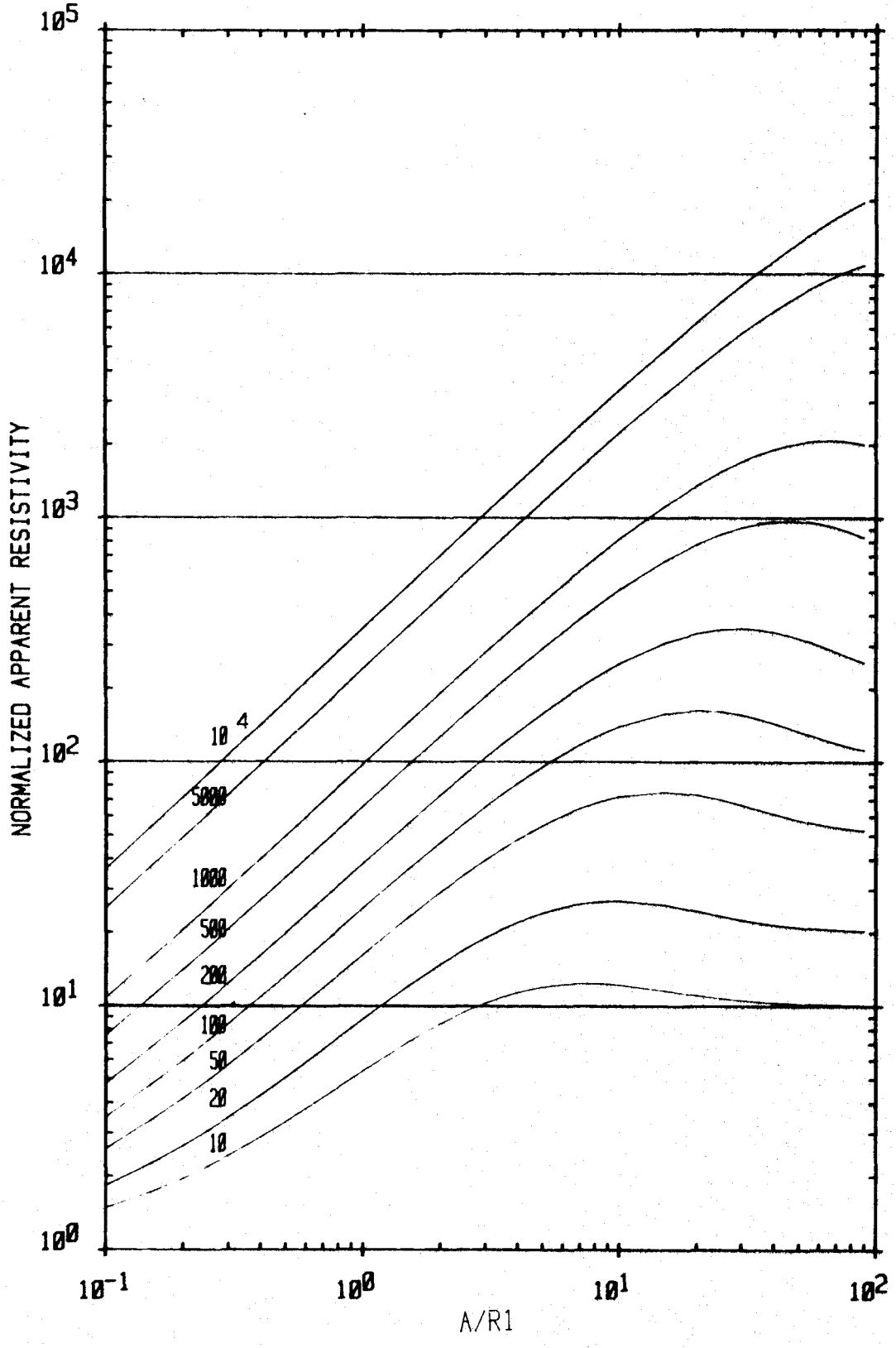

Fig. III-3. Normalized apparent resistivity versus normalized electrode spacing (normal array) for various values of $\rho_2/\rho_1 > 1$. Values of ρ_1/ρ_2 are given beside each curve. A is the current to potential probe distance; R_1 is the well radius.

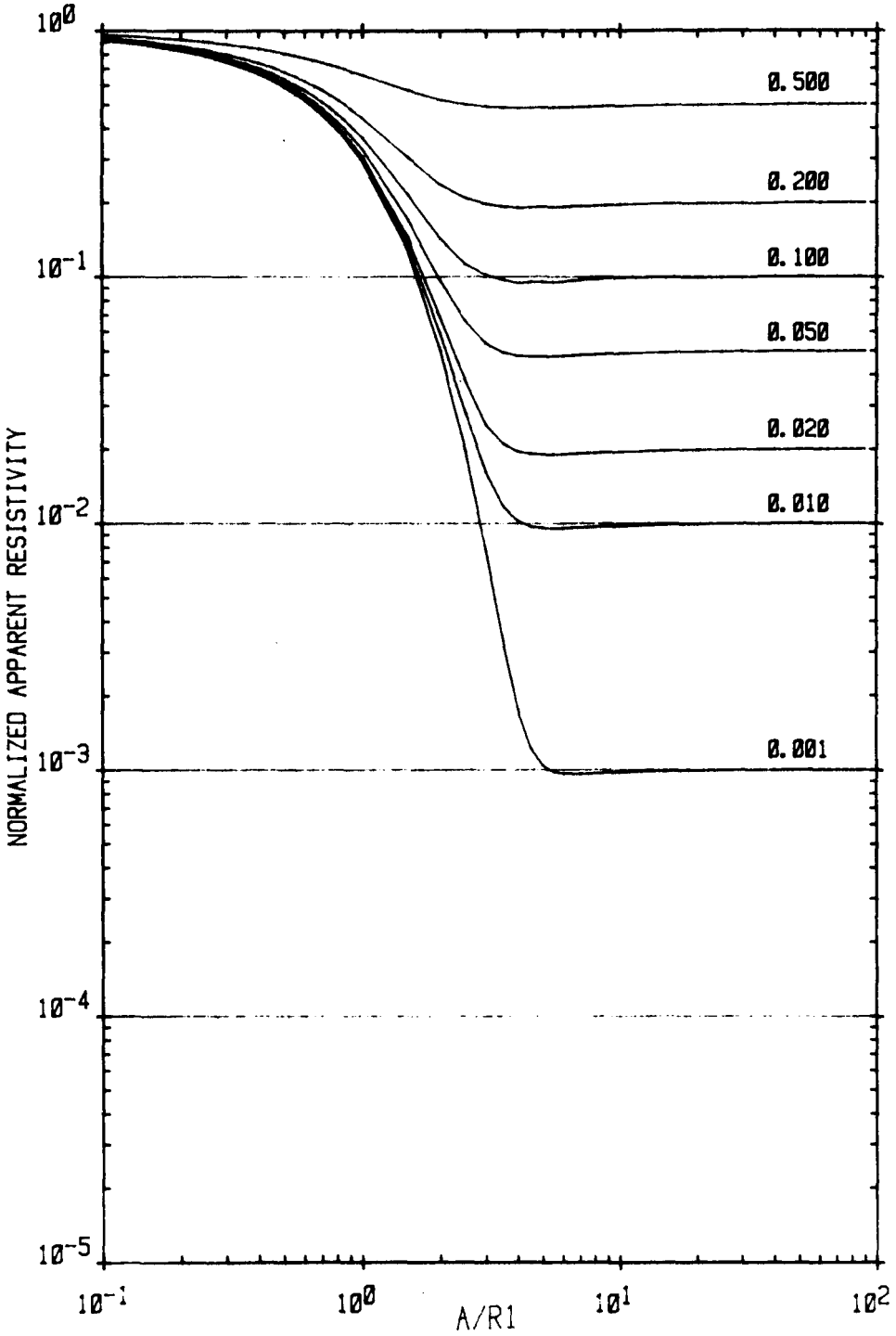

Fig. III-4. Normalized apparent resistivity versus normalized electrode spacing (normal array) for various values of $\rho_2/\rho_1 < 1$.

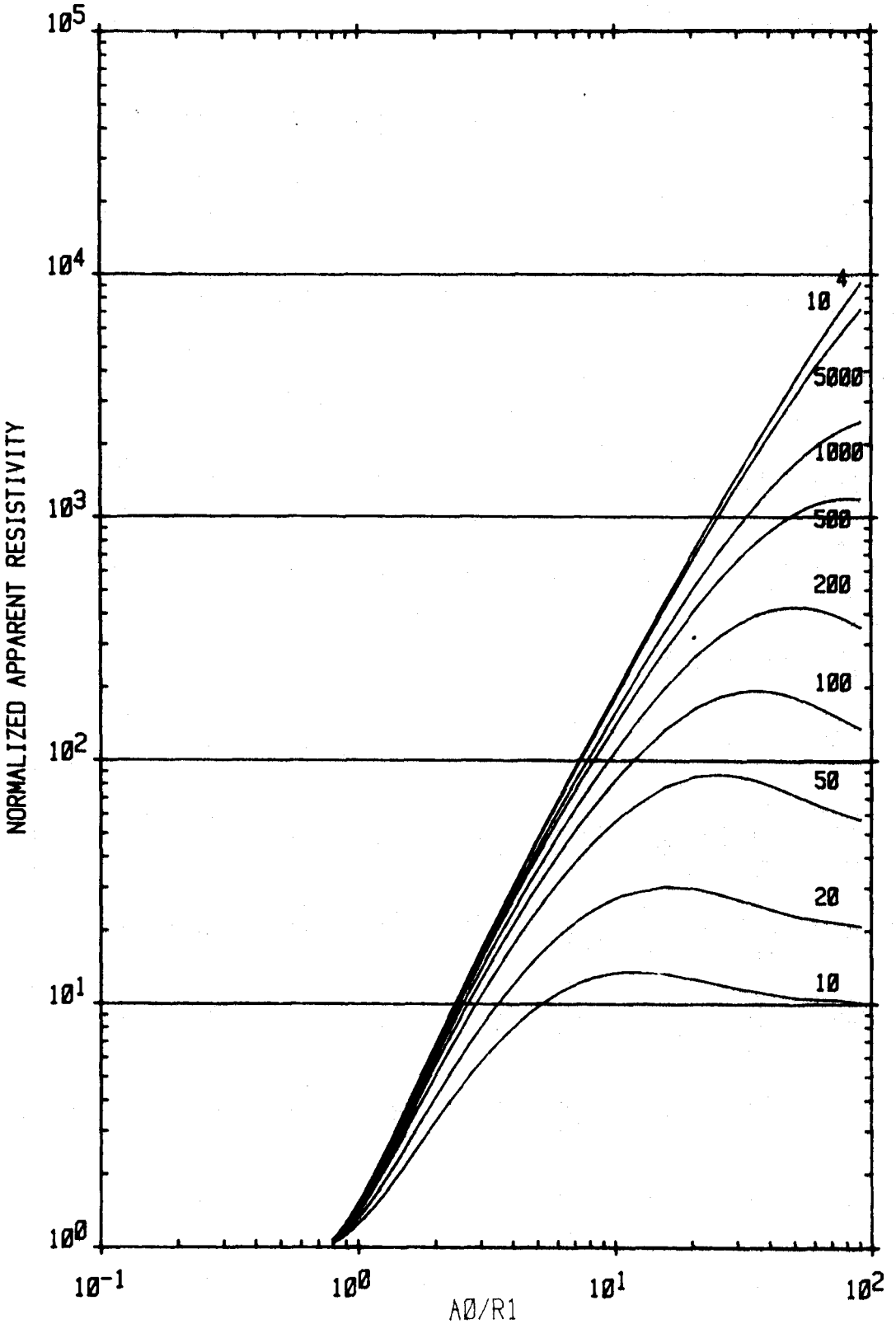

Fig. III-5. Normalized apparent resistivity versus normalized electrode spacing (modified Schlumberger array) for various values of $\rho_2/\rho_1 > 1$.

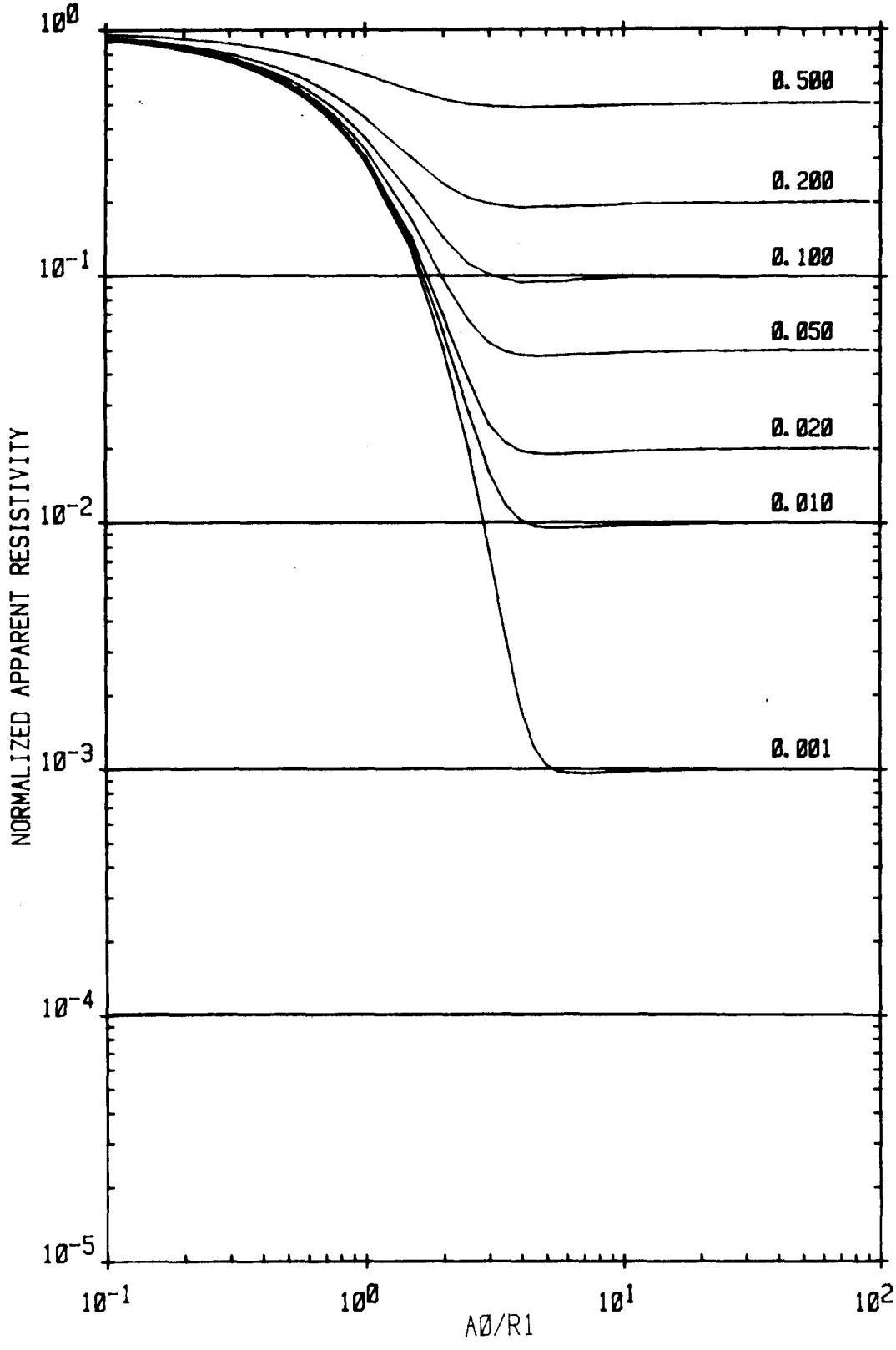

Fig. III-6. Normalized apparent resistivity versus normalized electrode spacing (modified Schlumberger array) for various values of $\rho_2/\rho_1 < 1$.

relative to the borehole radius. Clearly, the "borehole effect" is not a negligible problem. Note that for the $\rho_2/\rho_1 < 1$ cases (e.g. Figure III-4), the overshoot is minimal, which makes the "borehole effect" truly negligible.

The same type curves run for a modified Schlumberger array (Figures III-5 and 6) show similar behavior.

A three-layered system is depicted in Figure III-7. The general solutions for the potential in the three zones are:

$$V_p = \frac{I\rho_1}{4\pi z} + \int_0^\infty AI_o(mr)\cos(mz)\,dm \tag{19}$$

$$V_2 = \int_0^\infty [BI_o(mr) + CK_o(mr)]\cos(mz)\,dm \tag{20}$$

and

$$V_3 = \int_0^\infty EK_o(mr)\cos(mz)\,dm \tag{21}$$

The appropriate boundary conditions are:

$$\text{B.C.(1)} \quad V_p = V_2 \text{ at } r = R_1 \tag{22}$$

$$\text{B.C.(2)} \quad V_2 = V_3 \text{ at } r = R_2 \tag{23}$$

$$\text{B.C.(3)} \quad \frac{1}{\rho_1}\frac{\partial Vp}{\partial r} = \frac{1}{\rho_2}\frac{\partial V2}{\partial r} \text{ at } r = R_1 \tag{24}$$

$$\text{B.C.(4)} \quad \frac{1}{\rho_2}\frac{\partial V2}{\partial r} = \frac{1}{\rho_3}\frac{\partial V3}{\partial r} \text{ at } r = R_2 \tag{25}$$

The solutions for parameters A, B, C, and E are considerably more complex than for the two-layered system and are not given here.

Introduction of a third layer to the borehole electrical potential problem not only complicates the mathematical solution but also the manner in which such curves may be presented. Whereas for the two-layered system, the only options available are $\rho_2 < \rho_1$ and $\rho_2 > \rho_1$, the

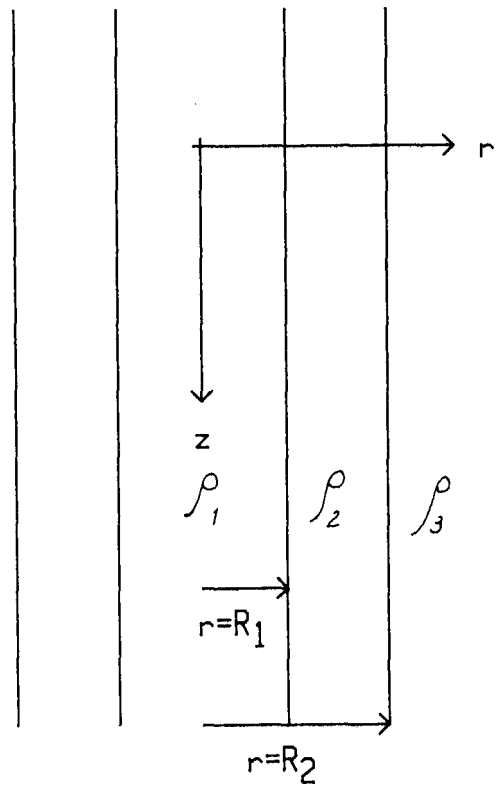

Fig. III-7. Model of a three-layered borehole system including an invaded zone. The resistivities are: Zone 1 ($r < R_1$) = ρ_1; Zone 2 ($R_1 \leq r$ KR_2) = ρ_2; Zone 3 ($r \geq R_2$) = ρ_3.

three-layered system includes many combinations of relative resistivity which could be observed. It is felt that only two situations, namely $\rho_1 < \rho_2 < \rho_3$ (salt water invasion), and $\rho_1 < \rho_3 > \rho_2$ (fresh water invasion), are practical in terms of standard material properties of oil/gas reservoir rock. Again, these situations were modeled for both the "normal" and "modified Schlumberger" arrays. Figures III-8 and III-9 show normal array response for $\rho_1|\rho_2|\rho_3$ ratios of 1|10|50 and 1|200|500. The former shows quite distinctive change in curve character as the radius of invasion ($r = R_2$) increases. As both invasion and formation resistivities increase, the curves become quite similar with small variation with increasing invasion. Note that all curves exhibit the overshoot phenomenon which again cautions against accepting implied "true formation" resistivities without considering the borehole effect. Figure III-10 shows the master curves for $\rho_1|\rho_2|\rho_3 = 1|500|10$. The influence of the invasion zone obviously increases as its radius increases. The character of the curves is quite distinctive which, for this resistivity ratio, indicates high interpretive value for analysis of fluid resistivity measurements.

Figures III-11, 12, and 13 show the modified Schlumberger array response for the same resistivity contrasts. The resulting curves are also quite distinctive in interpretive character although, again, for higher resistivity invasions and formations (e.g., Figure III-11) the curves are probably not distinct enough for an accurate interpretation of field data. As with the case for the "normal" array, all curves show an overshoot.

Current galvanic resistivity logs do not allow for more than two or three spacings. A variable spacing logging tool would need to be fabricated to make borehole measurements to make such master curves useful.

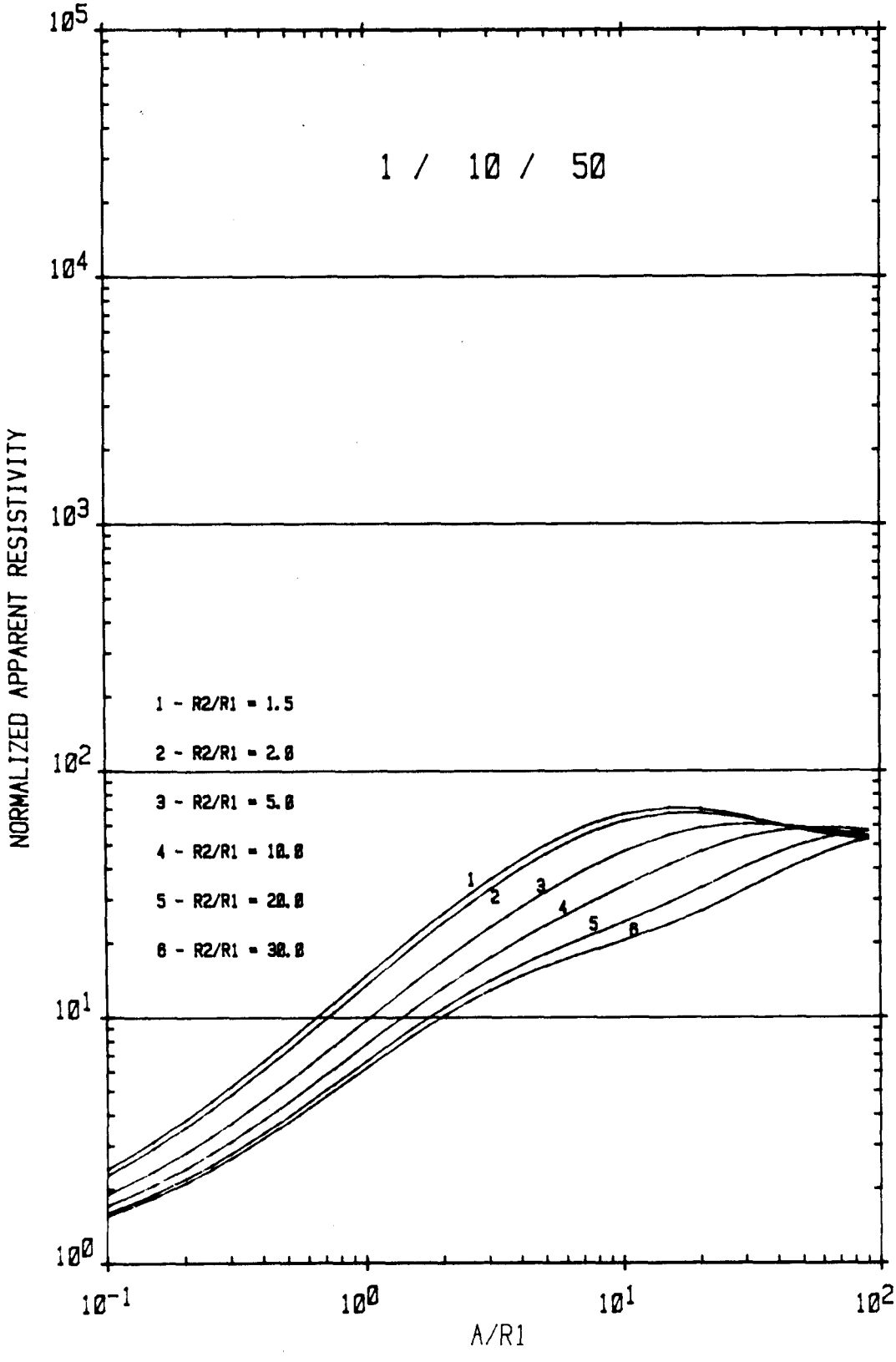

Fig. III-8. Normalized apparent resistivity versus electrode spacing (normal array) for $\rho_1/\rho_2/\rho_3$ = 1/10/50 for various depths of invasion

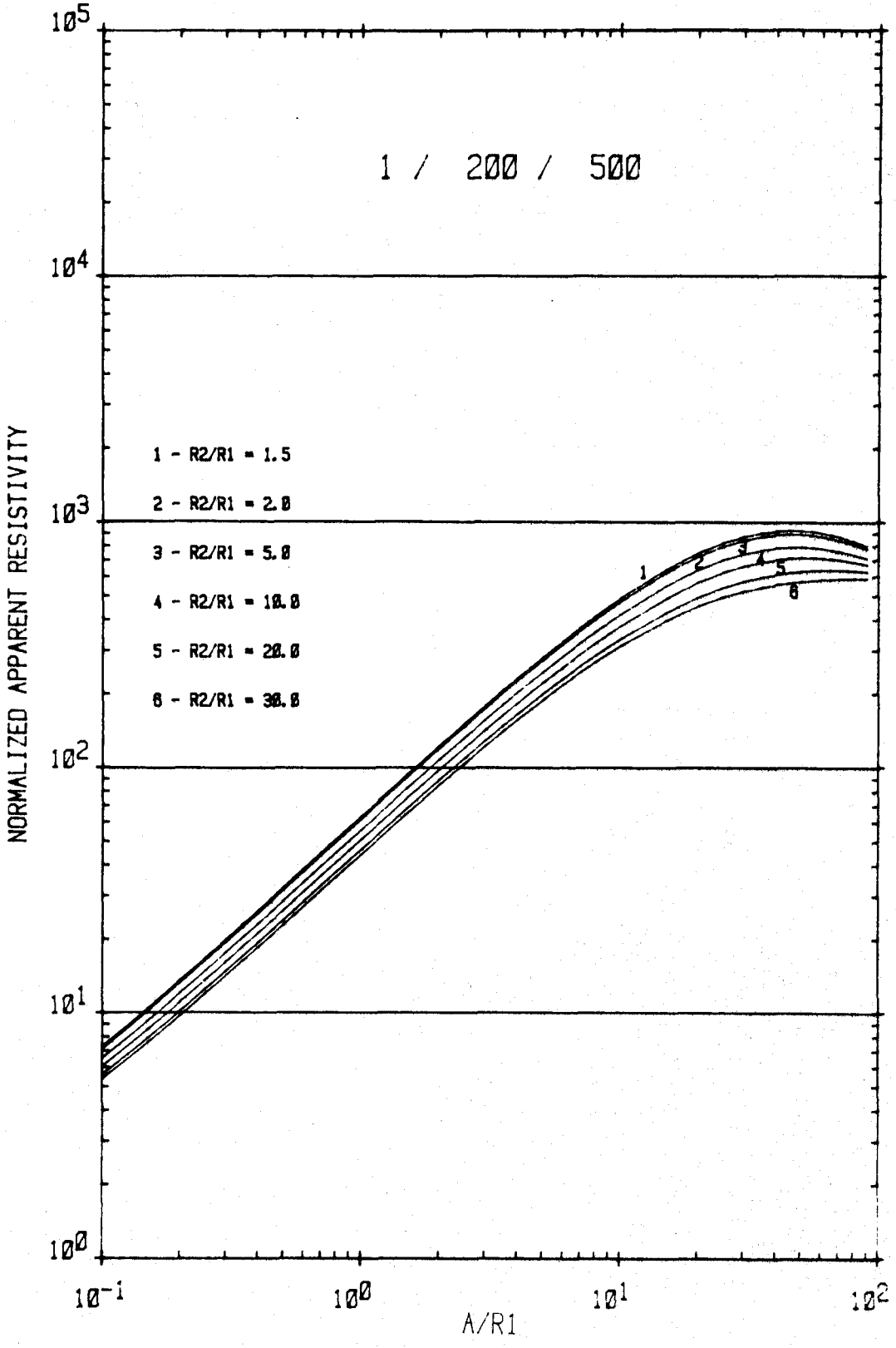

Fig. III-9. Normalized apparent resistivity versus normalized electrode spacing (normal array) for $\rho_1/\rho_2/\rho_3$ = 1/200/500 for various depths of invasion.

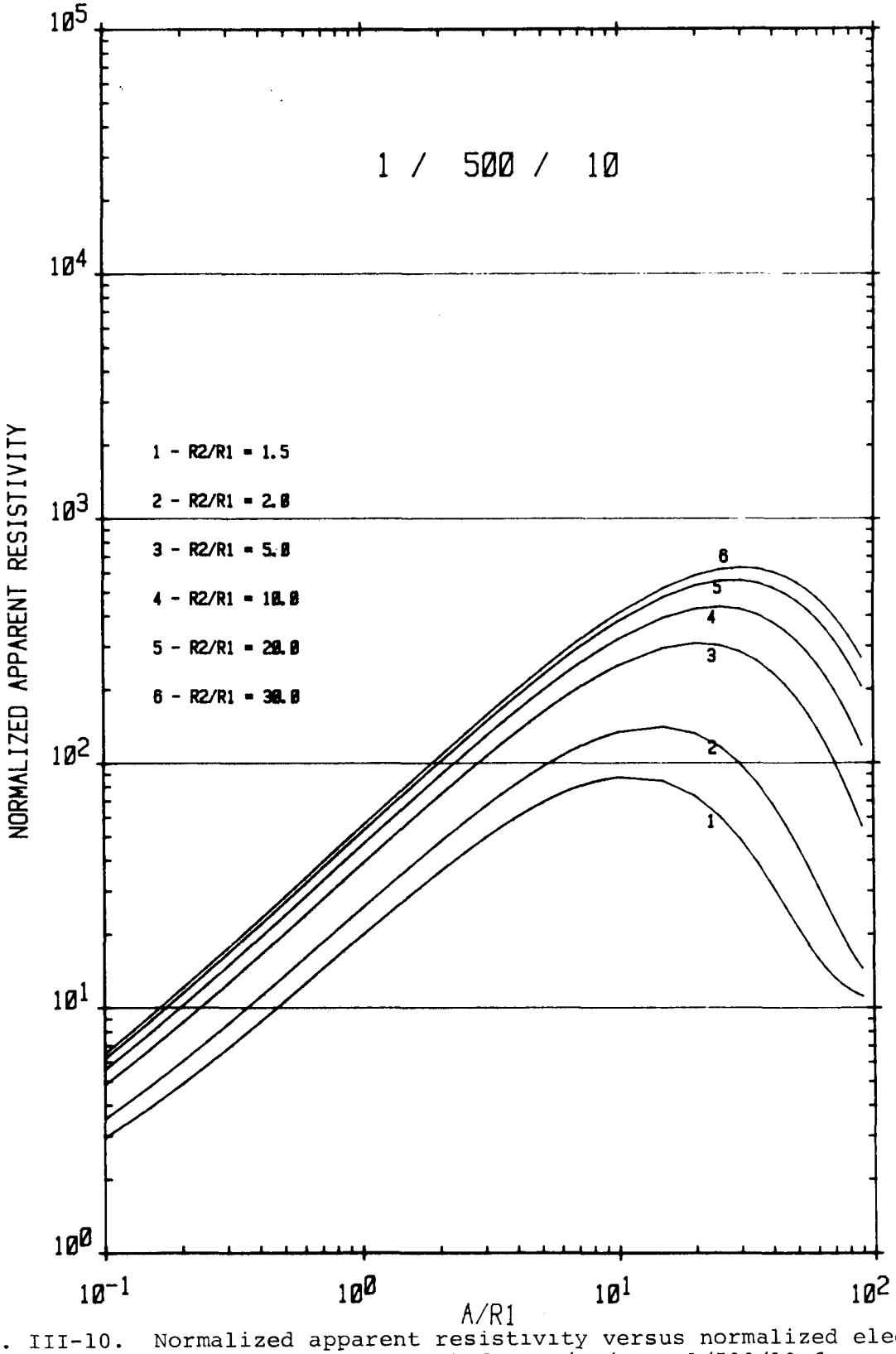

Fig. III-10. Normalized apparent resistivity versus normalized electrode spacing (normal array) for $\rho_1/\rho_2/\rho_3$ = 1/500/10 for various depths of invasion.

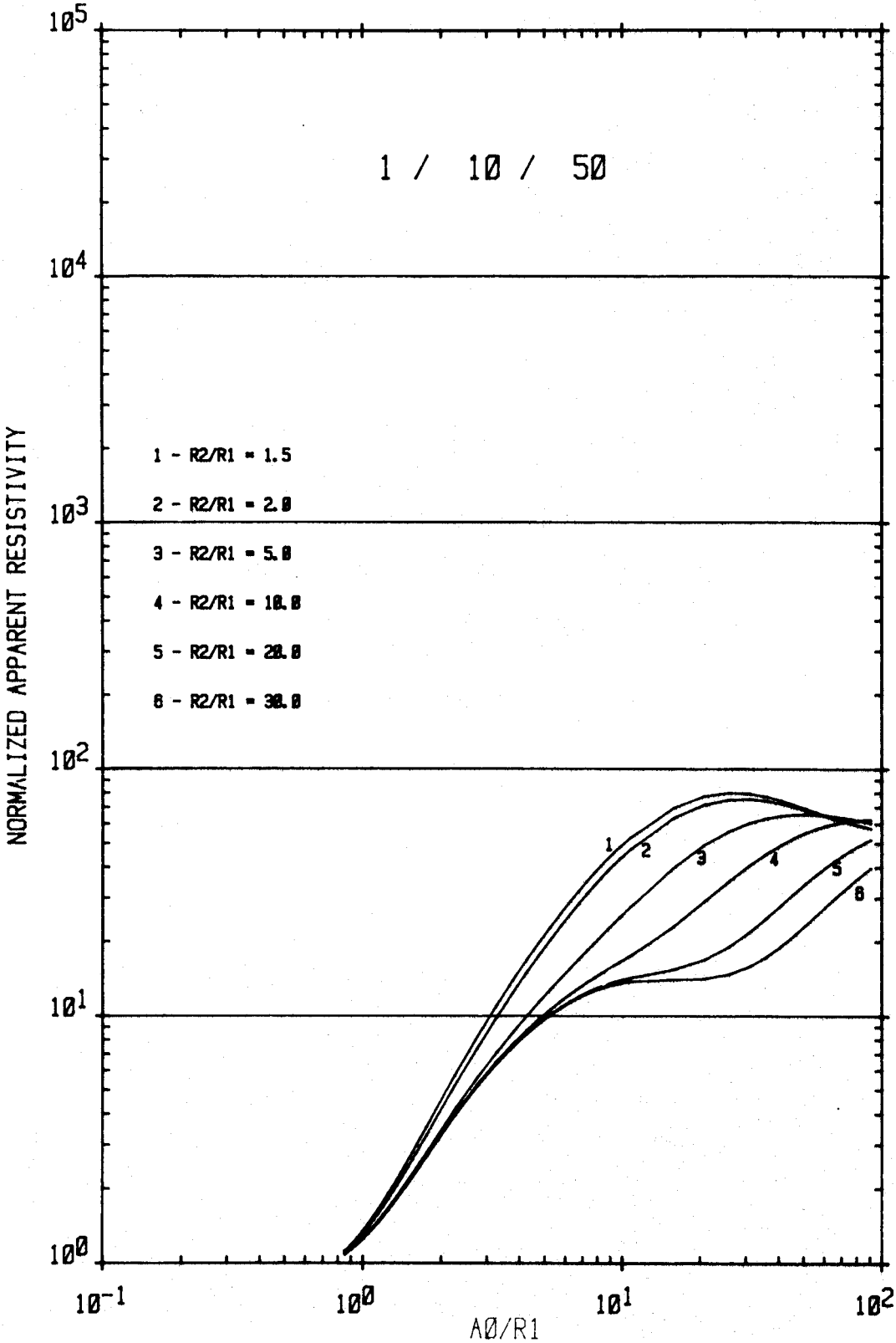

Fig. III-11. Normalized apparent resistivity versus normalized electrode spacing (modified Schlumberger array) for $\rho_1/\rho_2/\rho_3$ = 1/10/50 for various depths of invasion.

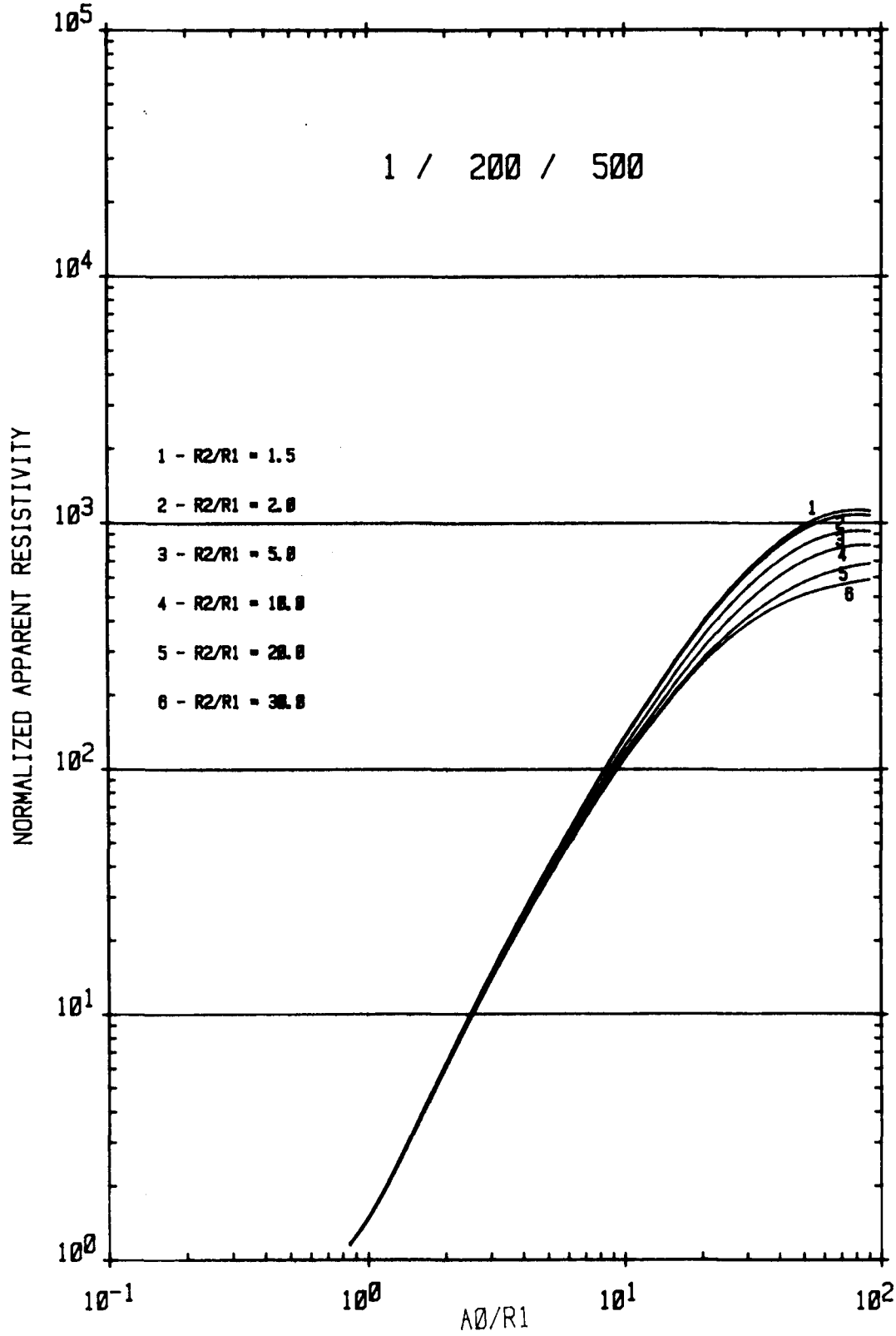

Fig. III-12. Normalized apparent resistivity versus normalized electrode spacing (modified Schlumberger array) for $\rho_1/\rho_2/\rho_3$ = 1/200/500 for various depths of invasion.

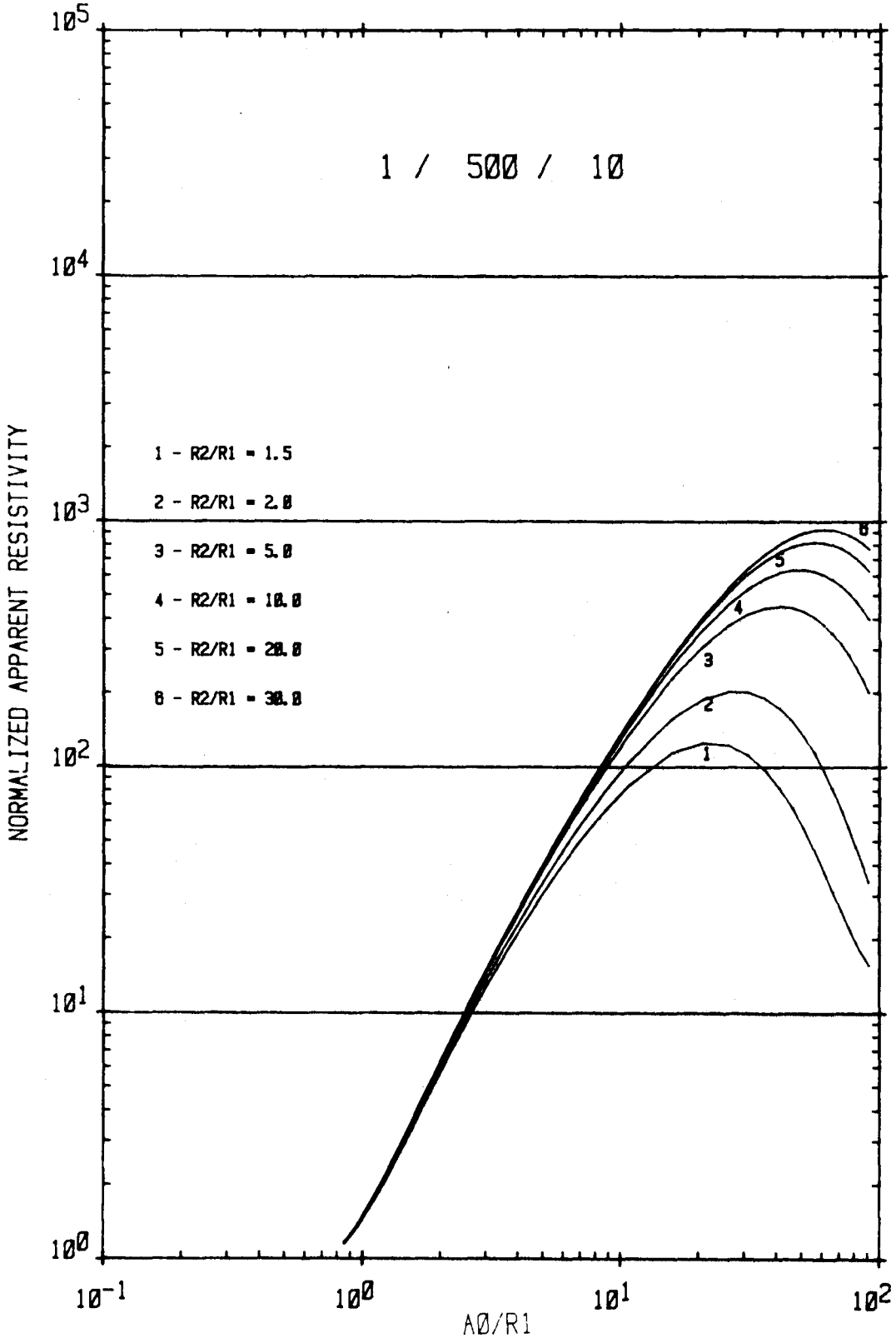

Fig. III-13. Normalized apparent resistivity versus normalized electrode spacing (modified Schlumberger array) for $\rho_1/\rho_2/\rho_3$ = 1/500/10 for various depths of invasion.

B. Electromagnetic (Induction) Logging

Induction probes have been used for some time to successfully measure formation resistivities at low (20 kHz) EM frequencies. In the interpretation of the measured signals, a convolution technique is used that neglects displacement currents and allows for only a simple set of electrical discontinuities such as occur at the formation layers. Recently[3] it has been recognized that high frequency (> 200 MHz) measurements can yield important additional information on, among other things, the pore water salinity, the pore size, and the electrical effects of shaliness. At these frequencies, displacement currents cannot be neglected and small material layers such as carried by mudcake may become important. To better understand the design parameters and data convolution techniques concerning proposed high frequency induction probes, a computer code is being developed to model coil responses in the earth. The source coil is approximated as a magnetic dipole, and it, along with the receiver coils, are oriented with their axes along the axis of the borehole. In the code, Maxwell's equations have been expressed in finite-difference form. Although the code can be applied to more general geometries, the earth is now modeled as three horizontal layers, each with uniform electrical parameters in between vertical interfaces at the drill-hole boundary, the edges of the saturated zones, the edges of the invasion zone, and the outer problem boundary. Each subdivision of the earth may be assigned a different permittivity, conductivity, and magnetic permeability. Although not presently in the code, equations have been formulated to include frequency-dependent electrical parameters.

C. Nuclear Magnetism Log (NML)

The NML is a curious phenomenon in that its concept as a logging tool was first published in 1960, yet today it is not a common commercial tool. The concept is also unique in that the log "sees" only free

fluid in rock pores and not bound or adsorbed waters associated with shales or hydrated minerals. The log behavior depends on many factors, including pore size distribution, paramagnetic substances in the matrix and in solution, and the pore fluid itself.

The bulk of published information relating observed nuclear magnetic resonance (NMR) behavior of saturated rocks to the pore size, matrix properties and fluid properties of these rocks has come from Shell Development Co. (Loren, Robinson, et al.) and from Chevron Oil Field Research Co. (Seevers, Timur, Brown, et al.). Also, most of these published data have dealt with laboratory, pulsed NMR experiments on core or chip samples as well as artificial aggregates. The most important results of these studies have been to show quantitative relationships between measured NMR behavior and a) pore size distribution, b) permeability, and c) residual oil saturation. An observation of published data is that very little testing of water-gas mixed phase media has been performed. As the proton density of the gas phase is pressure dependent, perhaps laboratory testing would require a pressure cell arrangement in conjunction with NMR experimentation. This is perhaps why little has been published in this regard.

To more deeply investigate the applicability of NML, T. L. Dobecki of Sandia visited Chevron Oil Field Research Laboratories over August 3 and 4, 1978, as the guest of Dr. Aytekin Timur. Our discussions included, among other possible logging techniques, NML and the state-of-the-art of downhole measurements. The more important observations/results obtained during this visit are summarized as follows. Current measurements (lab) on low permeability samples indicate that a dead time between sample energizing and measurement on the order of 1 millisecond (msec) is necessary; current downhole tools have a 12 msec dead time. Satisfactory measurements may be made, however, on core or chip samples right at the drill site using portable lab equipment; this does not measure at in situ pressures or non-invaded conditions, however.

Chevron and Sandia may soon enter into a cooperative research effort wherein typical samples of reservoirs of primary interest to the Enhanced Gas Recovery Program will be subjected to NMR analysis to determine how much information NMR can provide. The initial feeling is, however, that NMR analysis may prove useful for in situ permeability determination, yet may not prove sensitive enough to be useful for saturation determinations in the presence of significant borehole invasion.

D. Borehole Neutronics

Sandia presently has two programs funded by the National Uranium Resource Evaluation (NURE) Program for the development of downhole probes utilizing neutron generators. These programs are expected to have important spin-offs into the petroleum recovery area. The first program dealt with the development of a uranium assay probe and the accompanying neutron generator which is capable of producing 10^9 neutrons/second. This production rate is about an order of magnitude greater than that obtained from other commercially available devices and it will correspondingly increase the rate of data return in some logging applications. In a relatively newer program, Sandia has begun the development and calibration of a downhole gamma ray spectroanalysis probe. This probe will use a pulsed neutron source and a cooled germanium detector. Potentially, this probe can evaluate inelastic, capture and delayed radiation enabling an elemental analysis for all important materials including carbon. The fielding of this probe is expected in mid-1980.

E. Acoustic Logging

In addition to its dependence on virgin, matrix permeability, the producibility of tight gas sands or gas shales is often dictated by secondary porosity and permeability in the form of fractures. It is common, when such secondary permeability is not present or is minor, to

induce fracturing in the reservoir through explosive or hydraulic means. This implies a basic need to measure natural fracture density and orientation and elastic strength characteristics of the reservoir rock. Measurements of total seismic waveform propagation within the borehole and between a receiver in the borehole and a source at ground surface offers promise for such determinations. Developments to be considered include design of transmitter/receiver configuration for an in-borehole tool to accentuate either shear or compressional wave generation for accurate velocity and attenuation measurements. The design should allow for transmission paths to evaluate both vertical and horizontal fractures. Velocities derived from such measurements are also required to establish the elastic parameters of the reservoir and enclosing formations to evaluate proposed induced fracturing programs. Sandia is also investigating and developing a continuous wave seismograph technique for downhole velocity determinations using a surface source and downhole receivers. Such an arrangement measures the velocity of the formation and its fluids without being influenced by the borehole or the invaded zone, provided that invasion depth is not substantial.

To date, only the development of the sensor for the continuous wave log has been pursued.

References

1. Siegel, H. O., 1951, "Corrections for Masking, Drill Hole Pulse Logging," Newmont Exploration Files.
2. Kunz, K. S., and Moran, J. H., 1958, "Some Effects of Formation Anisotropy on Resistivity Measurements in Boreholes," Geophysics, V. 23, No. 4, pp. 770-795.
3. Poley, J. Ph., Nooteboom, J. J., and deWaal, P. J., 1978, "Use of V.H.F. Dielectric Measurements for Borehole Formation Analysis," The Log Analyst, May-June 1978, pp. 8-30.

IV. STIMULATION AND MINEBACK EXPERIMENT PROJECT

(D. A. Northrop, 4732, Editor)

The objective of the Stimulation and Mineback Experiment Project is to understand fracture stimulation techniques by directly observing induced fractures and relating their behavior to local and large-scale variations in geologic structure, material properties and in situ stresses as well as the mechanics of the fracturing process. Fracturing experiments are conducted in the volcanic tuffs that underlie Rainier Mesa at DOE's Nevada Test Site. The U12g tunnel complex provides the facilities for direct mineback of the fractures, exploratory coring to locate the fractures and determine their extent, measuring in situ stresses in regions of interest, obtaining material property samples at any location and conducting small scale experiments entirely underground. The site geology and evaluation methods were described in last year's report.[1]

Previous experiments include the Hole #3 Experiment[2] which examined two grout fractures that were propagated in the ashfall tuff, the Hole #5 Staged Proppant Experiment[1,3] and the Puff-N-Tuff experiment[3,4] which examined the containment-related problems induced by the release of post-detonation high pressure gases from a high explosive spherical charge.

Acknowledgments are due to Dr. Lynn D. Tyler and Dr. George B. Griswold for their participation in this program early in the year and also to William C. Vollendorf, Sharon J. Finley, many other Sandia personnel, and the skilled G-tunnel mining crew who conducted these experiments, mining operations, and evaluations at the Nevada Test Site.

A. Hole #5 Proppant Distribution Experiment (N. R. Warpinski, 4732)

The objective of this experiment was to investigate sand proppant transport and deposition during hydraulic fracturing. This experiment was designed, conducted and evaluated in 1976-77; complex fracture behavior was observed and reported in last year's annual report. This year, additional small volume hydraulic fracture tests and mineback activities were conducted in an attempt to quantify the reasons for the complex fracture behavior.

A detailed investigation of the in situ stresses in the vicinity of the Hole #5 Experiment was conducted using small volume hydraulic fractures to determine breakdown, fracturing and instantaneous shut in pressures. As shown in Fig. IV-1, seven zones in HFS #23 and nine zones in EV5#2 were fraced and subsequently mined back to provide information on fracture behavior and stress orientation. Table VI-1 shows the pressure data for HFS #23. P_c is the breakdown pressure, P_f is the fracturing pressure and P_{isi} is the instantaneous shut in pressure. The flow rates were 5 to 8 gal/min and the total volume pumped was usually less than 50 gal, injected in 2 or 3 stages. Only three zones exhibited breakdown spikes; in the other zones, the fluid was probably filling natural fractures, faults or bedding planes. Table IV-2 presents the pressure data for EV5#2 where only four zones exhibited breakdown spikes.

As can be seen from Fig. IV-1, there exists a complex system of faults that interacted with the minifracs and produced extremely erratic fracture behavior. Thus, the complex behavior of the Hole #5 fractures is also due to this fault system through the subsequent variations in the in situ stresses across the faults as well as the effect that the fault planes had on fracture propagation.

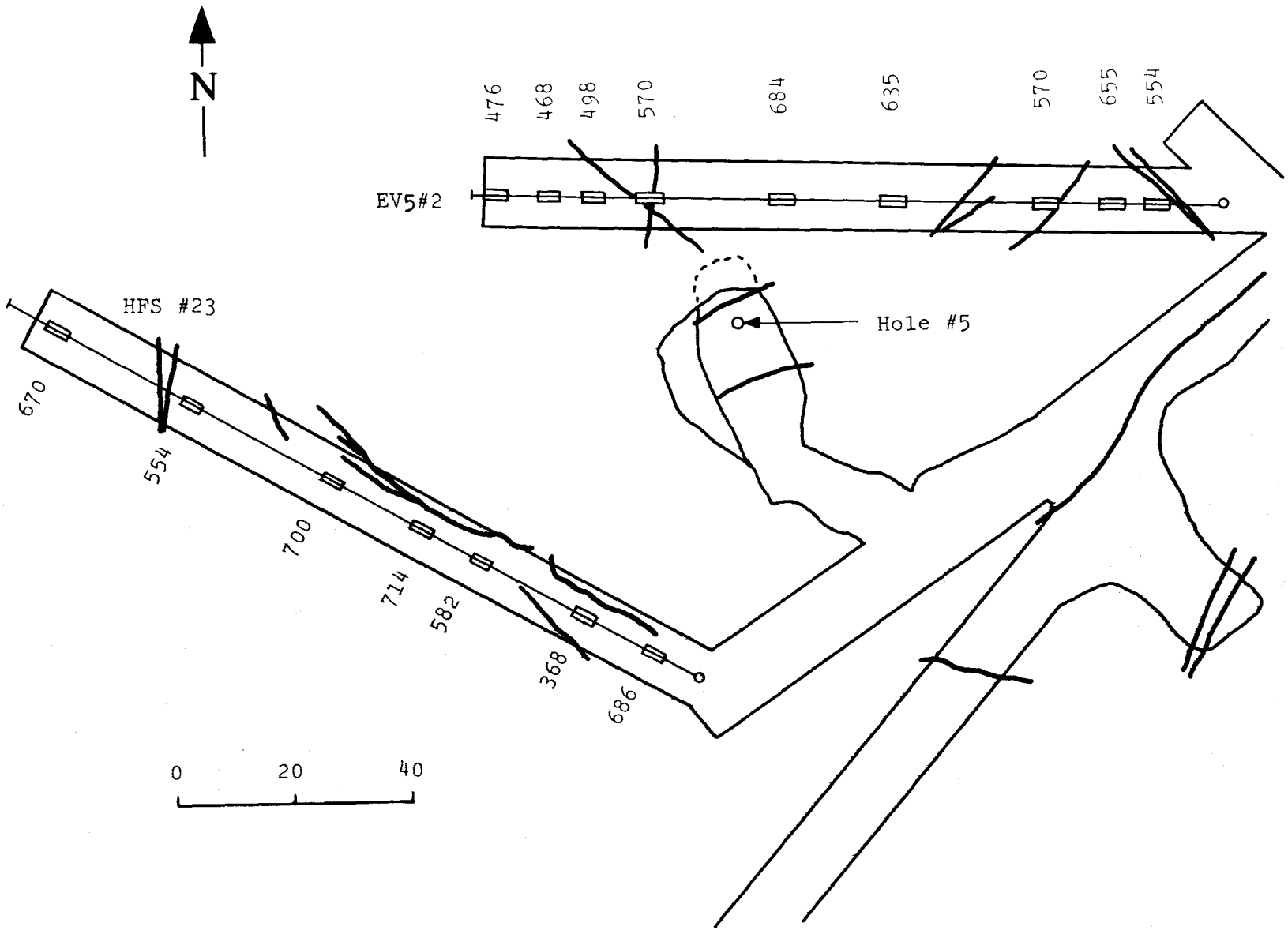

Fig. IV-1. Hole #5 Experiment Area showing fracture intervals and geologic faults.

Table IV-1. HFS #23 Small Volume Hydraulic Fracture Test Pressure Data

Flow Rate: 5-8 gal/min
Fluid: Dyed Water
Volume: < 50 gal

		Run #1			Run #2		Run #3	
Zone	(ft)	P_c(psi)	P_f(psi)	P_{isi}(psi)	P_f(psi)	P_{isi}(psi)	P_f(psi)	P_{isi}(psi)
1	126	-	715	670	750	650	750	710
2	99	821	735	571	714	536		
3	71	929	750	700	750	700	750	700
4	54	-	736	714	736	714	736	714
5	42	-	693	571	693	593	714	550
6	23	557	429	343	429	393	500	464
7	9	-	736	686	750	686		

Table IV-2. EV5#2 Small Volume Hydraulic Fracture Test Pressure Data

Flow Rate: 5-8 gal/min
Fluid: Dyed Water
Volume: 50 gal

		Run #1			Run #2		Run #3	
Zone	(ft)	P_c(psi)	P_f(psi)	P_{isi}(psi)	P_f(psi)	P_{isi}(psi)	P_f(psi)	P_{isi}(psi)
1	129	721	505	476	505	505		
2	119	-	625	468	494	468	520	468
3	111	711	575	493	571	503		
4	100	-	680	533	675	606		
5	78	850	780	684	814	684		
6	58	1201	735	601	720	669	700	659
7	33	-	660	570	660	570		
8	20	-	800	625	785	685		
9	12	-	640	554	615	554		

B. Hole #6 Formation Interface Experiment (N. R. Warpinski, 4732)

The understanding of fracture behavior at a geologic formation interface is important in the design of a hydraulic fracture stimulation. An experiment designed to address this question was formulated at a meeting of Amoco, Dowell, Halliburton, and Sandia representatives in Tulsa, OK, in February 1977. Hydraulic fractures would be created above and below an interface consisting of a welded ashflow tuff overlaying an ashfall tuff; these two formations which exhibit a significant difference in properties are discussed below. Colored cement would be used as the frac fluid to permit easy identification during mineback. The design called for injection of sufficient cement to create fractures of 50 ft. height and 600 ft. total length in each formation according to conventional calculations;* calculated fracture widths were 0.4 and 0.15 inches in the ashfall and welded tuffs, respectively.

Hole #6, with a collar elevation of 7555 ft. was drilled to a total depth (TD) of 1455 ft. The entire hole was cored, and a suite of logs was run. An ashflow unit, designated the Grouse Canyon Member of the Belted Range Tuff, was encountered from 1300 to 1352 ft. This member is comprised of an upper transition zone from 1300 to 1320 ft., a densely welded zone from 1320 to 1336 ft., and a lower transition zone from 1336 to 1346 ft. Below the ash flow unit is a peralkaline ashfall tuff designated Tunnel Bed 5 of the Indian Trail Formation. This experiment utilizes the contact between Tunnel Bed 5 and the dense welded zone of the Grouse Canyon Member for the interface; however, the interface is not discrete since the variation in properties occurs over a transition zone which is several feet wide.

The physical properties of eight core samples from this region of Hole #6 are shown in Table IV-3. The density, tensile strength, elastic modului and acoustic velocities of the welded tuff are much larger than

*Geertsma, J. and deKlerk, F., J. Pet. Tech., 21 1571-81, 1969, and Perkins, T. K. and Kern, L. R., J. Pet. Tech., 13 937-49, 1961.

TABLE IV-3. Physical Properties from Core Samples of Hole #6

DEPTH (ft)	TYPE	BULK DENSITY (gm/cc)	GRAIN DENSITY (gm/cc)	POROSITY (%)	TENSILE STRENGTH (psi)	MODULUS OF ELASTICITY (million psi)	POISSON'S RATIO	P WAVE VELOCITY (ft/sec)	S WAVE VELOCITY (ft/sec)
1297	Ashfall	1.95	2.49	35.0	35	1.22	0.213	9450	4870
1305	Transition	2.12	2.62	28.7	126	2.12	0.218	10100	5510
1313	Transition	1.92	2.63	40.3	108	0.80	-	7900	4430
1323	Densely Welded	2.42	2.65	12.8	820	5.07	0.213	14670	7080
1339	Transition	2.18	2.63	25.7	555	2.35	0.194	10800	5880
1343	Transition	2.14	2.47	20.1	29	2.20	0.265	11540	6280
1354	Ashfall	1.67	2.42	49.2	20	0.81	0.332	6190	3450
1363	Ashfall	1.68	2.42	48.6	39	0.30	0.206	5160	3130

the respective properties of the ashfall tuff and the porosity is considerably less. Physical properties were also calculated from the 3-dimensional velocity log. These results are plotted in Figs. IV-2 and IV-3 and are compared with the laboratory results. Only Poisson's ratio shows a poor correlation.

The treatment in the ashfall tuff (lower zone) was performed in August, 1977. As shown in Fig. IV-4, pea gravel was spotted to 1358 ft. and an inflatable packer was situated with the bottom of the element at 1352 ft. The 6 ft. open zone was fraced through NQ tubing (~2 3/8 in. ID) at 6 bbl/min with 5000 gal of green grout followed by 4000 gal of black grout injected into the formation. The complete pumping schedule is shown in Table IV-4. Bottom hole pressure and flow rate were recorded, but a wellhead pressure transducer malfunctioned. Four triaxial geophone packages grouted into the ashfall tuff 200 ft. away and 75 ft. below the packed off interval, recorded seismic signals during fracturing. The flow rate, bottom hole pressure, and seismic data are shown in Fig. IV-5.

The welded tuff zone was treated in October, 1977, because of delays due to lost pipe. At that time the hole had been reamed from 4 to 6 1/4 in., and TD was tagged at 1368 ft. As shown in Fig. IV-6, the hole was backfilled with pea gravel to 1331 ft., and the packer was set at 1324.5 ft. The formation was broken down with 30 bbl of water, shut in for a quiet period for acoustic signal detection, and treated with 5000 gal of blue grout at 6 bbl/min through HQ tubing (2 7/8 in. ID). The flow rate, well head pressure, and bottom hole pressure from an Amerada bomb and a Hewlett-Packard (HP) quartz crystal oscillator transducer were recorded during both breakdown and treatment. The data from the second zone are shown in Figs. IV-7 and IV-8. Figure IV-9 shows temperature surveys that were run before and after the frac job. The effect of the treatment can be seen in the open zone and the region where the packer element was situated.

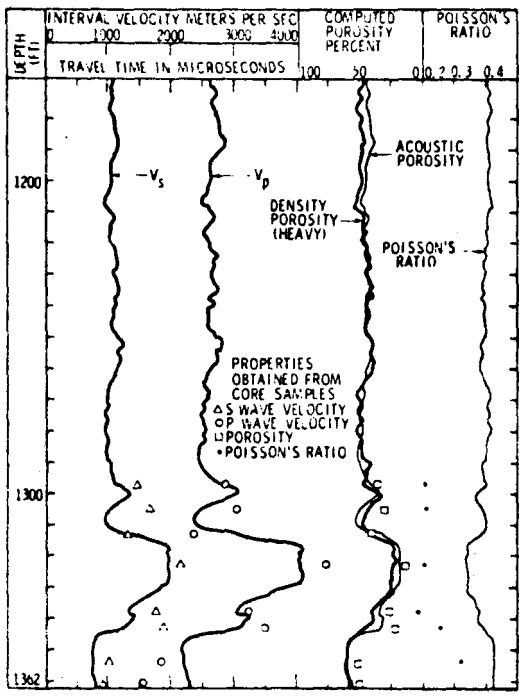

Fig. IV-2 Material Properties from Core Samples and Logs

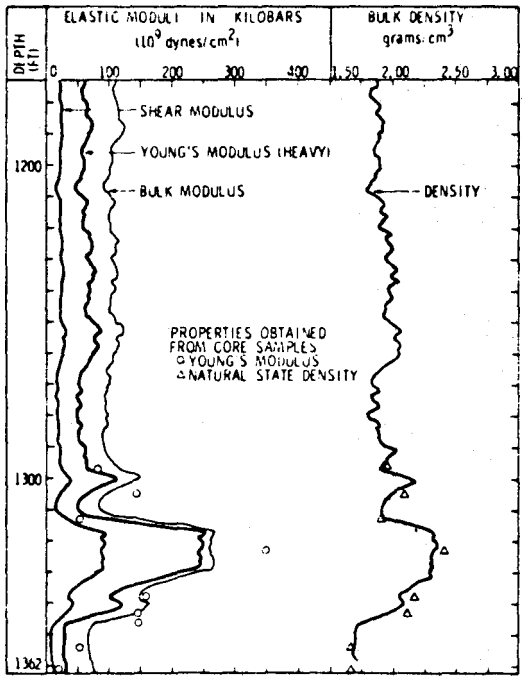

Fig. IV-3 Material Properties from Core Samples and Logs

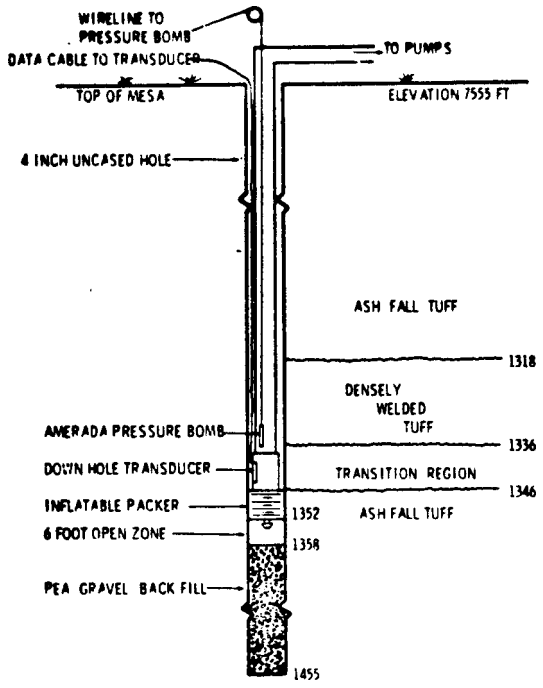

Figure IV-4 Ashfall Tuff Hydraulic Fracture Zone

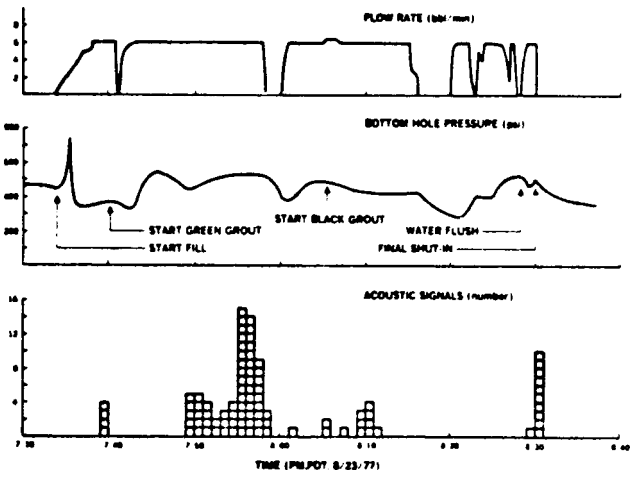

Figure IV-5 Hole No. 6 Ashfall Zone Treatment Data

TABLE IV-4

Treatment Schedule

Fluid: Nevada "A" Cement at 15.4 lb/gal

Viscosity: 128 cp (n' = 0.86, K' = 0.0031 lb-sec$^{n'}$/ft^2)

(η = 0.07 lbm/ft-sec, Ty = 0.23 lb/ft^2)

Flow Rate: 6 bbl/min

ASHFALL TUFF

Breakdown	1260 gal Water
Stage 1	5000 gal Green Cement
Stage 2	4000 gal Black Cement
Displacement	420 gal Water

WELDED TUFF

Breakdown	1260 gal Water
Fracturing	5000 gal Blue Cement
Displacement	420 gal Water

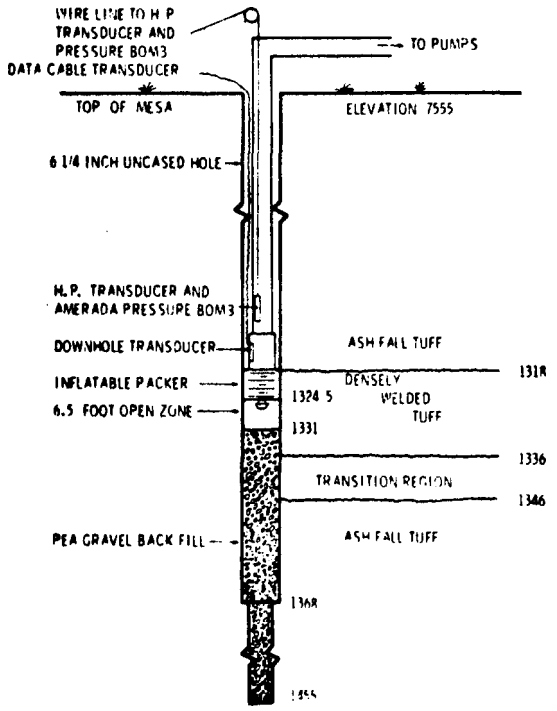

Figure IV-6 Welded Tuff Hydraulic Fracture Zone

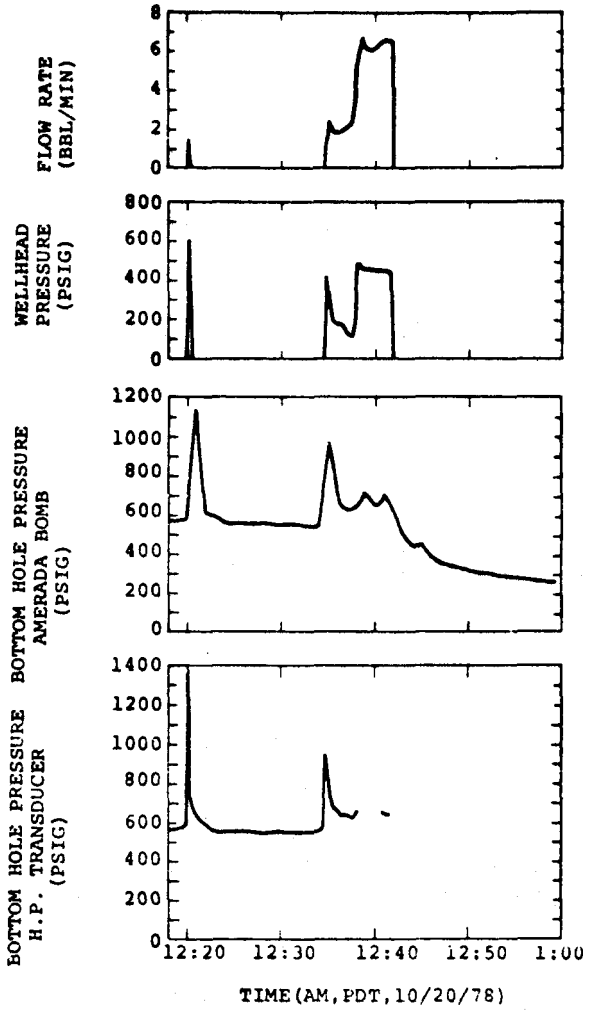

Figure IV-7 Hole No. 6 Welded Tuff Zone Breakdown Data

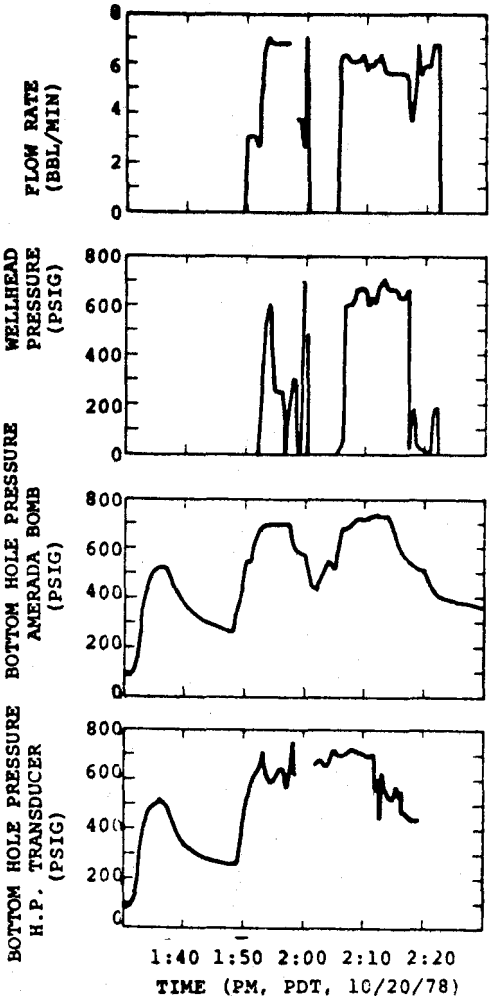

Figure IV-8 Hole No. 6 Welded Tuff Zone Treatment Data

The overall mineback area of the Hole #6 fractures is shown in Fig. IV-10. Mining began in September at point A and proceeded at a +13% grade to intercept the interface. In November the mining was suspended at point B in order to drill exploratory core holes to locate the fractures and provide holes for in situ stress measurements using small volume hydraulic fracture tests. Coreholes EV6 #1 and EV6 #2 were drilled horizontally in the ashfall tuff and EV6 #3 was drilled at +7° into the densely welded tuff. Green grout was detected in EV6 #1 and EV6 #3 at the positions indicated. The direction of the mineback was altered in order to intercept the projected fracture plane and the elevation of the drift was maintained at the interface to provide details of the fracture behavior there.

The green grout of the lower fracture was intercepted about 90 ft. from the borehole and it was clear that this was the tip of the fracture at this elevation. The mineback proceeded at the elevation of the interface through Hole #6 to a point 60 ft. past the hole where the fracture had again died out. A plan view of the mined out area where fractures were revealed is shown in Fig. IV-11, with the dip of the fracture at several locations indicated also. The direction of the fractures (N53°E) is consistent with the direction of the maximum principal in situ stress typically observed in G tunnel. The longitudinal view in Fig. IV-12 shows the stratigraphy relative to the mineback and the area where fractures were observed. The entire lengths of the fractures along the interface were mined out.

Cross section AA in Fig. IV-13 shows a location near where the fracture was first detected. The transition region, which was usually kept in the face of the drift, can, in general, be subdivided into three zones: (1) a basal, mostly non-welded, ash flow zone, (2) a hard, moderately welded, vitric zone, and (3) a non-welded zone comprised of a soft orange matrix with abundant hard lithics. Above the transition region is the densely welded tuff. The dip of the

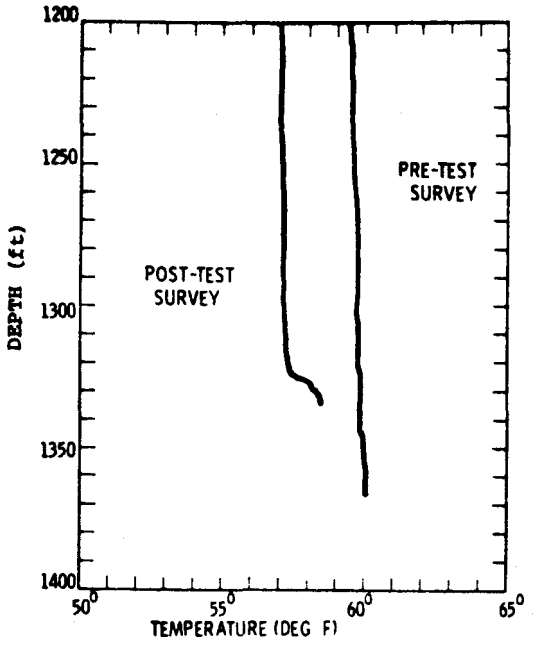

Figure IV-9 Temperature Surveys

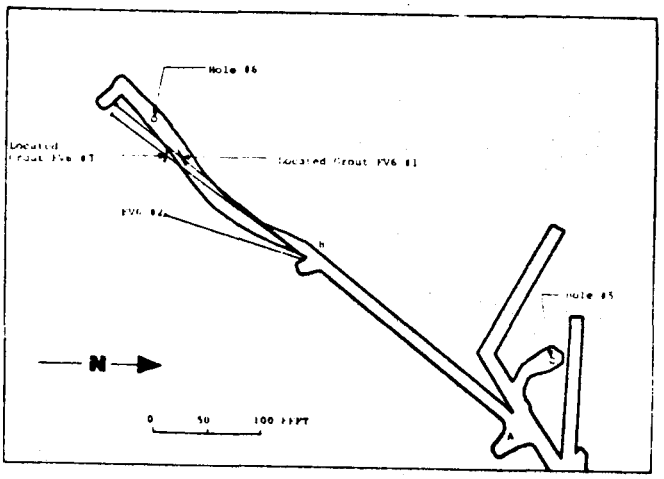

Figure IV-10 Plan View of Hole No. 6 Mineback Region

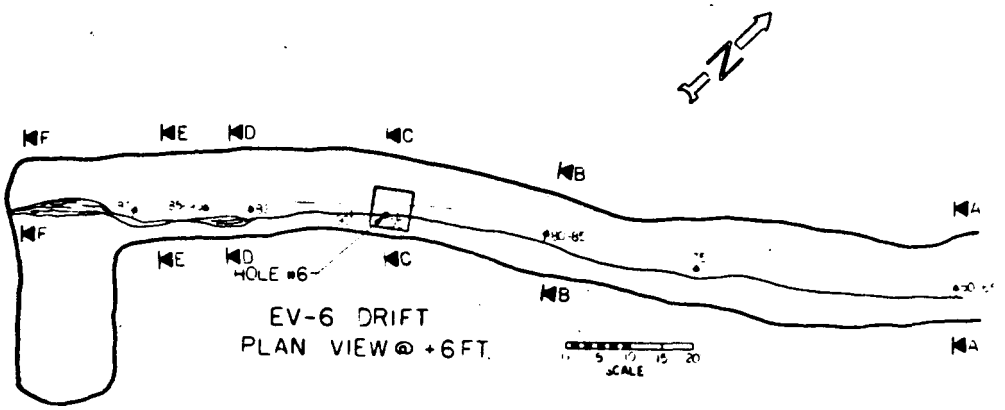

Figure IV-11 Plan View of Hole No. 6 Mineback

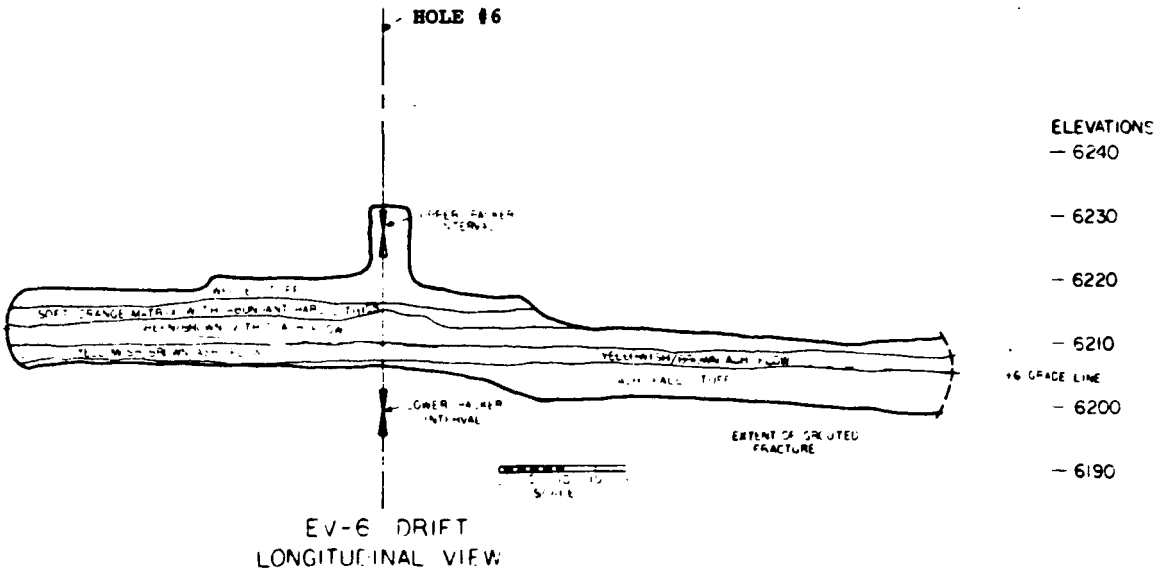

Figure IV-12 Longitudinal View of Hole No. 6 Mineback

fracture at this location is about 60° and only green grout was observed. The fracture had propagated through the hard, vitric zone but the effect of the different material properties could be clearly seen in the reduced width and increased stranding in this zone.

Closer to the borehole, both black and green grout were observed in the fracture, often in distinct laminae. As shown in Fig. IV-14 (section BB), the fracture becomes nearly vertical and considerably thicker. The transition zone apparently offered little resistance to fracture extension since the fracture propagated straight through. Very close to the borehole, the densely welded tuff was intercepted, and it was found that the fracture had also propagated into the welded tuff, but its width there was reduced by 50%. The primary fracture, however, had pinched out at tunnel level (about 10 ft. above the open interval where the fracture had initiated, as shown in Fig. IV-12) and a secondary fracture, which appeared to be a grout filled pre-existing fracture, became prominent and intersected the borehole.

The fracture at the borehole is shown in Fig. IV-15. It is vertical, about 10 mm wide in the ashfall tuff versus 5 mm wide in the welded tuff and filled with black, green and gray grout. When no blue grout from the upper fracture was seen as the mineback approached the hole, it was discovered that the concentration of blue dye in the cement was less than planned, and the upper fracture was actually gray. Gray grout had been noticed alongside the black and green fracture in many locations within about 30 ft. of the hole. A 6 ft. by 6 ft. rise was blasted up along the borehole and the fracture with black, green, and gray grout extended entirely through the interval where the upper frac was initiated. The upper frac, therefore, initiated in the same plane as the lower frac, but it was not always coexistent with the lower frac. In the welded tuff near the borehole there were abundant natural fractures that influenced the hydrofrac by offsetting the fracture

by as much as 2 ft. and terminating individual strands. In other cases, the grout has obviously filled some of these natural fractures.

Past the borehole, the fracture becomes quite complex. As shown in Figs IV-16 and IV-17, stranding is very common in the hard regions, such as the welded tuff and the vitric layer. In the soft region with the abundant hard lithics, the fracture typically meanders around the lithics, although it splits some occasionally. Figure IV-18 shows the fractures at the location where the mineback was terminated. Here, very little of the grout was observed in the transition region or the welded tuff. Mostly, the grout appeared to have filled natural fractures that were intersected by the hydraulic fracture.

After mineback was terminated, an exploratory coring program was begun to define further the extent of the fractures. By the end of September, seven coreholes had been drilled, and the results showing grout intersections are shown in Figure IV-19. The two holes up into the welded tuff intersected grout at several locations indicating severe branching of the fracture in the hard, fractured formation. Grout was observed in one of the coreholes in the ashfall tuff. Grout was not found in coreholes that were directed close to the interface or further away from the mined-out region. Thus, the fracture apparently propagated vertically rather than horizontally. Further coring is planned to delineate the fracture extremities.

The Hole #6 Formation Interface Fracture Experiment is an examination of fracture behavior at a geologic formation interface to determine if differences in material properties (and possibly in situ stresses) across an interface can deter the fracture from propagating through the interface. The entire length of the fracture along the interface was mined back, mapped, and photographed to provide detailed information for an analysis of this problem. The fracture in the ashfall tuff was, in general, well behaved, and

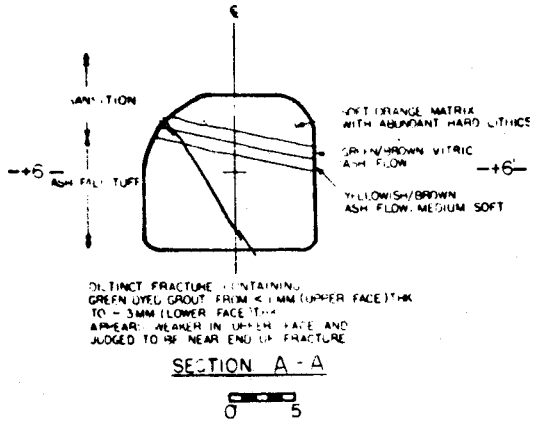

Figure IV-13 Face Map of Hole No. 6 Mineback

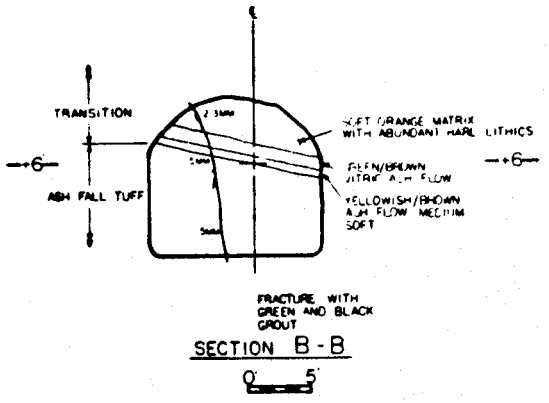

Figure IV-14 Face Map of Hole No. 6 Mineback

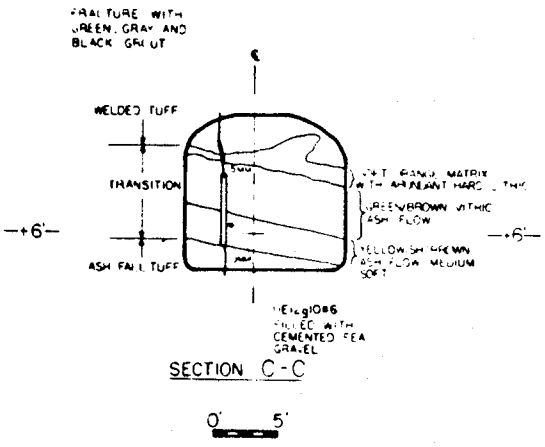

Figure IV-15 Face Map of Hole No. 6 Mineback

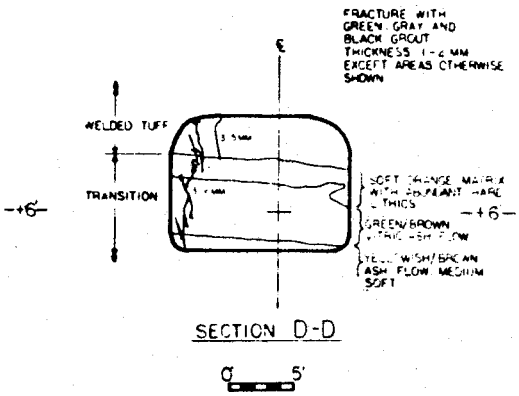

Figure IV-16 Face Map of Hole No. 6 Mineback

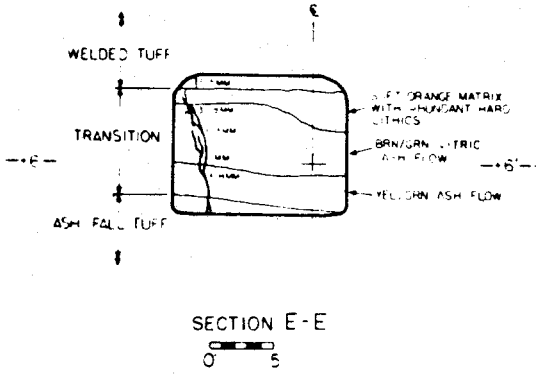

Figure IV-17 Face Map of Hole No. 6 Mineback

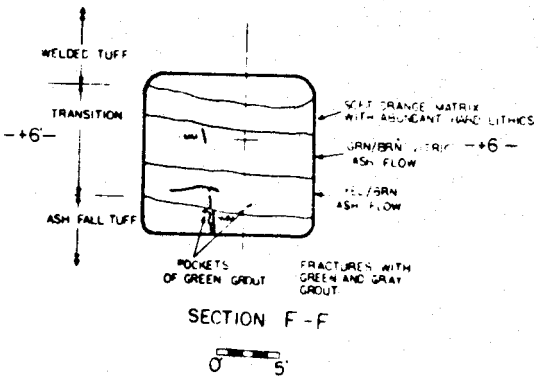

Figure IV-18 Face Map of Hole No. 6 Mineback

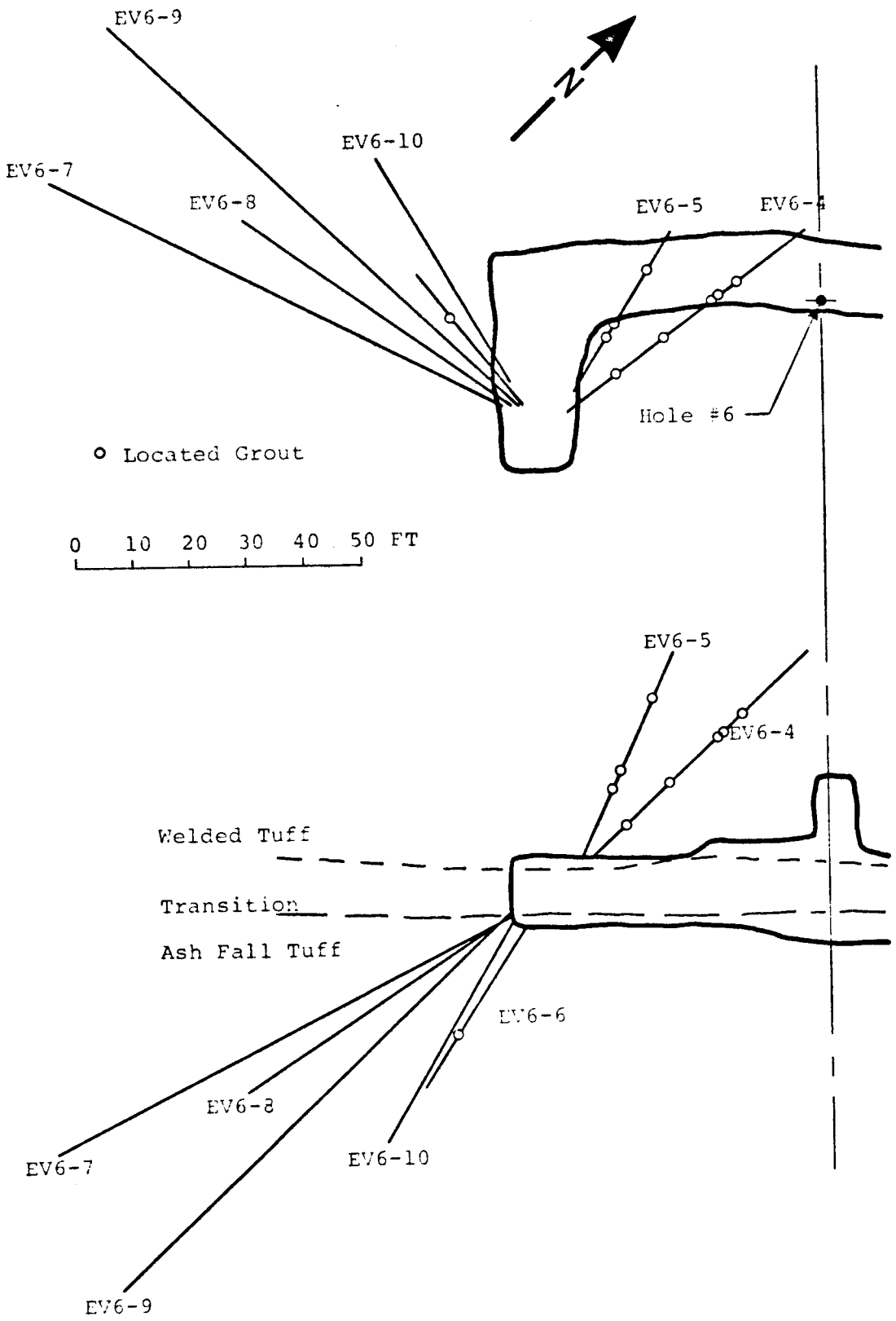

Fig. IV-19. Exploratory Coreholes and Grout Locations; Hole #6 Formation Interface Experiment.

the maximum width of the fracture was nearly that predicted by theory. However, the total length of the fracture at the interface was 150 ft. Thus, the fracture may have propagated downward as might be expected from the high density of the grout (1.9 g/cm). Unfortunately, the fracture in the welded tuff provides little information since it initiated alongside the lower fracture, and in many places was found alongside the lower frac.

Nevertheless, the results of the experiment are significant since the lower fracture readily broke into the welded tuff even though there is an order of magnitude difference in elastic modulus. Most of the simple analyses used to predict fracture behavior at an interface show that, all other things being equal, even a slightly greater elastic modulus is sufficient to confine the fracture. The results of this experiment, therefore, have important implications for the industry since it is usually assumed that the fracture will be confined to the pay zone.

Further work is under way to better characterize fracture behavior at the interface. Material properties of the ashfall tuff, welded tuff, and the tuffs of the various transition zones are being determined at several locations and in situ stresses will be determined by small-volume hydraulic fracturing on either side of the interface. In addition, the dynamic effects of the rate of fracture propagation at the interface will be examined by small-volume hydraulic fracturing and subsequent mineback.

C. Hydraulic Fracture Containment and Geometry (R. A. Schmidt, 4732)

This section deals with rock mechanics and our present ability (or inability) to understand and predict the growth characteristics of hydraulic fractures near a formation interface. Results from the Hole #6 experiment are examined in light of previous analytical and experimental studies. Consequently, severe limitations on quantitative predictability are recognized and plans are described that will hopefully alleviate this situation.

A hydraulic fracture is usually designed to be contained within the pay zone where it was initiated. Failure to do this results in an effective loss of the expensive fluid and proppant used to fracture the unproductive strata and some of the resource may even be lost if the fracture provides a leak path for the gas or oil to escape the pay zone. Other deleterious effects can also occur should the fracture penetrate a water-bearing zone. Due to the complexity of the problem, present design calculations assume, a priori, that the hydraulic fracture is contained and that a vertical fracture of constant height is created. Recent efforts, however, have demonstrated that fracture geometry and containment (or the lack of it) may be affected by parameters such as interface strength, in situ stress, rate effects on the fluid pressure distribution, and material properties such as Young's modulus and fracture toughness. While these parameters may be recognized as important, little has been done to test these effects and to develop quantitative criteria useful for design calculations. A summary of these parameters in general and their influence on the Hole #6 Experiment follow.

Interface Strength

Daneshy[5] investigated the strength of the interface in laboratory fracturing experiments and found that a fracture would

propagate across a well-bonded interface between dissimilar rocks. However, a weak interface, or an unbonded one, would arrest crack growth. One example of this is the fracture termination at a "clean" coal seam - shale interface observed during fracturing to promote methane drainage of the seam prior to mining.[6] In addition, the hydraulic fracture of the Hole #5 Experiment was observed to terminate at a "parting plane" which is merely an unbonded interface between two similar formations.[7] Hanson et al[8] have recently found that the stress perpendicular to an unbonded interface between blocks of the same material affects fracture penetration. A high normal stress was found effective in permitting the fracture to cross the interface, and this is presumably related to the higher achievable frictional stress and the ability of the interface to transmit shear stress.

These observations are supported by observation in fracture research of man-made composite materials. Composites are known to have a higher fracture toughness when the strength of the interface between the fibers and matrix is low enough to allow for crack tip blunting.

Observations during mineback of the Hole #6 Experiment indicate that the formation interface falls into the well-bonded category. The qualitative finding, then, that a well-bonded interface may not be effective in containing crack growth is supported by the observations at Hole #6 that the fracture did indeed cross the interface.

Variation in Minimum Principal Stress

Using a fracture mechanics approach Simonson et al[9] analyzed the effect of changes in the minimum principal stress on the stress intensity factor at the tip of a vertical hydraulic fracture. Their findings fall into two categories. 1) A fracture approaching an interface will tend to be arrested and contained if there is an abrupt increase in the minimum principal stress on the opposite side of that interface. Conversely, a decrease in this stress will encourage the crack to penetrate

the interface. 2) The gradient with depth of the minimum principal stress and the frac fluid density will determine the preference for growth in the vertical direction. High fluid densities and low stress gradients favor downward growth.

Examination of the Hole #6 data in light of these findings follow. 1) Pressure records from the frac job give the instantaneous shut-in pressure which is assumed equal to the minimum principal stress. Values of 400 and 430 psi were measured in the ashfall and welded tuff formations, respectively. This abrupt change is not large enough to conclude much in accordance with the first finding. 2) The density of the grout provided a pressure gradient of 0.8 psi/ft. and the gradient in the minimum principal stress is approximately 0.3 psi/ft. This indicates that downward growth is favored and, while observations show that the fracture did grow up through the interface, overall there appears to have been more downward growth.

Rate Effects

When rate effects are discussed, one must first realize that hydraulic fracturing is performed at rates that are considered quasi-static as far as strain rate effects in the rock are concerned (at least for most rocks of interest). The rate effects important in hydraulic fracturing are limited to the fluid flow aspects and the effects created on pore pressure and fluid pressure distribution in the crack. Hanson, et al[8] indicate that high flow rates and high fluid viscosities tend to encourage uniform growth along the entire crack front meaning the created fracture will tend to be "penny-shaped" with its center at the frac interval. That is, high pressure losses due to viscous drag and the resulting high input pressure overpowers the tendencies for the crack to grow upward or downward due to stress gradients or to be contained or affected by an interface.

These findings are too qualitative at present for much to be said concerning the Hole #6 experiment. However, it appears that rather uniform growth was observed and the degree to which this was caused by rate effects will be tested in the near future by further small-scale frac jobs near the same interface at various rates.

Material Properties

Many stress analyses have been performed on the problem of a crack approaching, reaching and passing through a material interface.[10-14] The stress analysis, however, is only part of the answer since without a fracture criterion one cannot predict when the crack will grow. The most obvious approach is to ignore the case of a crack whose tip rests at the interface and to examine the value of K as the crack tip approaches the interface and assume that crack growth simply requires a value of K equal to K_c.[9-10] This simplified approach leads directly to the prediction that a crack will be arrested in one material and will not even reach the interface if the second material has a higher modulus than the first. This results from the fact that for even a slight modulus increase the stress intensity factor goes to zero as the crack tip approaches the interface. Conversely, if the second material is of lower modulus than the first, the prediction is that crack growth will be enhanced and the crack will traverse the interface rapidly.

Observations of the fracture penetrating the interface in the Hole #6 Experiment contradict these findings. The formation interface chosen for this experiment involves a change in Young's modulus of more than an order of magnitude (0.3×10^6 psi for the ashfall tuff and 5.0×10^6 psi for the welded tuff) and yet containment was not achieved. Much experimental evidence for the fracture of composite materials also contradicts these analytical findings. Since the analytical calculations have been verified many times by various

investigators, one must conclude that the approach to the problem has been oversimplified.

One likely source of trouble is in modeling the interface as a discontinuity. The interfaces in hydraulic fracture continment problems and the Hole #6 experiment are often not discrete. Instead, the change in modulus is observed to occur over some finite distance. Even when the interface appears to be sharply defined with a discontinuous change of properties, there is a process zone at the crack tip where microcracking takes place in advance of the main crack. This process zone effectively averages the properties over some distance and is not modeled accurately by the analytical assumption of a sharp crack with infinite stresses at its tip. If the interface was "smeared" in the stress analysis it might be possible to avoid the situation by which K approaches zero as the interface is approached. Some analytical work by Atkinson [15] deals with the subject of stress analysis for a crack in a medium with a continuously varying modulus, but his work deals with mode III and a modulus variation inappropriate for the present problem.

Analysis of the problem of a pressurized crack approaching a smeared interface is being addressed from three directions:closed-form analysis, computer code calculations, and experimental studies. The closed-form analysis of this continuum mechanics problem is being handled primarily on contract to Tom Cook at the Southwest Research Institute. The basic approach taken is to use transform techniques to derive appropriate integral equations which are solved numerically. This approach is similar to that used previously by Cook for the problem of a crack approaching a discrete interface.

Code calculations on this problem were begun initially using the CHILES code.[16] While this code is excellent for crack problems using enriched elements near the crack tip, problems arose in applying

pressure loading to the crack surfaces near the tip. A similar code, APES,[17] also uses enriched elements but has additional features such as extra nodal points and the capability for pressure loading the crack tip. This code is now being modified so that it will run on the Sandia computers.

Experimental studies are needed in conjunction with the calculations to provide a well-controlled test bed for checking the validity of an appropriate fracture criterion. The stress analysis and one field experiment by themselves do not comprise a sufficient test. A solicited university proposal was received which deals with the fracture behavior of high-strength concrete specimens. These specimens are to be made in such a way as to result in a varying Young's modulus through the specimen which would model the smeared interface.

In addition, cores are being taken from the tunnel wall near the Hole #6 borehole. These cores will be machined and tested to provide the Young's modulus and fracture toughness data necessary as inputs to the code calculations. Hopefully, an adequate containment criterion will result.

D. Small Volume Hydraulic Fracturing (N. R. Warpinski, 4732, C. W. Smith, 1111, and R. A. Schmidt, 4732)

It is well known that the in situ stresses play a significant role in the behavior of hydraulic fractures. The orientation of a fracture is dictated by the overall stress field and the gradients of the stresses are possibly the deciding factors in whether a fracture propagates up or down and, thus, are a major influence on the overall fracture shape. Also, for novel fracturing techniques that initiate and extend multiple fractures, the in situ stresses must be overcome so that the fractures do not all propagate in the same direction.

A large number of in situ stress measurements are routinely made by the small volume hydraulic fracture technique (minifracs) to support the fracturing experiments conducted at the Nevada Test Site. This technique requires no delicate strain measurement or knowledge of the modulus of the rock and can be performed in any borehole at any depth. The minimum principal stress, σ_{min}, can be measured directly by

$$\sigma_{min} = P_{isi} \tag{1}$$

where P_{isi} is the shut in pressure. For a vertical borehole with the overburden stress aligned with borehole and the response of the rock assumed to be linear-elastic and isotropic, Kehle[18] and Fairhurst[19,20] show that a second equation which relates the breakdown or critical pressure, P_c, to the stress concentration in the wall of the borehole can be given by

$$P_c = 3\,\sigma_{min} - \sigma_{max} + T_o \tag{2}$$

where σ_{max} is the maximum horizontal stress, T_o is the tensile strength of the rock and it is assumed that the fluid is non-penetrating. It should be mentioned that although this is a direct stress measurement, there are inherent errors due to the determination of P_{isi} and rock mechanics considerations involved in the actual value of P_c that are not incorporated in Eq. 2. Also, the overburden stress σ_{ov}, is generally calculated from gravity considerations. Finally, since the orientation of the fractures must be obtained by impression packers or logging techniques, the apparent fracture direction at the borehole may be different from the direction farther out into the formation. At the Nevada Test Site, however, the fractures are mined back to determine their orientation and provide diagnostic information on the minifrac.

In our experiments, minifracs are performed from horizontal boreholes. In general, then, one of the stresses will not be aligned with the borehole and the simple theory outlined above does not apply. Fairhurst[19] demonstrated a method of solution for the more general case where the borehole axis makes any arbitrary angle with respect to the principal stresses. However, his actual calculations are also for the special case where one of the principal stresses is parallel to the borehole axis.

For a horizontal borehole, the assumption that one of the principal stresses, the overburden, is perpendicular to the borehole considerably simplifies the analysis and yet does not place severe restrictions on its applicability. For this case, Eq. 1 still holds but it is necessary to develop a breakdown criterion. To do this, the principal stresses must first be transformed into normal and shear stresses on axes aligned with the borehole and the vertical. These stresses are then applied to elasticity equations to give the stresses in the borehole wall. The stress state, which

includes shear stresses, is determined for all points around the borehole wall. Since breakdown is expected to occur when the maximum normal stress reaches the tensile strength, the calculated stress state must be transformed back to principal stresses. This gives the maximum and minimum normal stress at each point. The location around the wall that produces the greatest maximum (tensile) stress is the expected point of initial breakdown.

The maximum tensile stress criterion is a natural one which also yields a prediction for the orientation of the small fractures created by the initial breakdown. Certain combinations of in situ stress states and borehole orientations can give rise to a predicted breakdown orientation that differs significantly from the expected far-field orientation which is perpendicular to the least principal stress. This implies that direct observations of fracture orientations near the borehole may be helpful in verifying this analysis.

A computer code was written to handle these calculations since many transformations of stress are required and the closed-form solution is rather lengthy. Essentially, this calculation involves seven parameters: three in situ principal stresses, borehole orientation, tensile strength, Poisson's ratio, and breakdown pressure. The code can be used to predict P_c or one of the principal stresses if the other two are known. Since the minimum principal in situ stress is determined from Eq. 1, all three stresses can be determined from minifracs in two holes in different directions.

A number of minifracs were conducted in conjunction with the Hole #6 Formation Interface Fracturing Experiment. Holes EV6#1 and EV6#2 were cored nearly horizontally through the ashfall tuff below the welded tuff - ashfall tuff interface to locate the grouted fractures of the Hole #6 Experiment. Subsequently, minifracs were performed in 15 zones in corehole EV6#1 and 7 zones in EV6#2.

The instantaneous shut-in pressures obtained after fracturing were taken to be the minimum principal in situ stress and the results of these tests are shown in the map in Fig. IV-20. Indicated on the map are the minimum principal in situ stresses and the locations of the zones relative to Hole #6 and the grouted fractures. An attempt to fracture the welded tuff in Hole EV6#3 split the packer and no significant results were obtained. Of particular note, the main fracture from Hole #6 observed by mineback passed through the minimum in the minimum principal in situ stress, possibly choosing the path of least resistance.

These data, however, were suspect since only one zone out of the 22 tested exhibited a breakdown spike, even though the core that was recovered from both these holes was quite competent. The analysis for the breakdown of horizontal hole was then employed to examine the stress state around the boreholes and the subsequent breakdown criteria. In this region, the overburden stress is approximately 1300 psi and the maximum horizontal principal in situ stress (determined from Hole #6 fracturing data) is abut 800 psi. Hole EV6#1 was cored at 12° to the Hole #6 fractures and, therefore, 12° to the maximum principal horizontal stress; Hole EV6 #2 was cored at 31° to the maximum principal horizontal stress. Figure IV-21 shows the resultant stress distribution around the borehole of a typical zone in EV6#1, where the minimum principal in situ stress is 350 psi and the internal pressure is zero. Shown in Fig. IV-21 are the maximum and minimum principal stresses on the borehole wall as a function of the angle around the borehole (ϕ = 0 is horizontal). Under the conditions shown, the borehole wall around 90° and 270° is already under 261 psi tension and it only requires about 50 psi internal pressure to breakdown the formation assuming a 300 psi tensile strength. This pressure

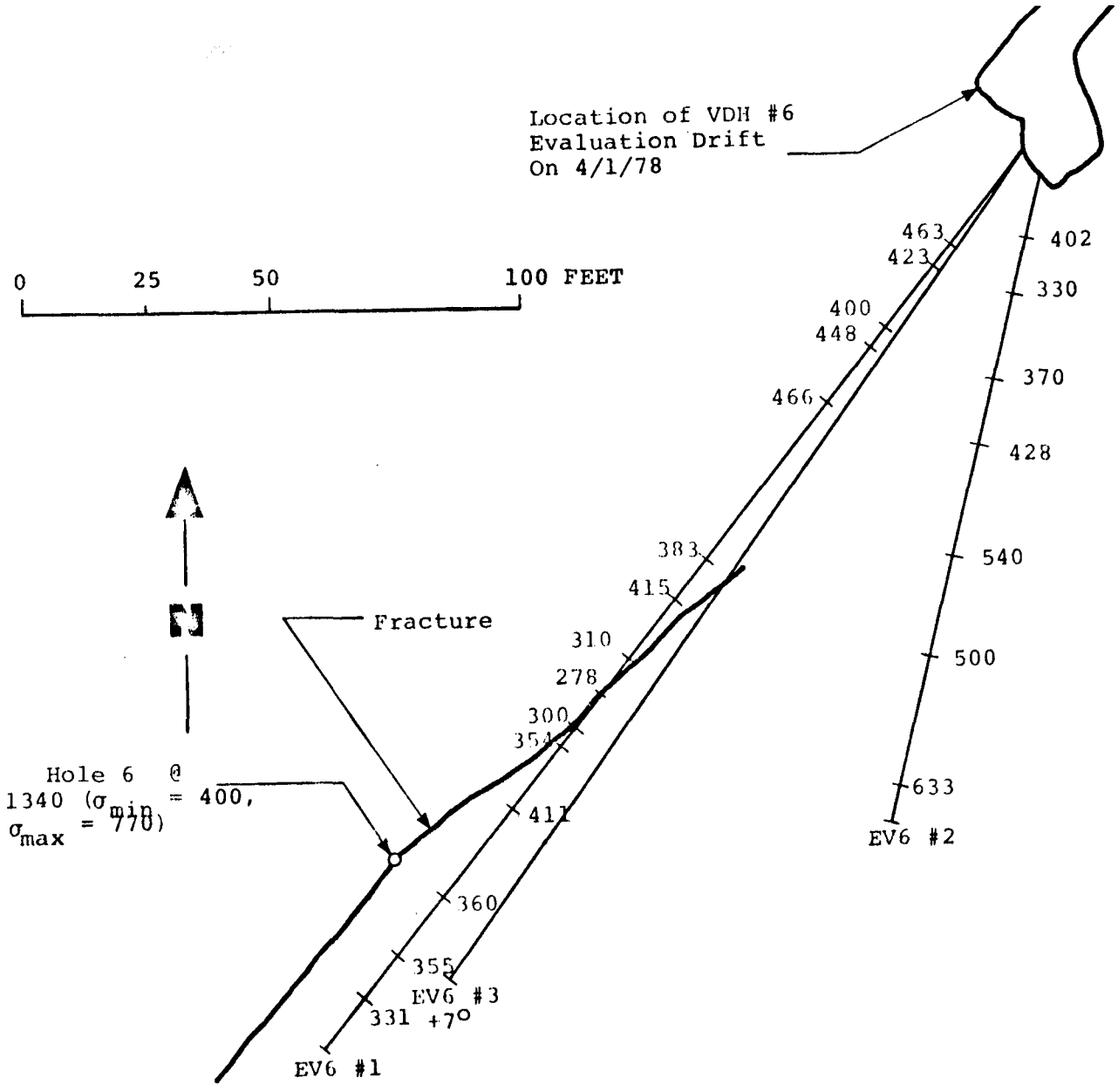

Fig. IV-20. In Situ Stresses in Ash Fall Tuff in the Vicinity of Hole #6

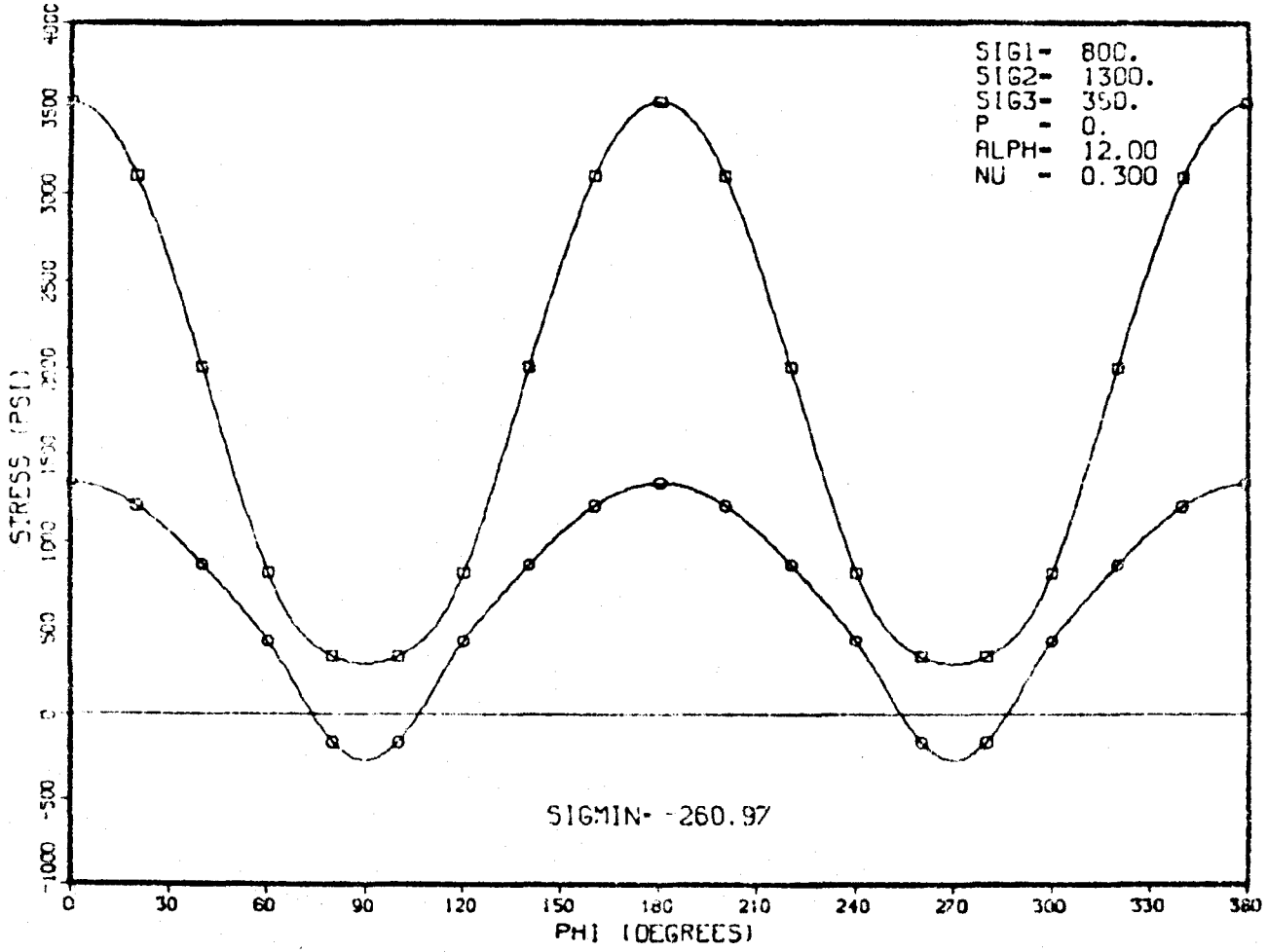

Figure IV-21 Principal Stresses Around the Borehole: No Internal Pressure, Borehole Wall in Tension

is less than the minimum principal in situ stress and, therefore, less than the fracturing pressure so that a breakdown spike will not be observed. In fact, in four zones of EV6#1 and one zone of EV6#2, the stresses may be such that breakdown can be produced simply by drilling the hole. On the other hand, if a hole is drilled perpendicular to the direction of the maximum principal horizontal in situ stress, a breakdown should be observed.

E. Complementary Studies

Two other activities were pursued concurrently in G-tunnel during the past year. Although these activities were not supported by DOE's Enhanced Gas Recovery Program, their results have direct application to natural gas stimulation. Thus summaries are presented here for completeness.

(1) High Energy Gas Frac (N. R. Warpinski, 4732, R. A. Schmidt, 4732, P. W. Cooper, 1132, H. C. Walling, 1136, and S. J. Finley, 4732)

This activity was conducted under Fossil Energy Development Program Funds received from DOE/Fossil Energy. The primary use of these funds is to examine the feasibility of new ideas or concepts.

The High Energy Gas Frac is a wellbore fracturing technique whereby multiple fractures are created and extended in a pay zone by imparting a controlled high intensity and short term load to the borehole. The concept of the High Energy Gas Frac is to tailor the pressure-time behavior of the deflagration of a suitable propellant to create multiple fractures and avoid limitations inherent in both hydraulic fracturing and explosive fracturing. Hydraulic fractures, which are propagated at pressures that are slightly higher than the minimum in situ stress and pumping times that are on the order of hundreds of seconds, typically produce only a single fracture whose orientation is aligned with the in situ stresses. Detonations, on the other hand, which usually have peak pressures that are orders of magnitude above the in situ streses and occur in microseconds, often cause considerable crushing of the rock and leave a residual compressive stress zone around the wellbore. This results in wellbore damage, and may seal off any cracks that are formed.

The High Energy Gas Frac imparts a controlled pressure load about one order of magnitude above the in situ stresses but below the flow stress of the rock to avoid crushing. This pressure

load is applied over an interval on the order of milliseconds to create and extend multiple fractures radially from the borehole. The initial loading rate must be large enough to initiate multiple fractures. The number of fractures appears to be rate dependent and is probably influenced by the velocity of sound in the rock, the size of the borehole, the in situ stresses and the number of available flaw sites for crack nucleation. The propellant must continue to burn for a short period so that the hot, high pressure gasses will enter the created fractures and extend them. There will be a limiting crack size if the fluid does not penetrate into the cracks. The pressure must be considerably above the in situ stresses so that the near wellbore stress field is dominated by the effect of the pressure in the cracks and wellbore resulting in fractures which propagate radially. However, if the pressure is too large and results in crushing, small particles may enter the cracks and seal them off. Under these conditions of elevated temperature, pressure and gas velocity it is also expected that the fractures will be somewhat self-propping and a number of high conductivity paths will remain after the pressure has decayed.

Three different propellants were tested in a volcanic ash fall tuff medium (density = 1.8 gm/cc, elastic modulus = 0.6 x 10^6 psi, permeability = 0.01 md, porosity = 40%) near an existing tunnel complex so that mineback of the tests would provide direct observational evidence to characterize the results. In each test, canisters containing 20 lb of propellant, ignitors and a fluid-coupled-plate pressure transducer were stemmed into an 8 in. diameter horizontal borehole, 20 ft. deep, with a high strength grout. The propellants utilized were JPN, a relatively slow burning rocket propellant, M26, a large bore gun ammunition having an intermediate burn rate, and M5, a small arms ammunition with a fast burn rate.

The results of the three tests showed phenomenologically different behavior. JPN, the slow propellant (burn time = 0.9 sec), had a pressure loading rate of 0.09 psi/μsec and a peak pressure of 6250 psi. The loading rate was too small to induce multiple fracturing and the peak pressure was too low to crush the rock. This test resulted in a single fracture that was similar in appearance to hydraulic fractures typically observed near this tunnel location. M26, the intermediate propellant (burn time = 9.4 msec) had a loading rate of about 20 psi/μsec and a peak pressure of 13,800 psi. This was sufficient to initiate and extend 12 separate fractures in random radial directions. Lengths of these fractures varied from 6 in. to 8 ft. There was no apparent crushing of the rock near the wellbore. The fast propellant (burn time $\sim$ 1 msec) had a pressure loading rate greater than 1500 psi/μsec and a peak pressure greater than 20,000 psi. These values were so large that considerable crushing of the rock near the wellbore was observed and only one fracture was extended a significant distance from the wellbore. Several incipient cracks ($\sim$4 in) that barely extended out of the crushed zones were also observed. The crushed cavity region was similar in appearance to typical contained high explosive shots conducted in tuff.

Analysis of the intermediate propellant test shows that a lower bound crack length of 1.6 ft is calculated by assuming a loaded borehole with no gas entering the fractures. On the other hand, if it is assumed that gas enters the fracture and the crack propagates at its maximum velocity for as long as the pressure is higher than the fracturing pressure in this medium, an upper bound crack of 30 ft is obtained. The observed crack lengths in general fall between these two bounds. Realistic calculations for these final crack lengths will require knowledge of the complex gas dynamics in the cracks.

The High Energy Gas Frac has been shown to be a viable technique for creating multiple, randomly oriented fractures in a borehole. This field test has demonstrated that a propellant can be suitably designed to provide (1) a large enough loading rate to initiate multiple fractures, (2) high enough pressures to extend fractures radially, but not so high as to exceed the flow stress of the rock and (3) sufficient gas generation to allow most of the fractures to be pressurized and propagated further.

The results of these experiments will be given in a future Sandia Laboratories Report: N. R. Warpinski, et al, "High Energy Gas Frac," SAND78-2342, December 1978.

(2) Nuclear Containment Studies (C. W. Smith, 1111)

The phenomena affecting the containment of underground nuclear detonations have been investigated for several years under funding by DOE's Division of Military Applications. A principal element of the nuclear containment work is the investigation of residual stress fields. These fields, produced by explosion dynamics, are believed to be the main containment vessel for underground nuclear detonations. Through a calculational and experimental program, we are attempting to identify the parameters significant to the formation of these residual stress fields. The experimental work is being pursued with small (8 to 1000 lb) high explosive detonations. Cavity pressure, dynamic stresses, and residual stresses are being measured with active instrumentation; the structure of these fields is being probed with post-shot hydraulic fracture and mineback techniques. These residual stress fields are of interest to natural gas recovery techniques that involve explosive stimulation methods.

Five high explosive charges (TNT) have been detonated this year: three 64 lb. events and two 8 lb. events. We have also constructed a test bed for a 1000 lb. explosion; this event will be extensively instrumented with stress gages to measure the dynamic and residual stresses in the tuff around the sphere.

We successfully measured the cavity pressure on three of the events, (RS4, RS5, and RS6). This is the value of pressure in the cavity shortly after the passage of the dynamic effects. It is of major calculational interest for this pressure is one of the "end products of the code calculations. Thus, reasonable agreement with experiment suggests that the overall detonation process has been well modeled.

The measurement technique consists of a nitrogen-filled pressure vessel located away from the high explosive charge, an explosively-actuated valve, and a high pressure tubing extending from the pressure vessel to the expected edge of the cavity. Ten milliseconds before the high explosive charge detonation, the explosive valve is fired and a flow of nitrogen started. As the explosive cavity grows, it engulfs the end of the high pressure tubing. The gas flow stops when the pressure in the cavity is equal to that in the pressure vessel.

Figure IV-22 shows the cavity pressure obtained on RS4, a 64 lb. event. Initially the pressure vessel shows 8400 psi. About 200 milliseconds after detonation the pressure has dropped to 7050 psi, which is the cavity pressure referred to above. Subsequently, the pressure decays slowly and shows 3750 psi at 600 sec. Cavity pressure from an approximate calculation are on the order of 7250 psi. RS5 and RS6, eight lb. TNT detonations, show cavity pressures of 5200 psi and 5800 psi, respectively.

Additional studies are subsequently performed on these experiments. A hole is drilled to the vicinity of the explosive cavity and small-volume hydraulic fracturing is done with dyed water at intervals along this hole. The region is then mined out to evaluate the behavior and orientation of the hydraulic fractures and to characterize the region near the detonation. In general, hydraulic fracture pressure data and orientations are unaffected beyond five to ten cavity radii from the center of the charge. At two cavity radii, breakdown and

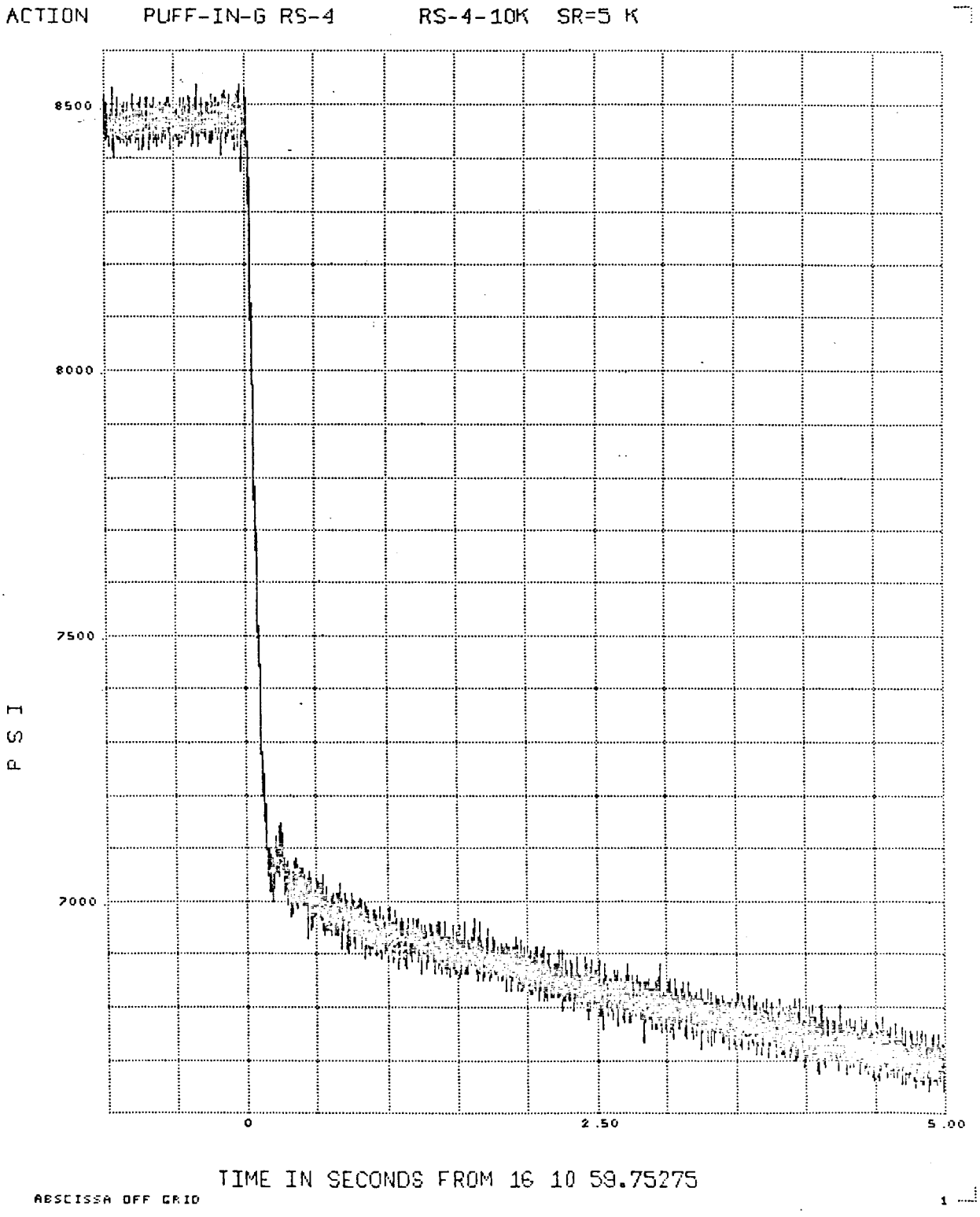

Figure IV-22. Cavity Pressure Measurement on RS-4

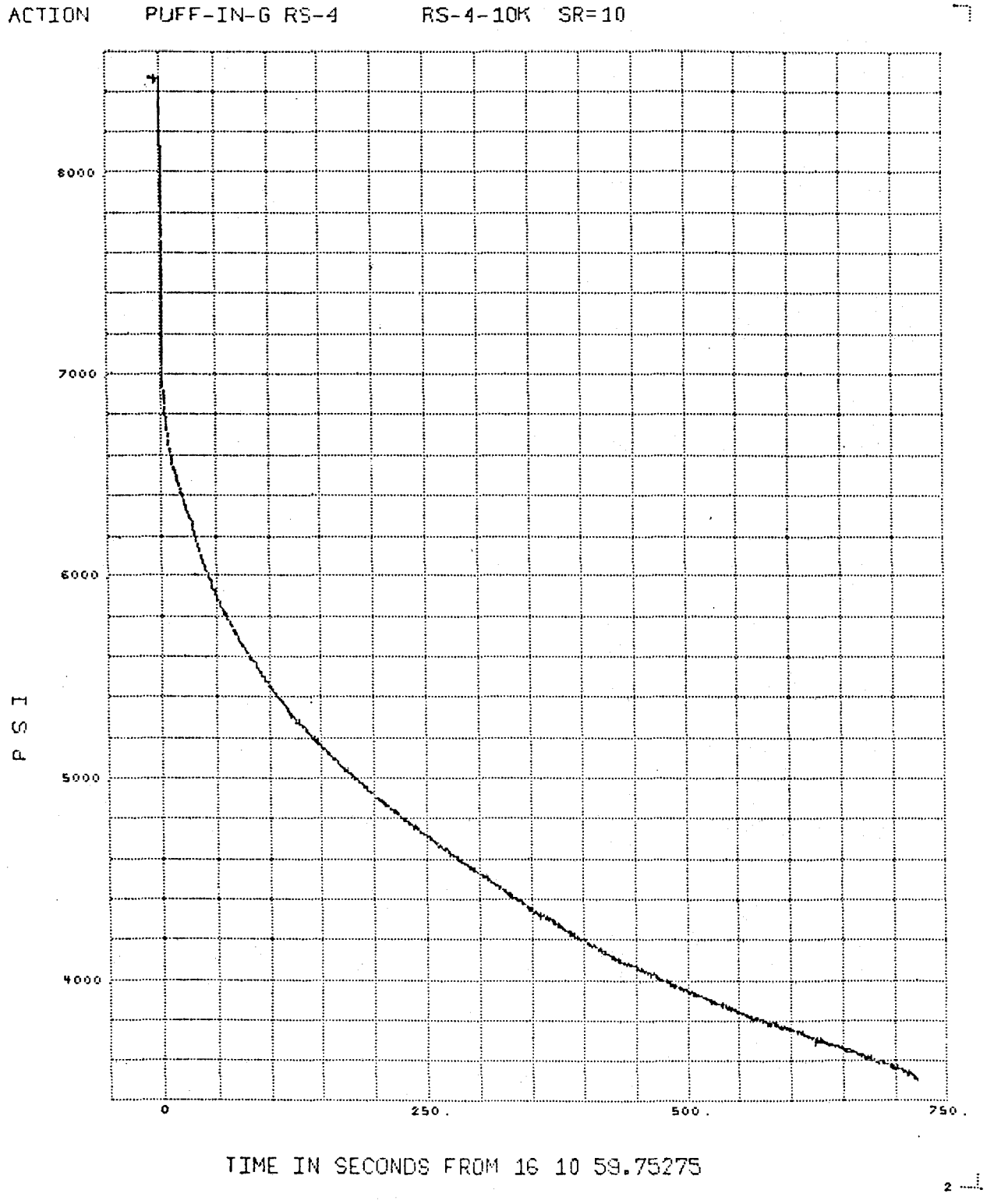

Figure IV-22. Continued

fracturing pressures are reduced and the observed dyed fractures is roughly spherical about the cavity. This location corresponds to a minimum in the calculated residual hoop stress obtained from a one-dimensional calculation. These calculations suggest that close to the cavity the tangential stress predominates, while further out the radial stresses are larger. This is consistent with the observation of mine-back of a series of circumferential fractures near the cavity wall ("onion skin") and small (∿1 ft) radial fractures at greater distances which may have been created by the subsequent hydraulic fracturing and which do not extend to the cavity.

The measured high cavity pressures and the observed fractures resulting from an explosive detonation support the concept of the formation of a containment cage which inhibits fracturing from the cavity. The observed cavity pressures are significantly greater than either the minimum in situ stress (∿ 1000 psi) or the vertical overburden stress (∿ 1300 psi) at these locations. In the absence of the residual stress field, these cavity pressures would be quickly relieved by creating and driving a fracture.

References (Section IV)

1. Northrop, D. A., and Schuster, C. L., editors, "Enhanced Gas Recovery Program Second Annual Report, October 1976 - September 1977," Sandia Laboratories Report SAND-77-1992, April 1978.

2. Tyler, L. D., and Vollendorf, W. C., "Physical Observations and Mapping of Cracks Resulting from Hydraulic Fracturing In Situ Stress Measurements," SPE 5542, 50th Annual Fall Meeting of the Society of Petroleum Engineers of AIME, Dallas, TX, September 28 - October 1, 1975.

3. Tyler, L. D., and Vollendorf, W. C., and Northrop, D. A., "In Situ Examination of Hydraulic Fractures," presented at Third ERDA Symposium for Enhanced Oil, Gas Recovery and Improved Drilling Methods, Tulsa, OK, August 30 - September 1, 1977.

4. Smith, C. W., Bass, B. C., and Tyler, L. D., "Puff 'N Tuff: A Residual Stress-Gas Fracturing Experiment," presented at the 19th U.S. National Symposium in Rock Mechanics, May 1-3, 1978.

5. Daneshy, A. A., "Hydraulic Fracture Propagation in Layered Formations," Soc. Petroleum Engineers Journal, February 1978, p. 33-41.

6. Elder, C. H., "Effects of Hydraulic Stimulation on Coalbeds and Associated Strata," R. I. 8260, U.S. Bureau of Mines, 1977.

7. Northrop, D. A., and Schuster, C. L., editors, "Enhanced Gas Recovery Program, Second Annual Report, Part I," SAND-77-1992, Sandia Laboratories Report, April 1978.

8. Hanson, M. E., et al., "LLL Gas Stimulation Program, Quarterly Progress Report, October through December 1977," Lawrence Livermore Laboratory Report UCRL-50036-77-4, January 1978.

9. Simonson, E. R., Abou-Sayed, A. S., and Clifton, R. J., "Containment of Massive Hydraulic Fractures," Soc. Petroleum Engineers Journal, February 1978, p. 27-32.

10. Cook, T. S., and Erdogan, F., "Stresses in Bonded Materials with a Crack Perpendicular to the Interface," Inter. J. of Eng. Sci., Vol. 10, pp. 677-697, 1973.

11. Erdogan, F., and Biricikoglu, V., "Two Bonded Half Planes with a Crack Going Through the Interface," Inter. J. of Eng. Sci., Vol. 11, pp. 745-766, 1973.

12. Atkinson, C., "On the Stress Intensity Factors Associated with Cracks Interacting with an Interface Between Two Elastic Media," Inter. J. of Eng. Sci., Vol. 13, pp. 489-504, Sept. 1972.

13. Laverenz, R. K., "A Finite Element Stress Analysis of a Crack in a Bi-Material Plate," Inter. J. of Fracture Mechanics, Vol. 8, No. 3, pp. 311-324, Sept. 1972.

14. Bogy, D. B., "On the Plane KElastostatic Problem of a Loaded Crack Terminating at a Material Interface," J. of Applied Mechanics, Vol. 38, pp. 911-918, August 1975.

15. Atkinson, C., "Some Results on Crack Propagation in Media with Spatially Varying Elastic Moduli," Inter. J. of Fracture, Vol. 11, No. 4, pp. 619-628, August 1975.

16. Benzley, S. E., and Beisinger, Z. E., "CHILES 2 - A Finite Element Computer Program that Calculates the Intensities of Linear Elastic Singularities in Isotropic and Orthotropic Materials," Sandia Laboratories Report SAND-77-1900, February 1978.

17. Gifford, L. N., and Hilton, P. D., "Stress Intensity Factors by Enriched Finite Elements," Engineering Fracture Mechanics, Vol. 10, pp. 485-496 (1978).

18. Kehle, R. D., "The Determination of Tectonic Stresses Through Analysis of Hydraulic Well Fracturing," Journal of Geophysical Research, Vol. 69, No. 2, January 15, 1964, p. 259.

19. Fairhurst, C., "Measurement of In Situ Rock Stresses with Particular Reference to Hydraulic Fracturing," Rock Mechanics and Engineering Geology, Vol. 2, 1964, p. 129.

20. Fairhurst, C., "Methods of Determining In Situ Rock Stresses at Great Depths," TN 1-68, Missouri River Division, Corps. of Engineers, Omaha, Nebraska, February 1968.

V. PUBLICATIONS, PRESENTATIONS AND OTHER COMMUNICATIONS

A. Publications and Presentations

1. C. L. Schuster and L. J. Keck, "Results from a MHF Surface Electrical Potential Mapping Experiment," presented by C. L. Schuster at the First Annual Eastern Gas Shales Symposium, October 17-19, Morgantown, WV, and published in the proceedings as MERC/SP-77/5, pp. 426-433, March, 1978.
2. L. D. Tyler, W. C. Vollendorf and D. A. Northrop, "In Situ Examination of Hydraulic Fractures," presented by L. D. Tyler and D. A. Northrop at the First Annual Eastern Gas Shales Symposium, October 17-19, 1977, Morgantown, WV, and published in the Proceedings as MERC/SP-77/5, pp. 37-48, March 1978.
3. H. M. Stoller, "Sandia's Role in the EGR Program," presented at the Fourth Semi-annual Enhanced Gas Recovery Review Meeting, Las Vegas, NV, March 21-23, 1978.
4. C. L. Schuster, "Fracture Diagnostics Activities," presented at the Fourth Semi-annual Enhanced Gas Recovery Review Meeting, Las Vegas, NV, March 21-23, 1978.
5. N. R. Warpinski, "Stimulation and Mineback Experiment Program," presented at the Fourth Semi-annual Enhanced Gas Recovery Review Meeting, Las Vegas, NV, March 21-23, 1978.
6. A. L. McFall, "Improved Pressure Core Barrel Development," presented at the Fourth Semi-annual Enhanced Gas Recovery Review Meeting, Las Vegas, NV, March 21-23, 1978.
7. D. A. Northrop and C. L. Schuster, Editors, "Enhanced Gas Recovery Program, Second Annual Report (Parts I and II), October 1976 through September 1977," Sandia Laboratories Report, SAND77-1992, April 1978.
8. C. L. Schuster and D. A. Northrop, Editors, "Enhanced Gas Recovery Program, First Quarterly Report: Fiscal Year 1978, October 1977-December 1977," Sandia Laboratories Report, SAND78-1172, June 1978.

9. C. W. Smith, R. C. Base and L. D. Tyler, "Puff 'N Tuff, a Residual Stress-Gas Fracturing Experiment," presented by R. A. Schmidt at the 19th Annual National Rock Mechanics Symposium, Lake Tahoe, NV, April 30 - May 3, 1978.

10. R. A. Schmidt and T. J. Lutz, "K_{IC} and J_{IC} of Westerly Granite," presented by R. A. Schmidt at the 11th National Symposium on Fracture Mechanics, Blackburg, VA, June 11-12, 1978.

11. R. A. Schmidt, "Laboratory Investigations of Rock Fracture with Applications to Energy Research," colloquium at Los Alamos Scientific Laboratory, Los Alamos, NM, July 27, 1978.

12. R. A. Schmidt, "Crack Propagation and Fracture in Rock," presented at a Gordon Research Conference, Tilton, NH, August 7-11, 1978.

13. D. A. Northrop, N. R. Warpinski, R. A. Schmidt, and C. W. Smith, "The Direct Observation of Hydraulic and Explosive Fracturing Tests," presented by D. A. Northrop at the Fourth Annual DOE Symposium on Enhanced Oil and Gas Recovery, Tulsa, OK, August 29-31, 1978, and published in the proceedings.

14. C. L. Schuster, "Massive Hydraulic Fracture Mapping and Characterization Program," presented at the Fourth Annual DOE Symposium on Enhanced Oil and Gas Recovery," Tulsa, OK, August 29-31, 1978, and published in proceedings.

15. C. L. Schuster and D. A. Northrop, Editors, "Enhanced Gas Recovery Program, Second Quarterly Report: Fiscal Year 1978, January through March 1978," Sandia Laboratories Report, SAND78-1672, September 1978.

B. Other Communications

1. R. J. Saucier and W. B. Bradley of the Shell Oil Company visited Sandia Laboratories on October 6, 1977, to review Sandia activities and to explore areas for further interaction and cooperation. A. B. Crawley, DOE/OGSIST, also attended this meeting.

2. D. A. Northrop, N. R. Warpinski and R. A. Schmidt met with Amoco personnel in Tulsa, OK, on November 29, 1977, to present an update of mineback program activities.
3. R. P. Trump, Gulf Research and Development Company visited Sandia Laboratories on December 12, 1977, to discuss enhanced gas recovery. He also visited the mineback activities at G tunnel, Nevada Test Site on the following day.
4. G. B. Griswold participated in a meeting to develop a core analysis program for the Western Gas Sands Project held at CER in Las Vegas, NV, on January 25, 1978.
5. R. L. Bullick and F. J. Humphrey, Exxon Production Research Company, visited the mineback activities in G tunnel, Nevada Test Site, during January 1978.
6. C. L. Schuster and R. W. Seavey visited CER in Las Vegas, NV, on January 5, 1978, to discuss the status of the mobile well logging laboratory and supporting equipment.
7. Sandia Laboratories hosted a one-day trip, on March 20, 1978, to the Nevada Test Site, in conjunction with the Fourth Semi-annual Enhanced Gas Recovery Review Meeting. About 20 people made the tour which featured detailed technical briefings on the mineback activities in G tunnel, a visit to Sedan Crater, and a tour of the NTS drill yard and drilling capability.
8. J. W. Reeves, E. I. DuPont Demours and Company, visited Sandia Laboratories on April 27, 1978, to discuss Sandia's programs in hydraulic fracture mapping and other activities.
9. D. A. Krycowski and E. I. Witterholt, Cities Service Research Labs, visited Sandia Laboratories to discuss Sandia's energy-related research activities.
10. D. A. Northrop, N. R. Warpinski and A. L. Stevens represented Sandia Laboratories at an EGSP Stimulation and Modeling Review Workshop held in Morgantown, WV, on May 18-19, 1978, and July 11-12, 1978.

11. D. A. Northrop briefed R. W. Taft and R. W. Newman, DOE/Nevada Operations Office, on the fossil-energy related experiments being conducted at the Nevada Test Site, Las Vegas, NV, June 8, 1978.
12. R. H. Maier, Gulf Universities Research Consortium, visited Sandia Laboratories on June 23, 1978, to discuss this program's methods of technology transfer to industry.
13. M. Sorrells, Teledyne-Geoteck, visited the Nevada Test Site to view the fracutre experiments as part of his analysis on the nature of seismis signals, August 1, 1978.
14. R. Huggins, R. Veatch and M. Smith, Amoco Production Company, visited the Nevada Test Site to view the fracture experiments as part of their continuing interaction with our program, August 22, 1978.
15. T. L. Dobecki and J. Castle visited Chevron Oil Field Research Laboratories on August 3, 1978, to discuss state-of-the-art and research advancements involving nuclear magnetic resonance techniques as applied to formation evaluation.

DISTRIBUTION:

US Dept. of Energy
MS D-107
Fossil Energy
Washington, DC 20545
Attn: G. Fumich, Prog. Dir.

US Dept. of Energy (16)
Div. of Fossil Fuel Extraction
MS D-107
Washington, DC 20545
Attn: R. Hertzberg, Director
J. W. Watkins, Dep. Dir.
D. Crane
C. Daffin
J. B. Smith
A. B. Crawley (10)

US Dept. of Energy
Div. of Program Control & Support
Office of Fossil Energy
Washington, DC 20545
Attn: C. W. Guidice, Acting Dir.

US Dept. of Energy (4)
Morgantown Energy Technology Center
P. O. Box 880
Morgantown, WV 26505
Attn: A. A. Pitrolo, Director
L. A. Schrider
C. A. Komar
R. L. Wise

US Dept. of Energy
Nevada Operations Office
P. O. Box 14100
Las Vegas, NV 89114
Attn: C. H. Atkinson

CER Corporation (2)
P. O. Box 15090
Las Vegas, NV 89114
Attn: G. R. Leutkenhans
R. L. Mann

US Dept. of Energy (2)
Bartlesville Energy Tech. Center
Bartlesville, OK 74003
Attn: R. T. Johansen
D. C. Ward

US Dept. of Energy
Special Programs Division
Albuquerque Operations Office
Albuquerque, NM 87185
Attn: D. K. Nowlin, Director

Lawrence Livermore Laboratory
Livermore, CA 94550
Attn: M. E. Hanson

Los Alamos Scientific (3)
Laboratory
Los Alamos, NM 87545
Attn: R. Brownlee, G-Division
W. G. Davey, Q-Division
W. J. Carter, G-7

Halliburton Services (2)
Research Center
Duncan, OK 73533
Attn: A. B. Waters
A. A. Daneshy

Shell Development Company
3737 Bellaire Boulevard
Houston, TX 77001
Attn: R. Saucier

Mobil Research and
Development Corporation
Field Research Laboratory
P. O. Box 900
Dallas, TX 75211
Attn: J. L. Fitch

Continental Oil Company (2)
Production Research Division
Ponca City, OK 74601
Attn: H. C. Walther
H. Wahl

Columbia Gas System Service (2)
Corp.
1600 Dublin Road
Columbus, OH 43215
Attn: R. Forrest
S. McKetta

Distribution, continued

Gas Producing Enterprises, Inc.
2100 Prudential Plaza
P. O. Box 749
Denver, CO 80201
Attn: R. Merrill

Dowell
P. O. Box 21
Tulsa, OK 74102
Attn: R. Steanson

Institute of Gas Technology
3424 S. State St.
Chicago, Ill 60616
Attn: P. Randolph

Amoco Production Co. (3)
P. O. Box 591
Tulsa, OK 74102
Attn: R. L. Huggins
R. W. Veatch
M. B. Smith

M. D. Wood, Inc.
1000 Elwell Court
Suite 218
Palo Alto, CA 94303
Attn: M. D. Wood

Gulf Research and Development Company
P. O. Drawer 2038
Pittsburgh, PA 15230
Attn: R. P. Trump

Terratek
University Research Park
420 Wakara Way
Salt Lake City, Utah 84108
Attn: A. S. Abou-Sayed

Dept. of Engineering Mechanics
The Ohio State University
Boyd Laboratory
155 West Woodruff Avenue
Columbus, OH 43210
Attn: Prof. S. H. Advani, Chairman

University of Minnesota
Dept. of Civil and Mineral Eng.
Minneapolis, Minn. 55455
Attn: Dr. Charles Fairhurst

School of Civil and Environmental Engineering
Hollister Hall
Cornell University
Ithaca, NY 14853
Attn: Dr. A. R. Ingraffea

US Geological Survey
345 Middlefield Road
Menlo Park, CA 94025
Attn: Dr. D. D. Pollard

Fracturing Technology, Inc.
10301 N.W. Freeway
Suite 202
Houston, TX 77092
Attn: A. R. Sinclair, President

Internal Distribution:

1	M. Sparks
1000	G. A. Fowler
1100	C. D. Broyles
1110	J. D. Kennedy
	Attn: C. R. Mehl, 1111
	C. W. Smith, 1111
1120	T. L. Pace
1130	H. E. Viney
	Attn: B. G. Edwards, 1131
	W. C. Vollendorf, 1131
4400	A. W. Snyder
4500	E. H. Beckner
4537	L. D. Tyler
4700	J. H. Scott
4710	G. E. Brandvold
4720	V. L. Dugan
4730	H. M. Stoller
4731	R. K. Traeger
4732	D. A. Northrop (25)
4733	C. L. Schuster (15)
4734	A. L. Stevens
4735	S. G. Varnado
4736	A. F. Veneruso
5500	O. E. Jones
	Attn: W. Herrmann, 5530
5800	R. S. Claassen
8266	E. A. Aas (1)
3141	T. Werner (5)
3151	W. L. Garner (3)
3172-3	R. P. Campbell
	for DOE/TIC (25)